

Titre: Optical differential phase-shift keyed signal generation,
Title: transmission and detection

Auteur: Yannick Lizé
Author:

Date: 2008

Type: Mémoire ou thèse / Dissertation or Thesis

Référence: Lizé, Y. (2008). Optical differential phase-shift keyed signal generation, transmission and detection [Ph.D. thesis, École Polytechnique de Montréal].
Citation: PolyPublie. <https://publications.polymtl.ca/8125/>

Document en libre accès dans PolyPublie

Open Access document in PolyPublie

URL de PolyPublie: <https://publications.polymtl.ca/8125/>
PolyPublie URL:

Directeurs de recherche: Nicolas Godbout, & Alan E. Willner
Advisors:

Programme: Unspecified
Program:

UNIVERSITÉ DE MONTRÉAL

OPTICAL DIFFERENTIAL PHASE-SHIFT KEYED
SIGNAL GENERATION, TRANSMISSION AND DETECTION

YANNICK KEITH LIZE
DEPARTEMENT DE GENIE PHYSIQUE
ECOLE POLYTECHNIQUE DE MONTREAL

THÈSE PRÉSENTÉE EN VUE DE L'OBTENTION
DU DIPLÔME DE PHILOSOPHIÆ DOCTOR
(GENIE PHYSIQUE)
MARS 2008

© Yannick Keith Lize, 2008.



Library and
Archives Canada

Published Heritage
Branch

395 Wellington Street
Ottawa ON K1A 0N4
Canada

Bibliothèque et
Archives Canada

Direction du
Patrimoine de l'édition

395, rue Wellington
Ottawa ON K1A 0N4
Canada

Your file *Votre référence*

ISBN: 978-0-494-41754-6

Our file *Notre référence*

ISBN: 978-0-494-41754-6

NOTICE:

The author has granted a non-exclusive license allowing Library and Archives Canada to reproduce, publish, archive, preserve, conserve, communicate to the public by telecommunication or on the Internet, loan, distribute and sell theses worldwide, for commercial or non-commercial purposes, in microform, paper, electronic and/or any other formats.

The author retains copyright ownership and moral rights in this thesis. Neither the thesis nor substantial extracts from it may be printed or otherwise reproduced without the author's permission.

In compliance with the Canadian Privacy Act some supporting forms may have been removed from this thesis.

While these forms may be included in the document page count, their removal does not represent any loss of content from the thesis.

AVIS:

L'auteur a accordé une licence non exclusive permettant à la Bibliothèque et Archives Canada de reproduire, publier, archiver, sauvegarder, conserver, transmettre au public par télécommunication ou par l'Internet, prêter, distribuer et vendre des thèses partout dans le monde, à des fins commerciales ou autres, sur support microforme, papier, électronique et/ou autres formats.

L'auteur conserve la propriété du droit d'auteur et des droits moraux qui protège cette thèse. Ni la thèse ni des extraits substantiels de celle-ci ne doivent être imprimés ou autrement reproduits sans son autorisation.

Conformément à la loi canadienne sur la protection de la vie privée, quelques formulaires secondaires ont été enlevés de cette thèse.

Bien que ces formulaires aient inclus dans la pagination, il n'y aura aucun contenu manquant.



Canada

UNIVERSITÉ DE MONTRÉAL

ÉCOLE POLYTECHNIQUE DE MONTRÉAL

Cette thèse intitulée:

OPTICAL DIFFERENTIAL PHASE-SHIFT KEYED
SIGNAL GENERATION, TRANSMISSION AND DETECTION

présentée par: LIZE Yannick Keith
en vue de l'obtention du diplôme de : Philosophiæ Doctor
a été dûment acceptée par le jury d'examen constitué de :

M. MACIEJKO Romain, Ph.D., président
M. GODBOUT Nicolas, Ph.D., membre et directeur de recherche
M. WILLNER Alan E., Ph.D., membre et co-directeur de recherche
Mme LACROIX Suzanne, D. Sc., membre
M. PLANT David, Ph.D., membre

To Maureen, Kathleen, Cynthia and Sandra,

"My name is Yannick, but you can call me doctor"
Yannick Keith Lize, 2008

Acknowledgements

Undertaking a Ph.D. is a strengthening experience of self-awareness, direction and reliance. Learning to endure and stay the course with a positive attitude is a fulfilling experience of which above all I enjoyed the challenges of defining problems and solving them. I want to acknowledge here the many people have made this work possible through their love, support and wisdom.

To Maureen, Kathleen, Cynthia and Sandra for your unconditional love, it's easy to be daring and push the limits when you know that whatever happens, you'll always be there for me, no matter what.

I would like to thank my supervisor Nicolas Godbout for saving me, for bailing me out when I was sinking. I want to thank my co-supervisor Prof. Alan E. Willner at the University of Southern California for his wisdom, counsel, support, understanding and supervision. You have been and continue to be a great mentor.

Thank you to Ben Eggleton, for making me a research scientist, for telling me what I would be judged by and how I should set my goals. You have given the drive to get all of this work done.

I want to thank everyone who had the patience and dedication to supervise me for one portion or another of this thesis: Rod Tucker and Thas Nirmalathas in Melbourne, Randy Giles and Xiang Liu at Bell Labs. I learned a lot from all of you.

To all those who supported me with their counsel and friendship, on whom I can

still count on for any silly question I come up with; Peter Winzer, René-Jean Essiambre, and Chris Doerr at Bell Labs, Christian Malouin at Stratalight, Kim Roberts at Nortel, John Cartledge at Queen's University, and many others. A special thanks to my Jedi Master Dan Marom for giving the confidence to battle the evil forces of Latex when writing this thesis.

To François Séguin for believing in my abilities to become a good industrial research scientist and giving me my first opportunity: your confidence has allowed me to make a successful transition from the university to the real world.

To all my co-authors and friends, Mathieu Faucher, Leigh Palmer, Louis Christen, Scott Nuccio, Pooryah Saghari, Saurabh Kumar, Moshe Nazarathy, Xiaoxia Wu, Yuval Atzmon, Robert Gomma, Jeng-Yuan Yang, Boris Kuhlmeijer, Maryse Aubé, Suzanne Lacroix, Alexandre Dupuis, Benoit Sévigny and Xavier Daxhelet.

I want to thank the cities of Baltimore, Berlin, Munich, New York, Orlando, Ottawa, San Diego, San Jose and Washington DC for providing food and shelter at a reasonable price during this writing process.

Résumé

Lors de l'encodage de l'information sur une onde électromagnétique, telle la lumière infrarouge pour la transmission dans la fibre optique d'un réseau de télécommunication, n'importe quelle propriété de la lumière cohérente peut être modulée. L'onde a une fréquence, une intensité, une polarisation et une phase. Jusqu'à tout récemment, les systèmes de communication optique utilisaient strictement la modulation d'intensité pour encoder l'information soit en format non-retour-à-zéro (NRZ) ou retour-à-zéro (RZ). Un certain nombre de formats de modulation optique avancés ont reçu une attention croissante au cours des dernières années. Un exemple est la modulation de phase différentielle (PSK pour « phase shift keying »), qui transporte l'information sur la phase optique. Puisque la phase absolue n'est détectable que par démodulation cohérente, l'encodage différentiel dans lequel la phase d'un bit subséquent est utilisée comme phase relative de référence, est devenu une méthode de choix. Le résultat est l'encodage en phase différentielle (DPSK pour « differential-phase-shift-keying »), qui repose non pas sur la valeur absolue de la phase mais sur la différence de phase optique entre bits successifs.

Dans cette thèse par articles, composée de six publications, nous étudions la *génération*, la *transmission* et la *démodulation* du DPSK dans les systèmes de transmission par fibre optique. Nous proposons une nouvelle façon d'encoder les paquets optiques en utilisant le DPSK dans notre étude de la *génération*. Nous étudions la *transmission* grâce à un nouvel outil de surveillance des effets utilisant la mesure des signaux d'horloge

assisté d'un interféromètre Mach-Zehnder ayant un délai partiel. La méthode permet la surveillance continue et sensible du rapport signal-sur-bruit optiques (OSNR pour « Optical Signal to Noise Ratio »), de la dispersion chromatique et de la dispersion des modes de polarisation. Ensuite nous examinons la démodulation de DPSK en analysant la réduction des tolérances ainsi que la pénalité de démodulation lorsque qu'un délai de plus qu'un bit est utilisé dans l'interféromètre. Nous proposons également une méthode optique de correction d'erreurs combinant les fonctions de logique binaire d'un démodulateur DPSK avec les fonctions de logique binaire électroniques dans le but d'améliorer la sensibilité et la tolérance aux effets de transmission. Enfin, nous redéfinissons la tolérance à la dispersion chromatique du Non-retour-zéro-DPSK et du Retour-à-zéro-DPSK lorsque les paramètres de démodulation tel que le filtrage optique et l'interfrange du démodulateur sont optimisés.

Abstract

When encoding information on an electromagnetic wave such as infrared light, to be transmitted through an optical fibre in telecommunication networks, any of the physical properties of light can be modulated. Light has a frequency, intensity, polarization and a phase. Until recently, optical communication systems strictly employed conventional intensity (IM) modulation signals in either non return-to-zero (NRZ) or return-to-zero (RZ) format. But a number of advanced optical modulation formats have attracted increasing attention in the last few years. One prime example is the phase-shift-keyed (PSK) family of formats which carry the information on the optical phase. Since absolute phase is not easily detected through coherent demodulation, differential encoding in which the phase of the preceding bit is used as a relative phase reference for demodulation has become a method of choice for phase modulated signals. The result in the differential-phase-shift-keyed (DPSK) formats, which carry the information in the difference in optical phase between successive bits.

In this thesis by article, composed of six papers, we investigate the *generation*, *transmission* and *demodulation* of DPSK in optical fibre transmission systems. We propose a novel way to encode optical packets using DPSK in our investigation of the *generation*. We also investigate transmission effects monitoring using a novel partial-bit delay interferometer-assisted clock tone monitoring method for sensitive optical-signal-to-noise ratio (OSNR), chromatic dispersion and polarization mode dispersion monitoring. Then we look at the demodulation of DPSK, first investigating the

reduced tolerances and power penalties of DPSK demodulation when more than one bit delay is used in the interferometer. We also propose an optical error correction method combining DPSK optical logic gates with electronic logic gates to improve receiver sensitivity and transmission impairment tolerances. Finally we redefine the previously assumed chromatic dispersion tolerances of Non-Return-to-Zero (NRZ) -DPSK, Return-to-Zero (RZ)-DPSK and Carrier-Suppressed-Return-to-Zero (CSRZ) -DPSK with optimized demodulation parameters of optical filtering and free-spectral range optimization.

Condensé en Français

Lors de l'encodage de l'information sur une onde électromagnétique, telle la lumière infrarouge pour la transmission dans la fibre optique d'un réseau de télécommunication, n'importe quelle propriété de la lumière cohérente peut être modulée. L'onde a une fréquence, une intensité, une polarisation et une phase. Jusqu'à tout récemment, les systèmes de communication optique utilisaient strictement la modulation d'intensité pour encoder l'information soit en format non-retour-à-zéro (NRZ) ou retour-à-zéro (RZ). Un certain nombre de formats de modulation optique avancés ont reçu une attention croissante au cours des dernières années. Un exemple est la modulation de phase différentielle (PSK pour « phase shift keying »), qui transporte l'information sur la phase optique. Puisque la phase absolue n'est détectable que par démodulation cohérente, l'encodage différentiel dans lequel la phase d'un bit subséquent est utilisée comme phase relative de référence, est devenu une méthode de choix. Le résultat est l'encodage en phase différentielle (DPSK pour « differential-phase-shift-keying »), qui repose non pas sur la valeur absolue de la phase mais sur la différence de phase optique entre bits successifs.

Dans cette thèse par articles, composée de six publications, nous étudions la génération, la transmission et la démodulation du DPSK dans les systèmes de transmission par fibre optique. Nous proposons une nouvelle façon d'encoder les paquets optiques en utilisant le DPSK dans notre étude de la génération. Il a été établi par d'autres auteurs que l'utilisation du DPSK combiné à la modulation d'intensité pour

encoder le message et l'adresse d'un paquet optique avec un récepteur équilibré pour détecter le DPSK résulte en une sensibilité record au récepteur autour -36 dBm à la fois l'adresse et le message pour un taux d'erreur de 10^{-9} . Malheureusement, la plupart des méthodes d'encode de paquet optique requièrent deux modulateurs optiques; un pour l'encodage du message et un autre pour l'adresse ce qui réduit considérablement la possibilité de l'implémentation d'un tel système à cause des coûts reliés à l'encodage. Notre méthode d'encodage utilise un seul modulateur pour l'encodage simultané du message ainsi que de l'adresse et ce avec une bonne sensibilité du récepteur. Nous présentons deux méthodes différentes pour l'encodage en utilisant un seul Mach-Zehnder modulateur :i) la modulation du point de croisement et ii) la modulation de du gain de l'amplificateur électrique.

Dans cette thèse, nous étudions également la transmission optique grâce à un nouvel outil de surveillance des effets utilisant la mesure des signaux d'horloge assisté d'un interféromètre Mach-Zehnder ayant un délai partiel. La méthode permet la surveillance continue et sensible du rapport signal-sur-bruit optique (OSNR pour « Optical Signal to Noise Ratio »), de la dispersion chromatique et de la dispersion des modes de polarisation. Les méthodes d'évaluation de performance d'un lien de transmission optique seront fort probablement une nécessité pour les futurs réseaux de télécommunication. À ce titre, il y a eu plusieurs méthodes rapportées dans la littérature pour réaliser une évaluation efficace des différents effets. Une façon simple et rentable pour le suivi du rendement est de mesurer la puissance RF dans le ton horloge en utilisant un filtre à bande étroite électrique et un wattmètre. Cette méthode peut

être utilisée pour suivre l'accumulation soit de CD ou de PMD. Malheureusement, il ne permet pas facilement l'isolation des deux effets et leur évaluation simultanée étant donné que les deux influencent la puissance du signal d'horloge. L'intensité de l'horloge est de plus dépendante de l'OSNR de sorte qu'il est difficile d'évaluer lequel des trois effets est responsable de la variation de la puissance d'horloge. Notre méthode permet cette évaluation indépendante et simultanée et ce pour plusieurs formats de modulation tel que le NRZ-OOK, le NRZ-DPSK et le Duobinaire optique.

Nous avons également évalué pour la première fois la réduction des tolérances ainsi que la pénalité de démodulation lorsqu'un délai de plus qu'un bit est utilisé dans la démodulation d'un signal DPSK. En dépit de l'intérêt grandissant pour le concept de la démodulation à délai multiple, très peu d'attention a été portée sur la pénalité encourue dans le système lorsque qu'un signal DPSK est démodulé dans un interféromètre ayant un délai plus grand qu'un bit. Nous présentons des résultats expérimentaux ainsi que d'analyse numérique et analytique sur la pénalité relié au désalignement de la fréquence entre la porteuse et le démodulateur, la largeur spectrale du laser de transmission ainsi que le décalage entre la longueur de bit transmis et le délai de l'interféromètre et démontrons que ces limitations peuvent réduire l'efficacité des méthodes multi-délais dans certaines applications.

Nous proposons également une méthode optique de correction d'erreurs combinant les fonctions de logique binaire d'un démodulateur DPSK avec les fonctions de logique binaire électroniques dans le but d'améliorer la sensibilité et la tolérance aux effets de transmission.

En dépit de ses performances supérieures à la modulation d'intensité, le DPSK a des exigences en OSNR 1.2 dB plus élevées que son homologue cohérent, le PSK pour un taux d'erreur de 10-3. Des stratégies de traitement multi-symboles ont été proposées pour réduire cette pénalité par la détection douce, incluant les techniques basées sur l'asservissement de la décision qui peuvent fournir 1-3 dB d'amélioration sur la sensibilité du DPSK. Cependant l'électronique analogue haute vitesse requise peut être difficilement implémentée avec les technologies actuelles. Notre méthode de détection utilise la décision dure plutôt que la détection douce, c'est-à-dire qu'une décision est prise sur chaque bit et qu'un signal numérique logique est produit. Nous appliquons ensuite du traitement logique numérique à la sortie de plusieurs interféromètres ayant un délai de démodulation différent pour réaliser des gains de traitement comparables. Nous avons démontré expérimentalement et numériquement notre méthode de correction d'erreur optique multi-chemins. La technique peut être facilement mise en œuvre en utilisant des interféromètres et des opérateurs logiques grande vitesse commercialement disponibles. Après la démodulation optique et la détection dure, les opérations logiques de base sont appliquées sur chaque chemin pour récupérer le signal et ensuite les erreurs peuvent être corrigées au moyen d'un simple vote majoritaire comparant les différents chemins [83].

Finalement, dans cette thèse nous avons redéfini la tolérance à la dispersion chromatique du Non-retour-zéro-DPSK et du Retour-à-zéro-DPSK lorsque les paramètres de démodulation tel que le filtrage optique et l'interfrange du démodulateur sont optimisés. Plusieurs publications ont démontré la performance des récepteurs

DPSK par rapport à certaines dégradations tel que le décalage du retard, décalage entre la fréquence de la porteuse et la fréquence de transmission de l'interféromètre, la dispersion chromatique (CD), la dispersion des modes de polarisation, les non linéarités dans la fibre de transmission. Ces dégradations affectent la phase du signal DPSK et réduisent la sensibilité de réception et la distance de transmission. Il a récemment été montré que l'augmentation de l'interfrange peut augmenter les tolérances au filtrage optique et la dispersion chromatique, mais la valeur des paramètres optimaux pour une valeur de filtrage ou une dispersion donnée n'avait jusqu'à maintenant jamais été établie. Qui plus est, l'effet combiné du filtrage et de la dispersion chromatique CD n'avait jamais été démontré

Grâce à nos simulations, nous avons déterminé que le filtrage optique optimal en détection dos à dos est d'environ $1.25xR$ pour NRZ-DPSK (R étant le débit de transmission), $1.75xR$ pour RZ-DPSK et $1.8xR$ pour CSRZ-DPSK. L'interfrange optimale varie selon la largeur spectrale du filtre mais est également très dépendante de la dispersion chromatique. Les résultats indiquent qu'autant un filtrage serré qu'une interfrange élevée augmente la tolérance à la dispersion, mais c'est la combinaison des deux qui conduit à des performances optimales CD.

Le resserrement de filtrage optique et l'augmentation de RSF peuvent être considérés comme mettant davantage l'accent sur le port constructif qui est en fait le format de modulation Duobinaire, au détriment du port destructif qui le format de modulation d'alternation de la marque d'inversée. Le Duobinaire est bien connu pour sa tolérance de dispersion chromatique, ce qui expliquerait l'augmentation des

performances.

Table of content

| | |
|--|--------------|
| DEDICATION | IV |
| ACKNOWLEDGEMENTS..... | V |
| RESUME | VII |
| ABSTRACT | IX |
| CONDENSE EN FRANÇAIS | XI |
| TABLE OF CONTENT | XVII |
| LIST OF FIGURES | XVIII |
| LIST OF SYMBOLS AND ABBREVIATIONS..... | XX |
| LIST OF APPENDICES | XXIII |
| INTRODUCTION | 1 |
| CHAPTER 1 | 5 |
| 1.1 Optical Label Encoding:..... | 8 |
| 1.2 Optical Performance Monitoring..... | 9 |
| 1.3 Multibit Delay DPSK Demodulation..... | 11 |
| 1.4 Optical Error Correction..... | 12 |
| 1.5 FSR Optimization: | 14 |
| CHAPTER 2 | 16 |
| 2.1 Optical Label Switching | 17 |
| 2.2 Optical Performance Monitoring..... | 20 |
| 2.3 Multibit Delay DPSK Demodulation..... | 25 |
| 2.4 Optical Error Correction..... | 29 |
| 2.4.1 <i>Theory</i> | 29 |
| 2.4.2 <i>Simulations & Experiment</i> | 34 |
| 2.5 Free Spectral Range and Optical Filtering Optimization..... | 36 |
| 2.5.1 <i>Theory</i> | 36 |
| 2.5.2 <i>Simulation Parameters</i> | 38 |
| CHAPTER 3 | 40 |
| 3.1 Optical Packets | 41 |
| 3.2 Performance Monitoring | 42 |
| 3.3 Multibit Delay DQPSK Demodulation | 43 |
| 3.4 DQPSK Optical Error Correction | 44 |
| 3.5 Optical Filtering & Free-Spectral-Range Optimization..... | 45 |
| CONCLUSION | 50 |
| REFERENCES | 52 |
| APPENDICES | 63 |

List of figures

| | |
|---|----|
| Figure 1. Properties of electromagnetic waves that can modulated to encode binary information on a CW lightwave to be transmitted in an optical telecommunication network. Most network currently use intensity modulation. DPSK uses the phase modulation to encode data..... | 3 |
| Figure 2. Difference between the absolute phase of a lightwave and the difference in phase between successive bits..... | 3 |
| Figure 3. Schematic of constant intensity DPSK known as non-return-to-zero (NRZ-) DPSK. | 6 |
| Figure 4. Schematic of pulse-carved DPSK known as return-to-zero (RZ-) DPSK. Typical pulse carving duty cycles of 33% (top) and 50% (bottom) are illustrated. RZ-DPSK is demodulated in the same manner as NRZ-DPSK..... | 7 |
| Figure 5. Schematic of pulse-carved DPSK known as return-to-zero (RZ-) with 67% duty cycles known as carrier-suppressed RZ- (CSRZ-) DPSK is demodulated in the same manner as NRZ-DPSK..... | 8 |
| Figure 6. Principle of operation for label encoding through bias modulation (a) and drive-voltage modulation (b). Empty (filled) circles illustrate payload modulation when label bit is a "1" ("0"). Diamonds mark the bias position..... | 19 |
| Figure 7. Simultaneous DPSK-payload/OOK-label encoding using a single MZM with label encoding through (a) bias modulation and (b) drive-voltage modulation..... | 20 |
| Figure 8. Partial-bit DLI for NRZ signals. A small fraction of the bit interferes with the following bit for pulse carving in the destructive port, resulting in a strong clock tone. There is little degradation at the constructive port due to the high FSR..... | 22 |
| Figure 9. Conceptual diagram of how the clock tone behaves after the constructive and destructive arm of the partial bit DLI under CD and PMD. The asymmetry in the behaviors allows the isolation of the two effects..... | 22 |
| Figure 10. Concept of $\frac{1}{4}$ -bit delay in the spectral domain. Most of the signal is notched out in the destructive port. The power ratio between the two arms is directly related to the OSNR..... | 25 |
| Figure 11. Spectral response (dash curve) of a 1-bit (left) and 2-bit (right) delay delay-line interferometer overlayed on a DPSK spectrum. The narrower spectrum increases frequency offset and laser linewidth sensitivity..... | 26 |
| Figure 12. The variable delay interferometer used for the experimental demonstration..... | 28 |
| Figure 13. Experimental setup to obtain receiver sensitivity and OSNR penalty measurements. Different bit delays are obtained through the variable delay interferometer while frequency offset penalty is obtained by tuning the tunable laser frequency..... | 28 |
| Figure 14. Conceptual diagram of multipath demodulation with majority vote error correction. The DPSK precoder uses a 4-bit delay. The optical logic is performed by the passive DLI DPSK demodulator. The electronic logic recovers the original signal before majority vote is applied..... | 30 |

| | |
|--|----|
| Figure 15. Experimental setup for the demonstration of multipath DPSK demodulation majority vote error correction. Using 3 commercial DLIs, three 10Gbps bit error rate tester and a 20Gs/s real time scope. Logic operations were processed offline. | 35 |
| Figure 16. DPSK spectrum with overlayed transfer functions for optical filtering and delay-line interferometer. Free-spectral-range larger than the bitrate and tighter optical filtering puts a greater emphasis on the optical duobinary (ODB) port (constructive) rather than the alternate-mark-inversion port (destructive). | 38 |
| Figure 17. Chromatic dispersion tolerances for RZ- and NRZ-, DPSK and DQPSK. The increase in chromatic dispersion when both optical filtering and FSR are optimized is greater percentage wise for the DPSK formats but roughly the same in absolute values. | 48 |
| Figure 18. Required values of optical filtering (OF) and free spectral range (FSR) normalized over baudrate for RZ- and NRZ- DPSK and DQPSK for optimized Q factor (when both OF and FSR are optimized simultaneously). | 49 |

List of symbols and abbreviations

| Symbol or abbreviation | Description |
|---------------------------|--|
| ASE | Amplified spontaneous emission |
| BER | Bit-error ratio |
| BW | Bandwidth |
| CD | Chromatic dispersion |
| dB | Decibel |
| DC | Direct current |
| DFE | Decision feedback equalization |
| DLI | Delay line interferometer |
| DM | Dispersion managed |
| DP | Differential precoding |
| DPSK | Differential phase shift keying |
| DQPSK | Differential quadrature phase shift keying |
| EDFA | Erbium doped fiber amplifier |
| EFEC | Enhanced forward error correction |
| ERFC | Complementary error function |
| ERFC ⁻¹ | Inverse complementary error function |
| FBG | Fiber bragg grating |
| FEC | Forward error correction |

| Symbol or abbreviation | Description |
|---------------------------|--|
| FFE | Feed forward equalization |
| FO | Frequency offset |
| FSR | Free spectral range |
| FWHM | Full width half maximum |
| IM | Intensity modulation |
| LW | Linewidth |
| MLSE | Maximum likelihood sequence estimation |
| MZI | Mach Zehnder interferometer |
| MZM | Mach Zehnder modulator |
| NRZ | Non-return-to-zero |
| OBS | Optical burst switching |
| ODB | Optical duobinary |
| OF | Optical filter |
| OOK | On-off keying |
| OPS | Optical packet switching |
| OSNR | Optical signal to noise ratio |
| OTDM | Optical time domain multiplexing |
| PMD | Polarization mode dispersion |
| PSK | Phase shift keying |
| RF | Radio frequency |
| RZ | Return-to-zero |

| Symbol or abbreviation | Description |
|-----------------------------------|----------------------------------|
| TF | Transfer function |
| TX | Transmitter |
| WDM | Wavelength division multiplexing |
| XOR | Exclusive OR |

List of Appendices

| | | |
|-------------|--|----|
| Appendix 1. | Single Modulator Payload/Label Encoding and Node Operations for Optical Label Switching..... | 64 |
| Appendix 2. | Independent and Simultaneous Monitoring of Chromatic and Polarization-Mode Dispersion in OOK and DPSK Transmission..... | 68 |
| Appendix 3. | Tolerances and Receiver Sensitivity Penalties of Multibit Delay Differential-Phase Shift-Keying Demodulation..... | 72 |
| Appendix 4. | Combination of optical and electronic logic gates for error correction in multipath differential demodulation..... | 76 |
| Appendix 5. | Free spectral range optimization of return-tozero differential phase shift keyed demodulation in the presence of chromatic dispersion..... | 86 |
| Appendix 6. | Chromatic dispersion tolerance in optimized NRZ-, RZ- and CSRZ-DPSK demodulation..... | 93 |

Introduction

Communication systems have developed at an incredible rate in the last 20 years. From links operating at kilobits per second to megabits, new systems have demonstrated the capacity to transmit information at gigabits and even terabits per second. Fibre-optic communication systems transmit information from one location to another by sending modulated light through an optical fibre cable. First developed in the 1970s, fibre-optic communication systems have revolutionized the telecommunications industry and played a major role in the advent of the information age. Because of its advantages over electrical and wireless transmission with respect to signal loss and interference, bandwidth and transmission distance, the use of optical fibre has replaced copper wire communications for undersea, long-haul and short haul communication. It is now even largely replacing copper wires for metro and office to office communication. The latest deployments even bring the optical fibre directly to subscribers' houses for high bandwidth applications.

When encoding information on an electromagnetic wave such as infrared light, any of the physical properties can be modulated. Light has a frequency, intensity, polarization and phase as illustrated in Figure 1. Until recently, optical communication systems strictly employed conventional intensity modulation (IM) signals in either non return-to-zero (NRZ) or return-to-zero (RZ) format. But a number of advanced optical modulation formats have attracted increasing attention in the last few years[1-3].

Some of these formats carry information through intensity modulation while additionally modulating the optical phase which has been shown to increase transmission robustness to chromatic dispersion, optical filtering and nonlinearities. Examples such as duobinary, alternate mark inversion (AMI), chirped return-to-zero (CRZ), and alternating-phase (AP) IM such as carrier-suppressed return-to-zero (CSRZ) are some of these formats. In contrast, phase-shift-keyed (PSK) formats carry the information in the optical phase itself. Since absolute phase is not easily detected through coherent demodulation [4], differential encoding is often used such that the phase of the preceding bit is used as a relative phase reference for demodulation. This is defined as differential-phase-shift-keyed (DPSK), a format carrying the information on the *change* in optical phase between successive bits as illustrated in Figure 2. DPSK is easily demodulated in a Mach Zehnder interferometer [5, 6] which allows for balanced detection of the signal using the difference in photocurrent between the detected constructive and destructive arm of the interferometer. Balanced detection lowers by 3dB the required optical signal-to-noise ratio (OSNR) for a given bit-error ratio (BER). DPSK has also been shown to be more robust to certain nonlinear effects [7] and coherent crosstalk [8]. Over the last few years, innovations such as forward-error correction (FEC), distributed Raman amplification, new transmission fibres including dispersion-managed (DM) fibres, and advanced optical modulation formats, have allowed wavelength-division-multiplexed (WDM) transmission systems to reach record capacities and distances. Many capacity and distance records at rates of 10 and 40 Gb/s per channel in the last few years used DPSK transmission [9-19].

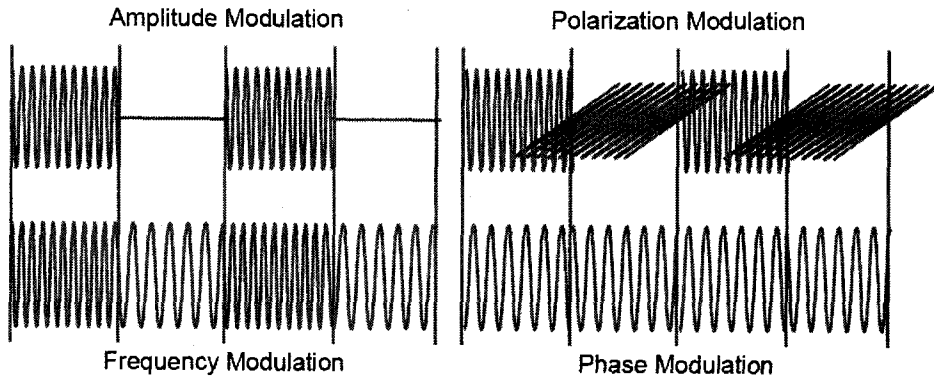


FIGURE 1. PROPERTIES OF ELECTROMAGNETIC WAVES THAT CAN MODULATED TO ENCODE BINARY INFORMATION ON A CW LIGHTWAVE TO BE TRANSMITTED IN AN OPTICAL TELECOMMUNICATION NETWORK. MOST NETWORK CURRENTLY USE INTENSITY MODULATION. DPSK USES THE PHASE MODULATION TO ENCODE DATA.

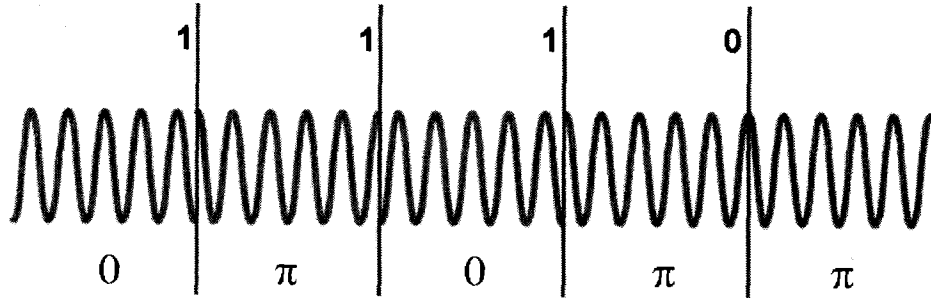


FIGURE 2. DIFFERENCE BETWEEN THE ABSOLUTE PHASE OF A LIGHTWAVE AND THE DIFFERENCE IN PHASE BETWEEN SUCCESSIVE BITS.

Interestingly enough optical DPSK-based telecommunication systems are not new. The format was studied in the 1980s for coherent fibre-optic systems and free-space optical transmission [4, 20-23]. But with the development of erbium-doped fibre amplifiers (EDFAs) interest in DPSK faded. For about a decade, intensity modulated WDM systems using EDFAs dominated long-haul optical communications. As WDM systems were pushed to ever-higher levels of performance, interest in DPSK re-emerged.

The goal of this thesis is to investigate the DPSK modulation format in fibre optic communications systems. The objective is to further the understanding on this modulation format and its application to fibre optics transmission to enable novel ways to utilize DPSK in optical telecommunication networks.

This thesis by articles is composed of six papers looking at *generation*, *transmission* and *demodulation* of DPSK. We propose a novel way to encode optical packets using DPSK in our investigation of the generation. We then investigate transmission effects monitoring using a novel partial-bit delay interferometer-assisted clock tone monitoring method for sensitive optical-signal-to-noise ratio (OSNR), chromatic dispersion (CD) and polarization mode dispersion (PMD) monitoring. Then we look at the demodulation of DPSK and investigate the reduced tolerances and power penalties of DPSK demodulation when more than one bit delay is used in the interferometer. We also propose an optical error correction method combining DPSK optical logic gates with electronic logic gates to improve receiver sensitivity and chromatic dispersion tolerances. Finally, we investigate the important effect of the optimization of the free-spectral range of the delay-line interferometer to improve chromatic dispersion tolerances.

Chapter 1

Literature Review

In differential phase shift keying, the information is not encoded directly on the phase of the lightwave but rather on the difference in phase between successive bits. As such DPSK is easily demodulated in a Mach-Zehnder interferometer using a one-bit delay in one arm. The demodulation allows for balanced detection since the constructive port and destructive port have complementary intensity modulated signals and balanced detection improves the receiver sensitivity or optical signal-to-noise ratio (OSNR) tolerances for a given bit-error ratio (BER) by 3dB. DPSK has also been shown to be more robust to certain nonlinear effects in [7] and coherent crosstalk [8]. There are different flavours of DPSK depending if pulse carving is used or not and on the duty cycle of the pulse carving. Constant intensity DPSK is referred to as non-return-to-zero (NRZ-) DPSK as shown in Figure 3.

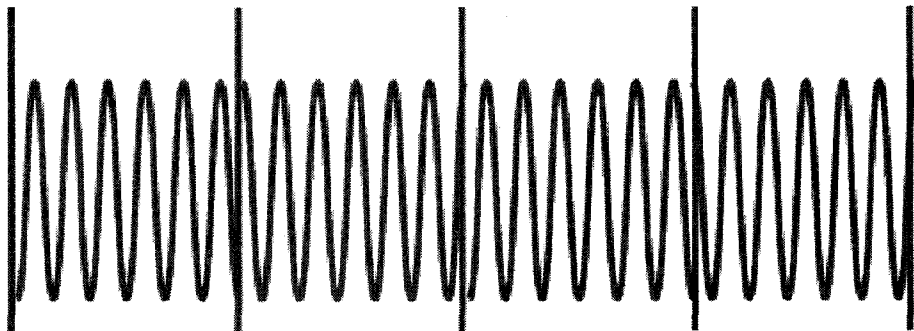


FIGURE 3. SCHEMATIC OF CONSTANT INTENSITY DPSK KNOWN AS NON-RETURN-TO-ZERO (NRZ-) DPSK.

Other flavours of binary DPSK use pulse carving of each bit to effectively increase tolerances to certain transmission effects such as polarization mode dispersion. Pulse-carved DPSK are known as return-to-zero (RZ-)DPSK and are defined by the duty cycle of the pulse carving. Typical pulse carving are 33% RZ-DPSK and 50% RZ-DPSK as illustrated in Figure 4. A third flavour is 67% RZ-DPSK also known as carrier-suppressed RZ- (CSRZ-) DPSK shown in Figure 5. All the different flavours of DPSK are demodulated in the same fashion in a delay-line interferometer. In the six papers of this thesis, we investigate the *generation*, *transmission* and *demodulation* of different flavours of DPSK. We present in this chapter the literature review for the different topics. In our investigation of DPSK *generation* we discuss in section 1.1 the literature on optical packet encoding related to our method of using orthogonal and simultaneous modulation of DPSK and intensity modulation for payload and label encoding respectively in a single modulator. We investigate real-time monitoring of *transmission* effects in an optical transmission link with an overview of the literature in section 1.2 related to our partial-bit delay interferometer-assisted clock tone

monitoring method for optical-signal-to-noise ratio (OSNR), chromatic dispersion and polarization mode dispersion monitoring. We discuss in section 1.3 the literature on the *demodulation* of DPSK starting with multibit delay demodulation. The literature on the novel field of optical error correction methods combining DPSK optical logic gates is discussed in section 1.4. Finally free-spectral range and optical filtering optimization method to increase chromatic dispersion and optical filtering tolerances are discussed in section 1.5.

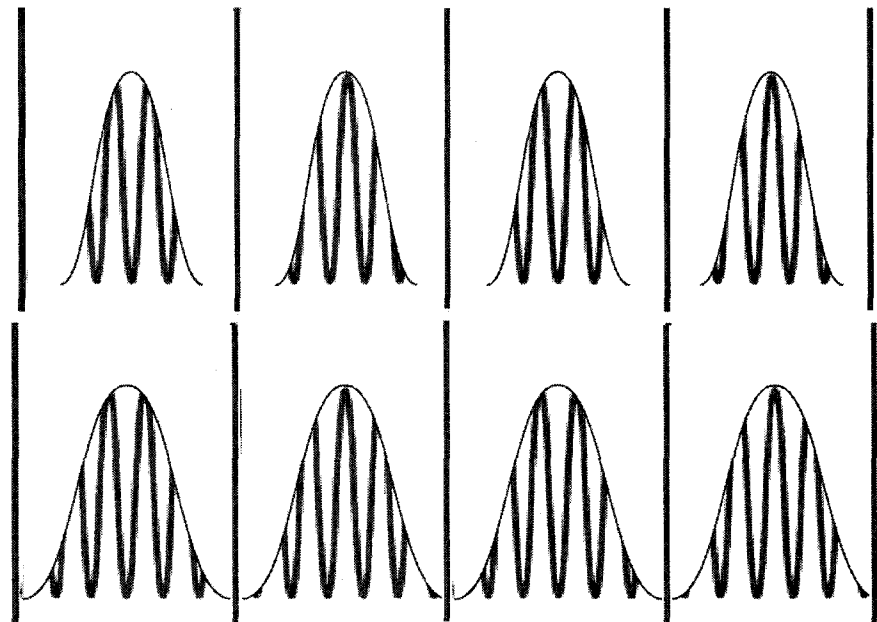


FIGURE 4. SCHEMATIC OF PULSE-CARVED DPSK KNOWN AS RETURN-TO-ZERO (RZ)-DPSK. TYPICAL PULSE CARVING DUTY CYCLES OF 33% (TOP) AND 50% (BOTTOM) ARE ILLUSTRATED. RZ-DPSK IS DEMODULATED IN THE SAME MANNER AS NRZ-DPSK.

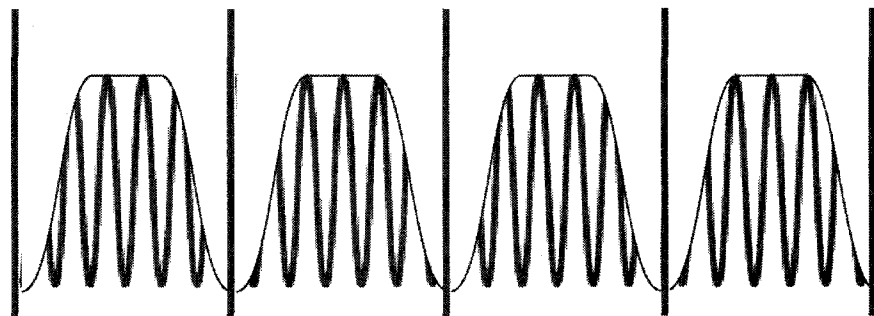


FIGURE 5. SCHEMATIC OF PULSE-CARVED DPSK KNOWN AS RETURN-TO-ZERO (RZ-) WITH 67% DUTY CYCLES KNOWN AS CARRIER-SUPPRESSED RZ- (CSRZ-) DPSK IS DEMODULATED IN THE SAME MANNER AS NRZ-DPSK.

1.1 OPTICAL LABEL ENCODING:

While the scalability of optical networks will become critical to meet the ever increasing demand for bandwidth for telecom applications, existing electronic technologies have bandwidth limitations with respect to processing and routing. Currently, an opto-electronic layer transmits optical data between nodes on the network by optical-electronic-optical (OEO) conversion, i.e. converting optical signals to electrical signals for processing and back again to optical for transmission. Although this has enabled great increases in the data carrying capacity of networks, the scalability of electronic processing and routing technology is lagging behind optics. Ultimately the amount of packet traffic that can be efficiently switched in networks will be restrained. Therefore, in order for networks of the future to take full advantage of the capacity offered by optical networking, the conversion of optical to electrical signals for packet routing must be minimized.

Optical packet switching (OPS) is regarded as next-generation transport

technologies that enable more efficient and flexible utilization of the capacity of optical networks [24]. One optically labeled packet transmission based on orthogonal intensity modulation/ differential phase shift keying (IM/DPSK) modulation format, in which the payload is intensity modulated while the label is carried by DPSK, has been proposed and demonstrated[25-28]. Another scheme utilizes frequency shift keying for the label, and intensity modulation for the payload [29]. Sub-carrier modulation and polarization shift keying [30-34] have also been demonstrated for label modulation. More recently, it was established that using DPSK/IM for payload/label modulation and using a balanced receiver for DPSK detection provides superior receiver sensitivity of around -36 dBm for both the label and payload at a bit error ratio (BER) of 10^{-9} [35-37]. In most optical label encoding schemes, two optical modulators are required, one for encoding the payload and the other for the label. A method for encoding both label and payload using a single modulator with good receiver sensitivity would be quite advantageous in a network. In the first article of this thesis, we demonstrate two novel payload and label encoding techniques based on a single Mach-Zehnder modulator (MZM) for DPSK/IM payload/label modulation. The methods provide superior receiver sensitivity with the advantage of using a single modulator for simultaneous payload and label encoding.

1.2 OPTICAL PERFORMANCE MONITORING

Optical performance monitoring has the potential to enable highly robust, stable, and scalable future optical networks. As such, there has been several methods reported

in the literature to achieve efficient monitoring of either Optical-Signal-to-Noise-Ratio (OSNR) [38-47], Chromatic Dispersion (CD) [48-62], or Polarization mode dispersion [63, 64]. Effective deterioration monitoring has the following characteristics:

(a) isolated monitoring of the specific impairment that is degrading the data signal in order to help with network diagnosis and adaptation; (b) minimized number of optical elements in order for the monitoring to be simple and cost-effective; and (c) different degrading effects simultaneously, such as CD, PMD, and OSNR. Despite the extensive amount of publications on optical performance, there has been little attention given to a method capable of combining all of the above advantages. Some methods may be susceptible to CD, PMD and/or OSNR and are limited to one modulation format. Other methods did present results monitoring two effects simultaneously [65-70] but a significant step forward would be a monitoring solution that simultaneously and independently monitors CD, PMD and OSNR using a single device and that for several modulation formats [71].

One simple and cost-effective approach for performance monitoring is to measure the RF power in the clock tone using a narrowband electrical filter and a power meter. This method can be used to track accumulation of either CD or PMD [52, 54, 64, 72, 73]. Unfortunately, it does not easily allow for isolated and simultaneous monitoring given that both effects will influence the clock tone power. Also, the intensity of the clock tone is OSNR dependent making it difficult to evaluate which of the three impairments is responsible for the variation in the clock tone power.

In the second article of this thesis, We propose and demonstrate numerically and

experimentally a $\frac{1}{4}$ -bit delay Mach-Zehnder interferometer (MZI)-assisted simultaneous and independent CD, PMD and OSNR monitoring method for NRZ-OOK, NRZ-DPSK and Duobinary modulation formats. The OSNR monitoring method can be extended to other modulation formats such as RZ-DPSK and RZ-OOK. By combining the $\frac{1}{4}$ -bit delay MZI methods, simultaneous, independent and sensitive monitoring of OSNR, CD and PMD can be performed with no degradation to the transmitted signal. The method is discussed in chapter 2.2.

1.3 MULTIBIT DELAY DPSK DEMODULATION

There has been much recent interest in the concept of modified DLIs with multi-bit-delay in one arm, demodulating the differential phase between two successive data bits that are a fixed number, d , of bit time slots apart. DPSK receivers equipped with such a function are used in different applications, for example, when demodulating data streams using polarization interleaving where the polarization of successive bits is orthogonal [74, 75]. This method has been shown to mitigate certain nonlinear effects but it entails using a demodulator with 2 bit delay such that bits with the same polarization are interfered together. Another example is in the demodulation of optical time-division-multiplexed (OTDM) data stream, such that each data bit is compared to a previous bit from the same transmitter [76]. This is also important in laboratory experiments when using a single transmitter, where the OTDM multiplexer does not provide phase stability. Lastly, multibit demodulation is very useful when using a DPSK receiver made of several DLIs in parallel each of a different bit delay, with the

DLI outputs all combined using post-processing, to achieve higher receiver sensitivity [77, 78]. Although DPSK demodulation has been extensively investigated, there has been little discussion on the actual system penalty incurred by multi-bit delay demodulation, mostly because such applications are quite recent.

In the third paper of this thesis we present experimental results, as well as numerical and analytic analysis of the penalties associated with multi-bit DPSK demodulation due to Frequency Offset (FO), laser linewidth and the bit delay offset. Simulation results along with a simple analytic model indicate that the OSNR penalty associated with detection through multi-bit delay scales as 0.2-0.35 dB per integer bit delay at 10Gb/s with a 10 MHz linewidth. As expected we find that the FO tolerance scales as the inverse of the bit delay. Furthermore the bit delay mismatch penalty increases for two-bit delay demodulation, but no further degradation occurs for longer delays. These key limitations may reduce the effectiveness of multi-bit delay methods in some applications.

1.4 OPTICAL ERROR CORRECTION

DPSK is currently being deployed as a data-modulation format for high-capacity and undersea optical communication systems mainly due to its 3 dB OSNR advantage over intensity modulation and its nonlinear tolerance [2, 3, 7, 8, 79]. However DPSK OSNR requirements are still 1.2 dB higher than for its coherent counterpart, PSK for a BER of 10^{-3} . Multi-symbol processing strategies have been proposed to reduce this penalty through soft detection, including decision feedback based techniques [77, 78],

80, 81], providing $\sim 1\text{-}3$ dB sensitivity improvements for DPSK optical transmission. However the analog or high-speed digital soft detection feedback electronics remain challenging to implement. It would be advantageous to attain comparable processing gains over multiple demodulation paths with hard detection rather than soft detection, i.e. by applying digital logic processing on the balanced outputs of multiple Mach-Zehnder interferometers. Forward error correction (FEC) is now commonly used in most types of long-haul transmission systems. With only a 7% overhead, enhanced FEC (eFEC) can convert a 2×10^{-3} error to 1×10^{-15} while Super FEC with a 25% overhead, can correct errors from as low as 6×10^{-3} [82]. When error rates exceed those values, FEC becomes somewhat inefficient. It would be useful to have an error correction algorithm that could take a poor error rate and bring it to a FEC-capable error rate without affecting the effective bandwidth of the transmission.

In the fourth article of this thesis, we propose and demonstrate experimentally and numerically an optical multi-path error correction technique for differentially encoded modulation formats. The scheme can be readily implemented using commercially available interferometers [79] and high-speed logic gates. After optical demodulation and hard detection, basic logic operations are applied on each path to recover the data signal. The partially correlated errors induced by ASE noise are then corrected using a simple majority-vote algorithm [83]. We find through numerical simulations that back-to-back DPSK receiver sensitivity is improved by 0.35 dB at BER of 10^{-3} with optimal filtering and 0.45dB in a 25GHz channel. In chromatic dispersion (CD) limited channels such as in fibre optic transmission, we numerically obtain a 1.6 dB

improvement and the tolerance to CD is increased by 25% from ± 1220 ps/nm to ± 1520 ps/nm. Experimentally we measured a 1.5 dB sensitivity improvement. The main advantage of the proposed method is that it does not require any data overhead and hence its performance improvement is attained without affecting the effective bandwidth of the transmitted data. This diversity demodulation scheme is compatible with and complementary to error correction techniques commonly used in optical transmission systems such as forward-error-correction (FEC). Since the error correction is obtained through hard detection, it is also compatible with soft electronic distortion compensation schemes such as feed forward equalization (FFE), decision feedback equalization (DFE), and maximum likelihood sequence estimation (MLSE) [84-86]. The scheme is differentiated from those presented in references [77, 78, 80, 81] in that it is a hard detection scheme and could therefore be combined with the other soft detection multipath-methods. Furthermore, we demonstrate in our work an experimental and numerical demonstration at 10 Gbps whereas references [77, 78, 80, 81] were numerical demonstrations.

1.5 FSR OPTIMIZATION:

In back-to-back configuration, the most efficient DLI for DPSK demodulation has a complete one-bit delay such that the phases of two adjacent bits are compared during the entire bit time for maximum eye opening. It has been shown that DLI degradations such as bit delay mismatch and frequency offset [87-89], transmission impairments such as chromatic dispersion (CD), polarization-mode-dispersion (PMD), and

nonlinearities [90-92] or the combination of DLI degradations and transmission impairments [93] can distort the phase of the DPSK signal and reduce receiver sensitivity. It was recently shown that free-spectral-range (FSR) optimization can increase optical filtering (OF) and CD tolerance for RZ-and NRZ-DPSK [94-97]. However, the full potential of optimized FSR DPSK systems has yet to be explored.

In the last two articles of this thesis, we first report results of FSR optimization for RZ-DPSK and then present a comprehensive numerical analysis of the parameter space of OF bandwidth and FSR for the NRZ-, RZ- and CSRZ-DPSK formats, establishing that concurrent FSR and OF optimization significantly improves CD tolerances. The impact of transmitter bandwidth on the optimized demodulation parameters mentioned in [94-96] is further investigated. Finally, OF and FSR optimization are applied to design high bitrate DPSK systems with increased DWDM channel density.

Chapter 2

Synthesis of Work

Radio-frequency DPSK has been around for many years and today is used in many communications protocols such as WiFi networks [98] and Bluetooth wireless communication [99]. But even *optical* DPSK networks are not a new concept; the format was studied in the 1980s for coherent fibre-optic systems and free-space optical transmission [4, 20-23]. However, with the development of erbium-doped fibre amplifiers (EDFAs) and the advent of wavelength division multiplexing (WDM), interest in DPSK systems faded. For about 20 years, intensity modulated WDM systems using EDFAs have dominated optical fibre communications. Today, as systems are pushed to ever-higher levels of performance and required bandwidth, there is a renewed interest in this efficient and robust modulation format.

The goal of this thesis is to investigate the DPSK modulation format from its generation, its transmission to its demodulation in fibre optic communications systems. The objective of the thesis is to further the understanding of this modulation format and its application to fibre optics transmission. This understanding enables novel ways to utilize DPSK in optical telecommunication networks in order to enhance the

performance.

This thesis by article is composed of six papers looking at the *generation, transmission* and *demodulation* of DPSK. We propose a novel method to encode optical packets using DPSK in our investigation of the generation in section 2.1. We also investigate transmission effects monitoring using a new partial-bit delay interferometer-assisted clock tone monitoring method for sensitive optical-signal-to-noise ratio (OSNR), chromatic dispersion (CD) and polarization mode dispersion (PMD) monitoring in section 2.2. Then we look at the demodulation of DPSK from multibit demodulation standpoint in section 2.3. We also propose an optical error correction method combining DPSK optical logic gates with electronic logic gates to improve receiver sensitivity and transmission impairments in section 2.4. Finally we redefine the previously assumed chromatic dispersion tolerances of NRZ-DPSK, RZ-DPSK and CSRZ-DPSK with optimized demodulation parameters of optical filtering and free-spectral range optimization in section 2.5.

2.1 OPTICAL LABEL SWITCHING

As discussed in chapter 1.1, it was established that using DPSK and intensity modulation (IM) for payload/label modulation and using a balanced receiver for DPSK detection provides superior receiver sensitivity of around -36 dBm for both the label and payload at a bit error ratio (BER) of 10^{-9} [35-37]. Unfortunately, most optical label encoding schemes require two optical modulators, one for encoding the payload and

the other for the label which can potentially be impractical in cost-conscious OPS network. Our method for encoding both label and payload uses a single modulator with good receiver sensitivity. We present two different methods for encoding both label and payload using a single Mach-Zehnder modulator (MZM) for DPSK/IM payload/label modulation.

The output optical field of a Mach-Zehnder modulator (MZM) biased at extinction can be expressed as

$$(2.1.1) \quad E_{\text{out}}(t) = E_{\text{in}} \frac{(e^{j\varphi_{\text{upper}}(t)} - e^{-j\varphi_{\text{lower}}(t)})}{2}$$

where E_{in} and E_{out} are the input and output optical fields, respectively, φ_{upper} and φ_{lower} are induced phase changes in the upper and lower arms of the MZM by applied voltages. With balanced driving, we have $\varphi_{\text{upper}}(t) = -\varphi_{\text{lower}}(t) = \varphi(t)$ and

$$(2.1.2) \quad \varphi(t) = \frac{\pi}{V_{\pi}} [V_p D_p(t) + \Delta V_{\text{bias}}]$$

where V_p is the amplitude of the data modulation, $D_p(t) = \pm 0.5$ is the ac-coupled payload modulation index, and ΔV_{bias} is the bias voltage offset from the extinction point.

A nonreturn-to-zero signal is generated with $V_p = \Delta V_{\text{bias}} = 0.5V_{\pi}$ and an ideal DPSK signal is generated with $V_p = V_{\pi}$ and $\Delta V_{\text{bias}} = 0$. One advantageous feature of DPSK generation is that even when the MZM is not fully driven or not perfectly biased, exact phase encoding can still be achieved over the center portion of each bit period. This feature is exploited to modulate the amplitude of a high-speed DPSK payload signal for

label encoding [100] as illustrated in Figure 6. In the first single MZM label/payload encoding scheme, the RF port of the MZM is used to encode the DPSK payload while the label is encoded by modulating the bias port between the null point and a small fraction of V_π . The phase modulation can be expressed as

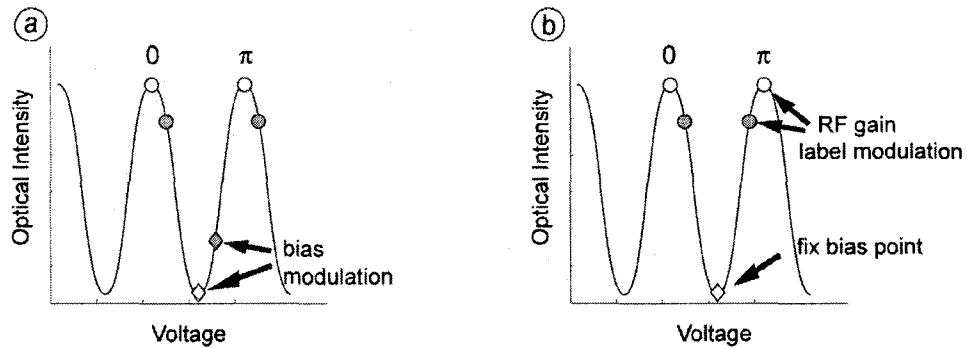


FIGURE 6. PRINCIPLE OF OPERATION FOR LABEL ENCODING THROUGH BIAS MODULATION (A) AND DRIVE-VOLTAGE MODULATION (B). EMPTY (FILLED) CIRCLES ILLUSTRATE PAYLOAD MODULATION WHEN LABEL BIT IS A “1” (“0”). DIAMONDS MARK THE BIAS POSITION.

$$(2.1.3) \quad \varphi(t) = \frac{\pi}{V_\pi} [V_p D_p(t) + V_l D_l(t) + \Delta V_{\text{bias}}]$$

where V_l is the amplitude of the label modulation and $D_l(t) = \pm 0.5$ is the label data. In the second method of encoding the label, the drive voltage output of the RF driver is modulated between V_p and $(V_p - V_l)$ by the label data. Preferably $V_p = V_\pi$. The phase modulation can be expressed as

$$(2.1.4) \quad \varphi(t) = \frac{\pi}{V_\pi} V_p D_p \left[1 - \frac{V_1}{V_p} (0.5 - D_1) \right]$$

The implementation of bias and RF voltage modulation is illustrated in Figure 7.

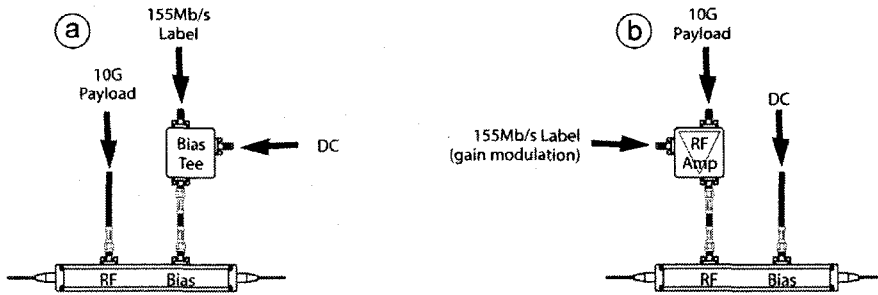


FIGURE 7. SIMULTANEOUS DPSK-PAYLOAD/OOK-LABEL ENCODING USING A SINGLE MZM WITH LABEL ENCODING THROUGH (A) BIAS MODULATION AND (B) DRIVE-VOLTAGE MODULATION.

2.2 OPTICAL PERFORMANCE MONITORING

Optical performance monitoring may be necessary for future scalable optical networks. As such, there have been several methods reported in the literature to achieve efficient monitoring of either Optical-Signal-to-Noise-Ratio (OSNR), Chromatic Dispersion (CD) or Polarization Mode Dispersion (PMD). One simple and cost-effective approach for performance monitoring is to measure the RF power in the clock tone using a narrowband electrical filter and a power meter. This method can be used to track accumulation of either CD or PMD. Unfortunately, it does not easily allow for isolated and simultaneous monitoring given that both effects will influence the clock tone power. Also, the intensity of the clock tone is OSNR dependent making

it difficult to evaluate which of the three impairments is responsible for the variation in the clock tone power. Our method uses a $\frac{1}{4}$ -bit delay Mach-Zehnder interferometer (MZI) to simultaneously and independently monitor CD, PMD with differential RF clock tone detection, and OSNR with DC power detection for the NRZ-OOK, NRZ-DPSK and Optical Duobinary modulation formats. The OSNR monitoring method can also be used with other pulse-carved modulation formats such as RZ-DPSK and RZ-OOK.

We use a DLI from ITF Laboratories [79, 101] but with a $\frac{1}{4}$ -bit-time delay in one arm without any modifications to the transmitter. The transmission peak of the interferometer is biased at maximum/minimum power in the constructive/deconstructive arm, and both DLI outputs are utilized in the monitoring process. As illustrated in Figure 8, the response in the constructive port is essentially transparent to the signal due to the high free-spectral range (FSR) (4x the data rate). The destructive output of the DLI is a return-to-zero (RZ) signal with a strong RF clock tone present. Inside the DLI, the signal interferes with itself for a $\frac{1}{4}$ of the bit period and interferes with the phase of the following bit for the other $\frac{1}{4}$ of the bit period, resulting in RZ pulses. The $\frac{1}{4}$ -bit-time value was chosen as a reasonable tradeoff between constructive port penalty for data detection and destructive port pulse-carving for monitoring. The 10-G clock tones on the two outputs of the $\frac{1}{4}$ -bit-delay DLI are dependent on dispersion and PMD as conceptualized in Figure 9. The increase in clock tone power with increasing CD at the constructive port is well known for NRZ [52]. At the destructive port, CD spreads the input pulses in time, thereby

lowering the peak power in the output RZ pulses and therefore the clock tone power. The dephasing effect of PMD on the clock tone reduces its intensity [102]. Utilization of this feature allows isolation and simultaneous measurement of CD and PMD. The monitoring can be loosely conceptualized by the two functions

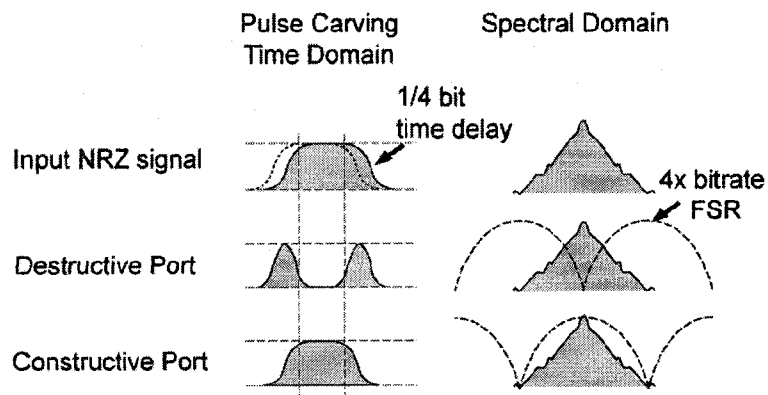


FIGURE 8. PARTIAL-BIT DLI FOR NRZ SIGNALS. A SMALL FRACTION OF THE BIT INTERFERES WITH THE FOLLOWING BIT FOR PULSE CARVING IN THE DESTRUCTIVE PORT, RESULTING IN A STRONG CLOCK TONE. THERE IS LITTLE DEGRADATION AT THE CONSTRUCTIVE PORT DUE TO THE HIGH FSR.

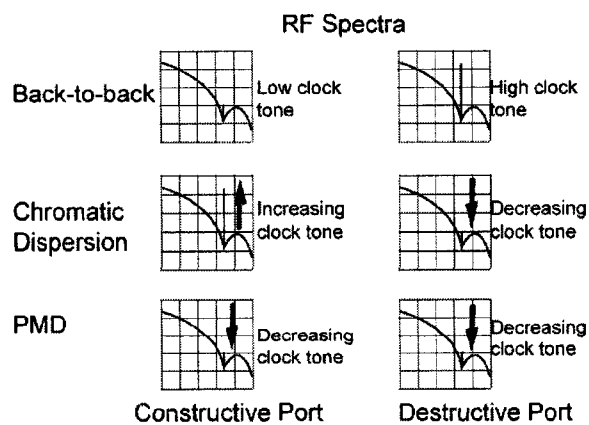


FIGURE 9. CONCEPTUAL DIAGRAM OF HOW THE CLOCK TONE BEHAVES AFTER THE CONSTRUCTIVE AND DESTRUCTIVE ARM OF THE PARTIAL BIT DLI UNDER CD AND

PMD. THE ASYMMETRY IN THE BEHAVIORS ALLOWS THE ISOLATION OF THE TWO EFFECTS.

$$(2.2.1) \quad f(CD) \Rightarrow P_{\text{const}}(\uparrow CD, \downarrow PMD) - P_{\text{dest}}(\downarrow CD, \downarrow PMD)$$

$$(2.2.2) \quad f(PMD) \Rightarrow P_{\text{const}}(\uparrow CD, \downarrow PMD) + P_{\text{dest}}(\downarrow CD, \downarrow PMD)$$

where P_{const} is the clock tone power at the constructive arm which grows with CD and decreases with PMD. P_{dest} is the clock tone power at the destructive arm which decreases with both CD and PMD. The inverse relationship allows for removal of the PMD in the subtraction and CD in the addition, thereby isolating both effects. This also has the added property of increasing the sensitivity of the CD measurement. Unfortunately this method is not appropriate for RZ-type formats since they already have strong clock tone power and do not benefit from the partial bit delay clock-tone generating DLI.

Unfortunately the CD and PMD monitoring is OSNR dependent. OSNR degradation reduces clock tone power similar to the effect of PMD on clock tone power. Hence the effect of PMD and OSNR cannot be differentiated in clock tone monitoring which could greatly reduce the usefulness if we did not have an independent OSNR monitoring method which would differentiate the contributions of PMD and OSNR on clock fading.

Monitoring methods using a delayline interferometer with a different delay have

been proposed for OSNR monitoring [40] and CD monitoring [103]. Using a $\frac{1}{4}$ bit delay interferometer to monitoring OSNR has 2 main advantages: i) it can be integrated with the CD and PMD monitoring in the electrical domain without requiring any extra optical devices, ii) it does not deteriorate the signal which passes through the interferometer unaffected.

In our $\frac{1}{4}$ -bit delay OSNR method, one output port gives constructive (P_{const}) while the other port provides destructive interference (P_{dest}). With increasing amplified spontaneous emission (ASE) noise power (i.e., decreasing OSNR) P_{dest} increases relative to P_{const} because of the random phase of the noise. The ratio of $P_{\text{const}}/P_{\text{dest}}$ can be roughly approximated as: $\text{Ratio} = (\frac{1}{4} P_{\text{signal}} + \frac{1}{2} \text{ASE}) / (\frac{1}{4} P_{\text{signal}} + \frac{1}{2} \text{ASE})$ and the OSNR is proportional to this ratio of $P_{\text{const}}/P_{\text{dest}}$. Since the phase relationship between successive bits is not important for monitoring, the method is applicable to multiple modulation formats. This principle can also be explained in the spectral domain as illustrated in Figure 10. Since a $\frac{1}{4}$ -bit delay MZI has a free spectral range (FSR) equal to 4 times the bit rate, most of the signal power goes to the constructive port. The noise then evenly distributes between the two ports. One advantage of our method is that the signal is not degraded at the constructive port as was demonstrated in [67]. The data signal can be normally detected in the constructive port and P_{const} can be calculated from the signal RF power. A low-cost photodiode can be used to measure P_{dest} in the destructive port.

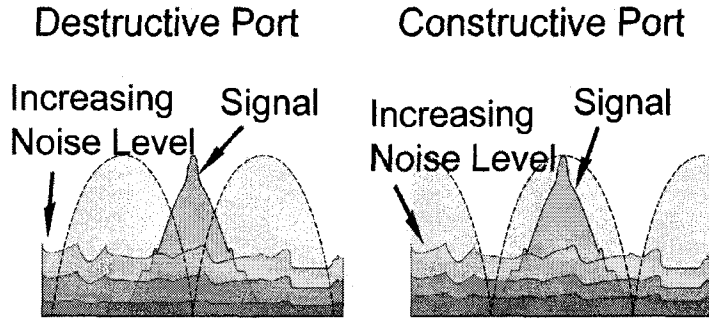


FIGURE 10. CONCEPT OF $\frac{1}{4}$ -BIT DELAY IN THE SPECTRAL DOMAIN. MOST OF THE SIGNAL IS NOTCHED OUT IN THE DESTRUCTIVE PORT. THE POWER RATIO BETWEEN THE TWO ARMS IS DIRECTLY RELATED TO THE OSNR.

The interferometer-assisted clock tone monitoring OSNR sensitivity can be eliminated in post-processing through multiplication with a fit factor corresponding to the measured OSNR value using the power ratio of P_{const} and P_{dest} . Therefore, OSNR, CD and PMD can be inferred simultaneously and independently. More details on the method are provided in chapter 3.2.

2.3 MULTIBIT DELAY DPSK DEMODULATION

Despite much interest in the concept of multi-bit-delay DPSK demodulation, there has been little discussion on the actual system penalty incurred by multi-bit delay demodulation. We present experimental results as well as numerical and analytic analysis of the penalties associated with multi-bit DPSK demodulation due to Frequency Offset (FO) between the transmitted laser and the DLI transmission peak, transmission laser linewidth (LW) and the offset between the transmitted bit length and the DLI bit delay and show that key limitations may reduce the effectiveness of

multi-bit delay methods in some applications.

The concept of multibit-delay is associated in spectral domain to a reduction in FSR of the demodulator as illustrated in Figure 11. Over a realistic fibre optic link it has been shown that the total linear and non-linear phase-noise has a nearly Gaussian distribution[104]. Extending the Gaussian approximation to laser-induced phase-noise[105], a simple analytic model is derived for multi-level DPSK detection, with Q-factor calculated from total demodulated Gaussian noise given by

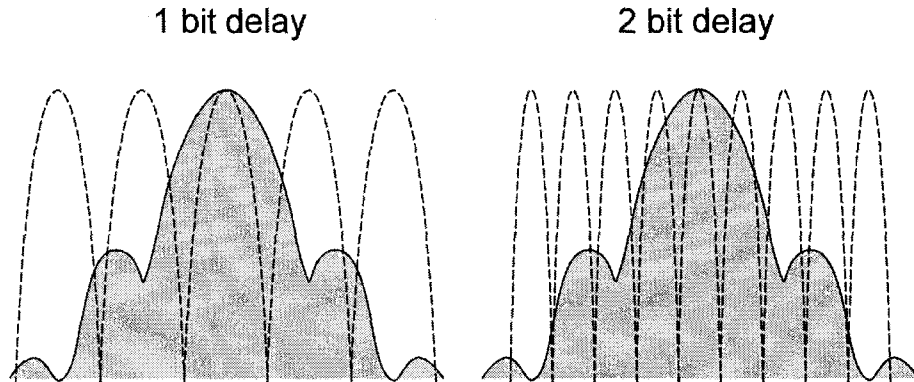


FIGURE 11. SPECTRAL RESPONSE (DASH CURVE) OF A 1-BIT (LEFT) AND 2-BIT (RIGHT) DELAY DELAY-LINE INTERFEROMETER OVERLAYED ON A DPSK SPECTRUM. THE NARROWER SPECTRUM INCREASES FREQUENCY OFFSET AND LASER LINewidth SENSITIVITY.

$$(2.4.1) \quad Q^2 = (\pi / M - \gamma)^2 / (\sigma_{LN+NL}^2 + \sigma_{LPN}^2)$$

where $\gamma \equiv 2\pi\Delta\nu_c Td$ is the phase-offset between the two DLI arms, with $\Delta\nu_c$ the frequency offset away from the optimal optical carrier, σ_{LN+NL}^2 is the variance of the linear and non-linear phase-noise, and the laser phase-noise (LPN) variance is given in

the first perturbation order by the expression

$$(2.4.2) \quad \sigma_{LPN}^2 = 2\pi\Delta\nu_{LW}T(d-1/3)$$

with $\Delta\nu_{LW}$ the FWHM laser LW, T^{-1} the bitrate, and d the integer number of bit delays. The OSNR penalty in dB units is readily extracted from (2.4.1) and (2.4.2) with its functional dependence due to the combined effect of LW, FO and multi-bit bit delays

$$(2.4.3) \quad -10\log_{10}[1-2M\Delta\nu_cTd] + 10\log_{10}\left[1 + \frac{2\pi\Delta\nu_{LW}T(d-\lambda)}{\sigma_{LN+NL}^2}\right]$$

Analytical results were obtained using a value of σ_{LN+NL}^2 such that for zero LW and FO penalties, the linear phase noise induces a BER of 10^{-9} while the non-linear phase noise power is zero.

For our experimental results, we constructed the stable delay interferometer with tunable delay providing an FSR ranging from 3.2 GHz to 11 GHz illustrated in Figure 12. Two 3dB fibre couplers were spliced together; one branch wound onto a fixed wheel and the other branch wound on two half wheels with tunable separation, stretching the fibre to provide the variable time delay. We used 10 m of fibres for 10 cm of stretching to ensure maintain the intergrity of the stretched fiber. The extinction ratio exceeded 15 dB and BER was measured for a 10 Gb/s NRZ-DPSK signal for several values of OSNR and FSR using the setup of Figure 13. A polarization controller was used to ajust the signal to the best polarization.

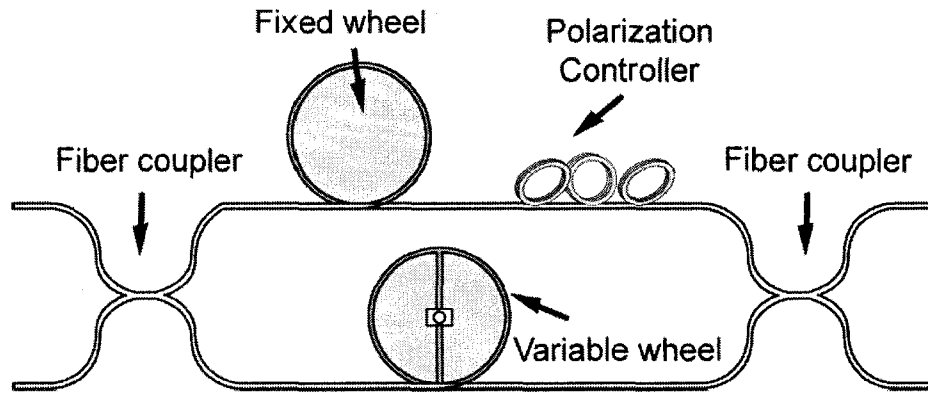


FIGURE 12. THE VARIABLE DELAY INTERFEROMETER USED FOR THE EXPERIMENTAL DEMONSTRATION.

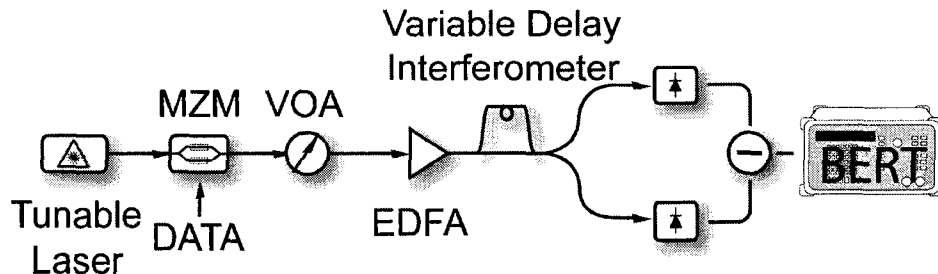


FIGURE 13. EXPERIMENTAL SETUP TO OBTAIN RECEIVER SENSITIVITY AND OSNR PENALTY MEASUREMENTS. DIFFERENT BIT DELAYS ARE OBTAINED THROUGH THE VARIABLE DELAY INTERFEROMETER WHILE FREQUENCY OFFSET PENALTY IS OBTAINED BY TUNING THE TUNABLE LASER FREQUENCY.

Simulations were performed for a 10 Gb/s RZ-DPSK signal on a 10 MHz LW laser using 12.5 GHz 3rd order Gaussian optical filtering and 8 GHz Lorentzian electrical filtering at the receiver. A Karhunen-Loeve expansion for non-Gaussian noise statistics was used with 512 bits simulated at 64 samples per bit. Complete BER versus OSNR curves were simulated and the OSNR penalty at $BER=10^{-9}$ was inferred from those curves through a linear fit of the $\log(\log(BER))$ curve.

2.4 OPTICAL ERROR CORRECTION

DPSK OSNR requirements are still 1.2 dB higher than for its coherent counterpart, PSK for a BER of 10^{-3} . Multi-symbol processing strategies have been proposed to reduce this penalty through soft detection, including decision feedback based techniques [77, 78, 80, 81], providing $\sim 1\text{-}3$ dB sensitivity improvements for DPSK optical transmission, however the analog or high-speed digital soft detection feedback electronics remain challenging to implement. Our method uses hard detection rather than soft detection, i.e. a decision is made on each bit to obtain a digital logic signal and then applying digital logic processing on the balanced outputs of multiple Mach-Zehnder Delay Interferometers (DLI) to attain comparable processing gains. We demonstrate experimentally and numerically our optical multi-path error correction technique for differentially encoded modulation formats. The scheme can be readily implemented using commercially available DLIs [79] and high-speed logic gates. After optical demodulation and hard detection, basic logic operations are applied on each path to recover the data signal and errors are corrected using a simple majority-vote comparison of the paths[83].

2.4.1 Theory

The optical error correction scheme takes advantage of the combination of the optical logical XOR function of the DLI and electronic binary logic gates. A simple logic representation of the system is illustrated in Figure 14. A modified 4-bit form of

Differential Precoding (DP) is performed at the transmitter prior to optical modulation. The received signal is corrupted by amplified spontaneous emission (ASE) noise accumulated along the transmission fibre from amplifiers. Optical demodulation is performed using multiple demodulation paths each consisting of a DLI with a different integer bit-delay. The bits are then detected. The output of the 4-bit delay DLI recovers the proper transmitted bits, since a 4-bit differential precoder is used at the transmitter. Electronic logic blocks consisting of XOR gates and delays follow the outputs of the 2-bit and 1-bit delay DLIs, re-aligning the three paths together. Finally error-correction is performed through a simple majority vote algorithm. The digital processing can be described by the following equations where $\oplus, \&, |$ respectively denote the XOR (addition-modulo-2), AND, OR logic functions:

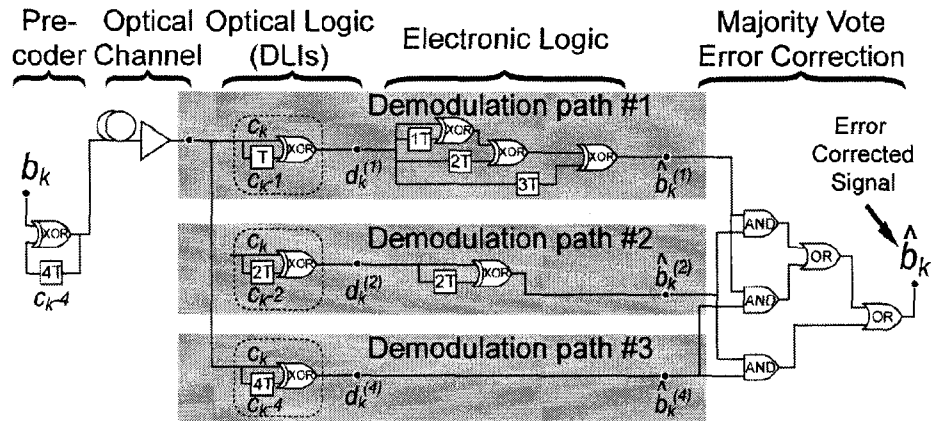


FIGURE 14. CONCEPTUAL DIAGRAM OF MULTIPATH DEMODULATION WITH MAJORITY VOTE ERROR CORRECTION. THE DPSK PRECODER USES A 4-BIT DELAY. THE OPTICAL LOGIC IS PERFORMED BY THE PASSIVE DLI DPSK DEMODULATOR. THE ELECTRONIC LOGIC RECOVERS THE ORIGINAL SIGNAL BEFORE MAJORITY VOTE IS APPLIED.

$$(2.4.1) \quad c_k = b_k \oplus c_{k-4}$$

represents the differential encoder using a four bit delay where b_k is the information message bit in time bin k , and c_k is the differentially encoded message transmitted in the channel. Next,

$$(2.4.2) \quad \begin{aligned} d_k^{(1)} &= c_k \oplus c_{k-1} \oplus \varepsilon_k^{(1)} \\ d_k^{(2)} &= c_k \oplus c_{k-2} \oplus \varepsilon_k^{(2)} \\ d_k^{(4)} &= c_k \oplus c_{k-4} \oplus \varepsilon_k^{(4)} \end{aligned}$$

represent the optical differential demodulations for the 1-bit, 2-bit and 4-bit delay DLIs, where d is the data after optical demodulation of c , and ε is the noise in the transmitted time bins. Then,

$$(2.4.3) \quad \begin{aligned} \hat{b}_k^{(1)} &= d_k^{(1)} \oplus d_{k-1}^{(1)} \oplus d_{k-2}^{(1)} \oplus d_{k-3}^{(1)} \\ \hat{b}_k^{(2)} &= d_k^{(2)} \oplus d_{k-2}^{(2)} \\ \hat{b}_k^{(4)} &= d_k^{(4)} \end{aligned}$$

represent the electronic XOR gates necessary to realign all 4 paths to the initial signal where

$$(2.4.4) \quad \hat{b}_k = \hat{b}_k^{(1)} \& \hat{b}_k^{(2)} \mid \hat{b}_k^{(1)} \& \hat{b}_k^{(3)} \mid \hat{b}_k^{(2)} \& \hat{b}_k^{(3)}$$

represents the majority vote error correction algorithm using the bit stream from all three DLIs.

Referring to the bit intervals $T=1/R$ (with R the bitrate) the DP performs a modulo-2 addition of the current transmitter output bit with the input data bit $4T$ seconds earlier, i.e. it implements an accumulator with 4-bit delay, whereas conventional DPSK uses a DP with 1-bit delay.

First, assuming that there are no errors, i.e. $\varepsilon_k^{(1)} = \varepsilon_k^{(2)} = \varepsilon_k^{(4)} = 0$. Applying the identity $\alpha \oplus \alpha = 0$, it follows that the output of the 4-bit delay DLI (yielding the estimate $\hat{b}_k^{(4)}$) correctly recovers the transmitted stream, and so do $\hat{b}_k^{(2)}$ and $\hat{b}_k^{(1)}$:

$$\begin{aligned}
 \hat{b}_k^{(4)} &= d_k^{(4)} = c_k \oplus c_{k-4} = b_k \oplus c_{k-4} \oplus c_{k-4} = b_k \\
 \hat{b}_k^{(2)} &= d_k^{(2)} \oplus d_{k-2}^{(2)} = (c_k \oplus c_{k-2}) \oplus (c_{k-2} \oplus c_{k-4}) \\
 &= c_k \oplus c_{k-2} \oplus c_{k-2} \oplus c_{k-4} = c_k \oplus c_{k-4} = d_k^{(4)} = b_k \\
 \hat{b}_k^{(1)} &= d_k^{(1)} \oplus d_{k-1}^{(1)} \oplus d_{k-2}^{(1)} \oplus d_{k-3}^{(1)} \\
 (2.4.5) \quad &= c_k \oplus c_{k-1} \oplus c_{k-1} \oplus c_{k-2} \oplus c_{k-2} \oplus c_{k-3} \oplus c_{k-3} \oplus c_{k-4} = c_k \oplus c_{k-4} = b_k
 \end{aligned}$$

Extending the model to include the additively injected error indicators $\varepsilon_k^{(i)}, i=1,2,4$ at the DLI outputs yields after some manipulation

$$(2.4.6) \quad \hat{b}_k^{(\Delta)} = b_k \oplus \eta_k^{(i)}, \quad i \in \{1, 2, 4\}$$

where $\eta_k^{(i)}$ are effective binary noise streams at the majority-vote input, given by

$$(2.4.7) \quad \eta_k^{(1)} \equiv \varepsilon_k^{(1)} \oplus \varepsilon_{k-1}^{(1)} \oplus \varepsilon_{k-2}^{(1)} \oplus \varepsilon_{k-3}^{(1)}, \quad \eta_k^{(2)} \equiv \varepsilon_k^{(2)} \oplus \varepsilon_{k-2}^{(2)}, \quad \eta_k^{(4)} \equiv \varepsilon_k^{(4)}$$

Notice that the underlying noise bits of the form $\varepsilon_k^{(i)}$ are not statistically

independent, hence nor are the effective noise bits $\{\eta_k^{(1)}, \eta_k^{(2)}, \eta_k^{(4)}\}$ independent.

It is apparent that (2.4.6) defines an effective binary channel wherein b_k repetition-coded with 3-fold diversity, i.e. the same bit is transmitted over three scalar binary channels corrupted by the partially correlated effective noises. The proposed decoding scheme applies a simple majority-vote strategy reducing the probability of errors, relative to a single use of either one of the three paths, and also provides improvement relative to conventional DPSK. When errors are uncorrelated in each demodulation path, the correction rate of majority vote is determined by the individual Error Rates (ER):

$$(2.4.8) \quad [ER^{(1)} \cdot ER^{(2)} \cdot (1 - ER^{(4)})] + [ER^{(1)} \cdot (1 - ER^{(2)}) \cdot ER^{(4)}] + [(1 - ER^{(1)}) \cdot ER^{(2)} \cdot ER^{(4)}]$$

This is the upper limit of majority vote error detection. Since there is only partial correlation between the effective noise bits, there is a low probability that two or three of the paths assume the same value simultaneously. The majority vote correction method is analogous to what has been proposed in the RF domain at MHz speed [17]. Combining soft FEC or soft detection techniques with this method could be done immediately after the interferometers before a hard decision is made to obtain

$$d_k^{(1)}, d_k^{(2)}, d_k^{(4)}$$

2.4.2 Simulations & Experiment

Monte Carlo simulations were performed using a $2^{15}-1$ pseudo random bit sequence (PRBS) at 10 Gb/s with 12.5 GHz optical filter and 8 GHz electrical filtering at the receiver. Using these parameters we find an improvement in receiver sensitivity of 0.35dB at BER of 10^{-3} . Our simulation of BER versus OSNR curve for standard back-to-back DPSK agrees with previously published results yielding confidence in our numerical results. We also provide the theoretical limit of majority vote error correction (ideal majority vote) assuming the errors were completely uncorrelated, confirming that in multi-path demodulation, errors are partially correlated. The theoretical limit when the demodulation paths are completely independent allows a 1.2×10^{-2} error rate to become 2×10^{-3} suitable for eFEC or it allows a 2.1×10^{-2} error rate to reach 6×10^{-3} suitable for Super FEC. In a back-to-back transmission, errors are somewhat correlated in each demodulation path such that the gain reduces correcting a 2.6×10^{-3} BER to a 2×10^{-3} BER and 6.92×10^{-3} BER to a 6×10^{-3} BER. Transmission impairments (i.e. CD, PMD, non-linear phase noise, cross-phase-modulation), and receiver degradations (i.e. non-ideal filtering, DLI's frequency offset) result in decorrelated errors between demodulation paths. Error propagation does occur due to the 4-bit precoding doubling the errors of the 2-bit delay demodulation and quadrupling the errors in the 1-bit delay. Nonlinear phase is an important degradation in DPSK transmission systems. The other multipaths schemes [77, 78, 81, 106] also exhibited increased performance in the presence of nonlinear degradations, which can be explained by the decorrelation of errors between the paths. We would expect

majority vote error correction to perform closer to its theoretical limit in the presence of non-linear phase degradation.

We performed experimental verification using $2^{15}-1$ PRBS pattern phase-modulated at 10Gbps and then sent through a variable attenuator and erbium amplifier as illustrated in Figure 15. The DPSK demodulators from ITF Laboratories had FSR's of 10GHz, 5GHz and 2.5GHz providing 1,2 and 4 bit delay. A 70 Ghz optical filter was used and the three photodiodes had bandwidths of approximately 8GHz. The three paths were detected simultaneously using three receivers and three bit-error-rate testers. Only the destructive arm of the DLI was detected since we lacked access to three balanced receivers. The detected bits were then fed into a 20Gsample/s real time oscilloscope with sufficient memory for offline-processing of 500 000 bits for each path. Experimental and simulation results are found in the article [80].

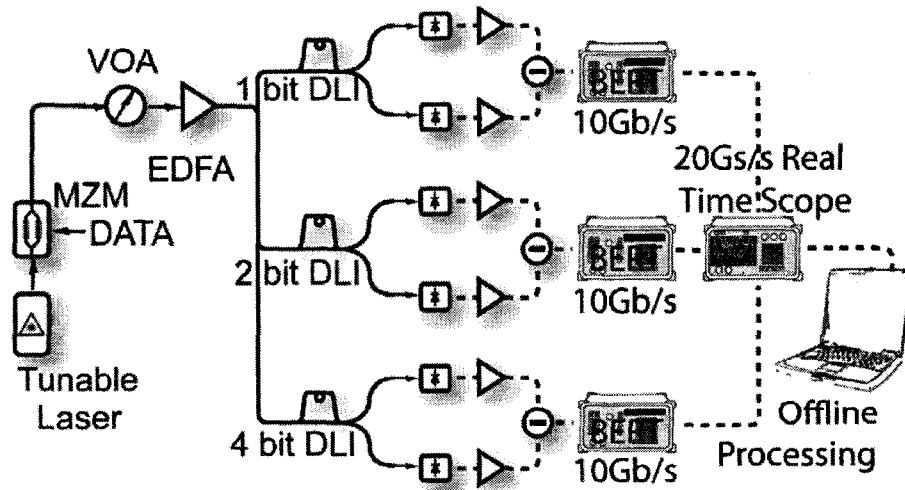


FIGURE 15. EXPERIMENTAL SETUP FOR THE DEMONSTRATION OF MULTIPATH DPSK DEMODULATION MAJORITY VOTE ERROR CORRECTION. USING 3 COMMERCIAL DLIs,

THREE 10GBPS BIT ERROR RATE TESTER AND A 20GS/S REAL TIME SCOPE. LOGIC OPERATIONS WERE PROCESSED OFFLINE.

2.5 FREE SPECTRAL RANGE AND OPTICAL FILTERING OPTIMIZATION

There has been several publications demonstrating that DLI degradations such as bit delay mismatch and frequency offset [87-89], transmission impairments such as chromatic dispersion (CD), polarization-mode-dispersion (PMD), and nonlinearities [90-92] as well as the combination of DLI degradations and transmission impairments [93] can distort the phase of the DPSK signal and reduce receiver sensitivity and transmission distance. It was recently shown that increased free-spectral-range (FSR) can better the optical filtering (OF) and CD tolerances of RZ-and NRZ-DPSK [94-97], but the value of the optimal parameters for any value of OF or CD was not reported. Moreover, the combined effect of OF and CD had never been discussed.

2.5.1 Theory

The optimization obtained through increasing the FSR of the Delay Interferometer (DI) can be explained using the equivalent baseband model detailed in [107], representing the DPSK link as two parallel paths with Transfer Functions (TF) given in our modified notation by the product $H_L(f) \equiv H_T(f)H_F(f)H_o(f)H_{\pm}(f)$ of the TF $H_T(f)$ of the Transmitter (TX) pulse-carver, the fibre dispersion $H_F(f)$, the OF $H_o(f)$ and the TFs describing the DI propagation to the constructive / destructive DI ports:

$$(2.5.1) \quad H_{\pm}(f) = [\exp(-j2\pi f/FSR) \pm 1]/2$$

The benefit of taking $FSR > R$, (with $R = T_b^{-1}$ the bitrate) is then interpreted as an equalization measure; by reducing the TX and/or OF bandwidths (BW) CD tolerance is improved and ASE noise reduced, however this in itself introduces inter-symbol interference (ISI), which is subsequently equalized by increasing the FSR of the filters. The enhanced BW filters then act as equalizers for the other TFs in the chain $H_L(f)$. While the ASE noise reduction due to tighter optical filtering is undone to some extent by the noise enhancement through the enhanced BW equalizers, an improvement in CD tolerance is evidently achieved. This intuitive argument does not address the Electrical Filter (EF), $H_e(f)$ following balanced photo-detection. However it is expected that its impact be secondary when tight OF is used.

The tighter optical filtering and increased FSR can be seen as putting a greater emphasis on the optical Duobinary (ODB) port versus the alternate mark inversion port in the DPSK balanced detection as illustrated in Figure 16. ODB is well known for its chromatic dispersion tolerance.

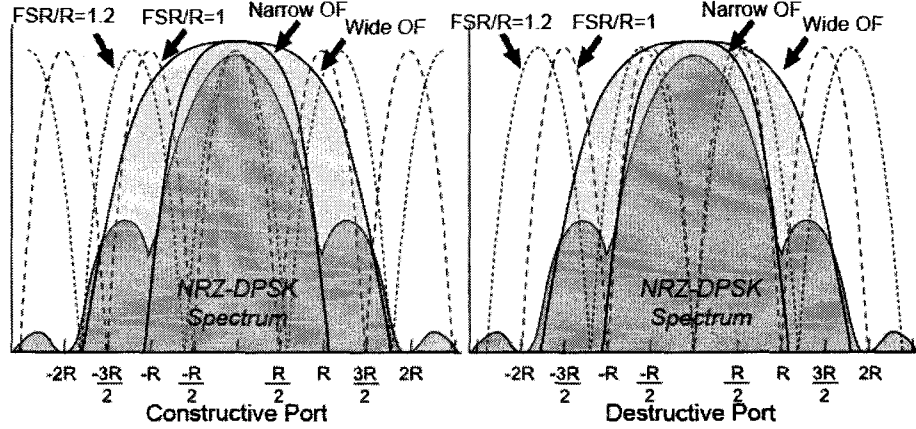


FIGURE 16. DPSK SPECTRUM WITH OVERLAYED TRANSFER FUNCTIONS FOR OPTICAL FILTERING AND DELAY-LINE INTERFEROMETER. FREE-SPECTRAL-RANGE LARGER THAN THE BITRATE AND TIGHTER OPTICAL FILTERING PUTS A GREATER EMPHASIS ON THE OPTICAL DUOBINARY (ODB) PORT (CONSTRUCTIVE) RATHER THAN THE ALTERNATE-MARK-INVERSION PORT (DESTRUCTIVE).

2.5.2 Simulation Parameters

We performed the simulations using normalized parameters such that our results can be applied to any bitrate. Simulations were performed for a C-band DPSK signals at bitrate R , modulated with a Mach-Zehnder modulator (MZM) with 20 dB of extinction ratio. The RZ- and CSRZ-DPSK signals were generated using a second MZM driven by a $R/2$ clock with a V_π drive voltage for CSRZ-DPSK and R clock with V_π drive voltage for RZ-DPSK. At the receiver, the signal was filtered through a 2nd order Gaussian OF and demodulated in a MZ DLI. Balanced detection was followed by $\frac{3}{4}R$ 4th-order Bessel electrical filter. The bit error rate (BER) was estimated by means of a Karhunen-Loeve expansion for non-Gaussian noise statistics, with 1024 simulated bits at 64 samples per bit in a simulation BW of $25R$. The OSNR in 0.1 nm was set

using $\text{OSNR} = 10\log(R)$ dB corresponding to 10, 16 and 20 dB of OSNR at 10, 40 and 100 Gb/s respectively. The CD was varied from 0 to 272 in normalized units of 10^3 (Gb/s) 2 ps/nm using $\text{CD}_{\text{index}} = R^2 L D$ [107] where L is the fibre length and D the CD in ps/nm/km. The Q parameter was calculated from the BER value as in [95] using :

$$(2.5.2) \quad Q = 20 \log \sqrt{2} \operatorname{erfc}^{-1}(2\text{BER})$$

with erfc^{-1} the inverse complementary error function.

Through our simulations, we have determined that the optimal OF for NRZ-, RZ- and CSRZ-DPSK for a one-bit delay, back-to-back demodulation to be around $1.25R$ for NRZ-, $1.75R$ for RZ- and $1.8 R$ for CSRZ-DPSK. The optimal FSR varies over the OF BWs but is also very dependent on CD. The results indicate that either tighter optical filtering or larger FSR tends to increase CD tolerance but it is their combination which leads to optimal CD performance.

Chapter 3

General Discussion

The general goal of this thesis is to investigate different aspect of the DPSK modulation formats in optical fibre telecommunication transmission. When we began our work, DPSK was a popular topic at technical conferences but no commercial systems utilizing the format were available. Although the first commercial systems were deployed by Tyco Telecommunications now over a year and a half ago, and the new high bitrate 40Gb/s systems are now being deployed using DPSK, the results presented in this thesis are still of interest to optimize the performance of such systems. The next generation of optical communication systems may be using more advanced modulation formats such as differential quadrature phase shift keying (DQPSK), using four phase states instead of two. This format has been receiving a lot of attention lately by research groups worldwide. For similar reasons DPSK was getting attention a few years ago: increased receiver sensitivity and greater tolerance to some transmission effects such as CD and PMD. The results of our work could be expanded to apply to new modulation formats. For example our optical error correction scheme can be expanded to higher level differential phase modulated signals.

Because of the specific method of precoding of DQPSK, we would expect errors to be less correlated than for DPSK, which would improve the error correction capability of the algorithm.

In this chapter, we revisit our work in the perspective of the next generation of modulation formats and try to understand how the lessons learned in this thesis could be applied and extended. This chapter serves as a starting point for future work.

3.1 OPTICAL PACKETS

Optical packet switching (OPS) though regarded as next-generation transport technologies are still in the somewhat distant future. All of the optical traffic is currently point-to-point links with lightpath switching. Packet switch network are more efficient at utilizing the available bandwidth and are used in many types of communication systems other than fibre optic systems. OPS and OBS could revolutionize optical telecommunication networks but as well as technological challenges, the optical components necessary for such systems are currently too costly for cost-effective deployment. Optical modulators represent a major cost of optical transmitters, our solution of using a single modulator for both payload and label modulation would represent a significant cost advantage. Further work is necessary to reduce the cost of demodulators, developing fast and efficient optical switches and control electronic for packet by packet optical routing. Another step in this direction is our demonstration of a low-cost spectrally-periodic fibre Bragg grating (FBG) for DPSK demodulation[108]. We demonstrated balanced DPSK demodulation using the

FBG demodulator exhibiting no penalty compared to a standard MZI. FBG are potentially cheaper to manufacture on a large scale than all-fibre or free-space devices which would be quite interesting for low-cost OPS networks.

3.2 PERFORMANCE MONITORING

There have been several methods reported in the literature to achieve efficient monitoring of either Optical-Signal-to-Noise-Ratio (OSNR), Chromatic Dispersion (CD) or Polarization mode dispersion (PMD). We demonstrated a $\frac{1}{4}$ - bit delay Mach-Zehnder interferometer (MZI)-assisted simultaneous and independent CD, PMD and OSNR monitoring method for NRZ-OOK, NRZ-DPSK and Duobinary modulation formats. Optical performance monitoring would be equally important for future DQPSK systems. There have been reports on monitoring method for DQPSK at recent conferences but there is no reported method to monitor CD, PMD and OSNR simultaneously and independently. Since DQPSK is also a phase modulated signal, our method of $\frac{1}{4}$ bit delay-assisted clock tone and DC power monitoring for CD, PMD and OSNR monitoring could possibly be extended to this modulation format. Furthermore, other advanced modulation formats such as coherent detection of phase modulated format (PSK & QPSK), which is becoming increasingly researched could possibly also take advantage of the monitoring method.

One drawback of the MZI-assisted method is that performance monitoring ought to be cost effective. Unfortunately, commercial MZI are possibly too pricy for performance monitoring to be deployed on a large scale. A promising extension of the

MZI-assisted method would be to use a spectrally periodic filter instead of a more expensive interferometer. We demonstrated that such filters have the same properties as MZI and demonstrated balanced DPSK demodulation using a spectrally-periodic fibre Bragg grating (FBG) with no penalty compared to a MZI [108]. FBG are potentially cheap to manufacture on a large scale. Using such a filter would enable large scale deployment of the monitoring method.

3.3 MULTIBIT DELAY DQPSK DEMODULATION

The interest in the concept of modified multi-bit-delay DPSK demodulation to demodulate polarization-interleaved [74, 75], or optically time-division-multiplexed (OTDM) data stream, [76] or DPSK optical error correction using several DLIs of various bit delays [77, 78], can also be useful for DQPSK modulation formats. Similar to DPSK demodulation, there has been little discussion on the system penalty incurred by multi-bit delay demodulation for DQPSK demodulation.

We demonstrated that multibit delay DPSK demodulation is 2x more sensitive to frequency offset penalty [109], and DQPSK was demonstrated to be 6x more sensitive than DPSK [87, 89, 110]. This would indicate that multibit DQPSK demodulation would be very sensitive to frequency offset between the transmitting laser and the demodulator, polarization dependent frequency offset and laser linewidth. This increased sensitivity may seriously limit multibit applications for DQPSK systems.

3.4 DQPSK OPTICAL ERROR CORRECTION

DPSK is currently being deployed as a data-modulation format for high-capacity and undersea optical communication systems mainly due to its 3 dB OSNR advantage over intensity modulation and its non-linear tolerance [2, 3, 7, 8, 79]. However DPSK OSNR requirements are still 1.2 dB higher than for its coherent counterpart, PSK for a BER of 10^{-3} . We demonstrated experimentally and numerically our optical multi-path error correction technique for differentially encoded modulation formats. The scheme can be readily implemented using commercially available DLIs [79] and high-speed logic gates. After optical demodulation and hard detection, basic logic operations are applied on each path to recover the data signal and errors are corrected using a simple majority-vote comparison of the paths [83]. In a back-to-back transmission, errors are somewhat correlated in each demodulation path such that the coding coding is limited, correcting a 2.6×10^{-3} BER to a 2×10^{-3} BER and 6.92×10^{-3} BER to a 6×10^{-3} BER. We demonstrated that transmission impairments such as chromatic dispersion (CD), polarization mode dispersion (PMD), non-linear phase noise, cross-phase-modulation), and receiver degradations such as non-ideal filtering, DLI's frequency offset result in decorrelated errors between demodulation paths.

Multibit delay error correction scheme for DQPSK would first require the understanding of the tolerances of multibit delay DQPSK demodulation discussed in 3.3. The error correction scheme was demonstrated to be efficient at correction frequency offset errors which could be important in multibit DQPSK. Moreover, because of the specific precoding necessary for DQPSK, we would expect error errors

to be less correlated than in multibit DPSK. It would require more complex electronics but the lower symbol rate of DQPSK would mean cheaper components. Moreover, the decorrelation of errors in DQPSK would make the error correction scheme significantly more effective.

3.5 OPTICAL FILTERING & FREE-SPECTRAL-RANGE OPTIMIZATION

Optical filtering and free-spectral-range optimization has a dramatic effect of the chromatic dispersion tolerances of DPSK. Other important transmission impairments may also be affected by the optical filtering and FSR.

One example is polarization mode dispersion (PMD). We demonstrated that FSR optimization has little effect on first order PMD impairments [94]. However, little attention has been given to the effect of OF and FSR on second order PMD (SOPMD) by research groups. SOPMD can significantly degrade signals, especially in legacy optical fibres, high bitrate system and long distance transmission. SOPMD is defined by two different effects: i) PMD induced signal depolarization and ii) polarization dependent chromatic dispersion. It is difficult to have an intuition on the effect on OF and FSR on depolarization but it is easy to assume that tolerances to polarization dependent chromatic dispersion could be increased through tight optical filtering and larger FSR.

In all long-haul fibre optic transmission and high bitrate systems with higher peak power, nonlinear effects can be very detrimental. Nonlinear effects can be thought as

intra-channel effects, which are effects that happen on a single WDM wavelength and *inter-channel* effects which are effects emanating from the interactions within neighboring channels. Alternatively nonlinear effects can be categorized as *signal-signal* interactions or *signal-noise* interactions. The impact of nonlinearities on different modulation formats depends strongly on the characteristics of the optical network [3] since so many elements such as chromatic dispersion map, noise level, channel separation all interplay. It is not easy to predict the effect FSR optimization and tight optical filtering on self-phase modulation, an intra-channel signal-signal effect. Another important effect, nonlinear phase noise, which is a signal-noise effect which can be either intra-channel (SPM induced) or inter-channel (cross-phase modulation, or XPM, induced). Once again, since chromatic dispersion, noise accumulation and nonlinear effects strongly interplay, it would be quite interesting to understand and demonstrate the effect of OF and FSR optimization and could be the subject of future work.

Finally, DQPSK is 4x less sensitive to chromatic dispersion than un-optimized DPSK but the same optimization can potentially be applied to make DQPSK even less sensitive to chromatic dispersion. This is of great importance for short haul high bitrate systems at 40Gb/s or even 100Gb/s. One main detrimental effect of these systems is chromatic dispersion and increasing the tolerance of DQPSK increases transmission distance and reduces the need for expensive chromatic dispersion compensation. It is fair to assume that OF and FSR optimization could be used to further increase CD tolerances. Recent demonstrations on the effect of FSR on optical

filtering in DQPSK demodulation were reported [111, 112], similar to the reports on DPSK optimization [94-96] are a promising indication that the optimization would similarly increase chromatic dispersion.

We recently obtained such results for DQPSK demodulation. With optimal parameters, CD tolerance increases by nearly 10% for NRZ-DQPSK as illustrated in Figure 17. As can be observed in the figure, the NRZ-DQPSK improvement in CD tolerance contrasts with that of NRZ-DPSK which improves by 20% with optimal FSR and OF 10^3 (Gb/s) 2 ps/nm using $CD_{index} = (2R)^2 LD$ [107] where again R is the symbol rate, L the fibre length and D the CD in ps/nm/km. This is explained by the fact that increasing the FSR of the demodulator of the Q channel for example, means that some of the signal in the I channel is accepted. Nevertheless, since DQPSK is already more tolerant to CD, the CD tolerance improvement in absolute value in normalized units of is similar for NRZ-DQPSK (40×10^3 (Gb/s) 2 ps/nm) than NRZ-DPSK (35×10^3 (Gb/s) 2 ps/nm). One can also deduce the optimal FSR depending on the OF used; since the contour plot of [113] are skewed, it can concluded that when tighter OF is used, increasing the FSR is beneficial as was observed in [111]. For a NRZ-DQPSK system, we conclude that using a constant FSR/R of 1.2 yields only a small 0.2dBQ penalty with no CD but optimized for 400×10^3 (Gb/s) 2 ps/nm and for a wide range of OF bandwidth.

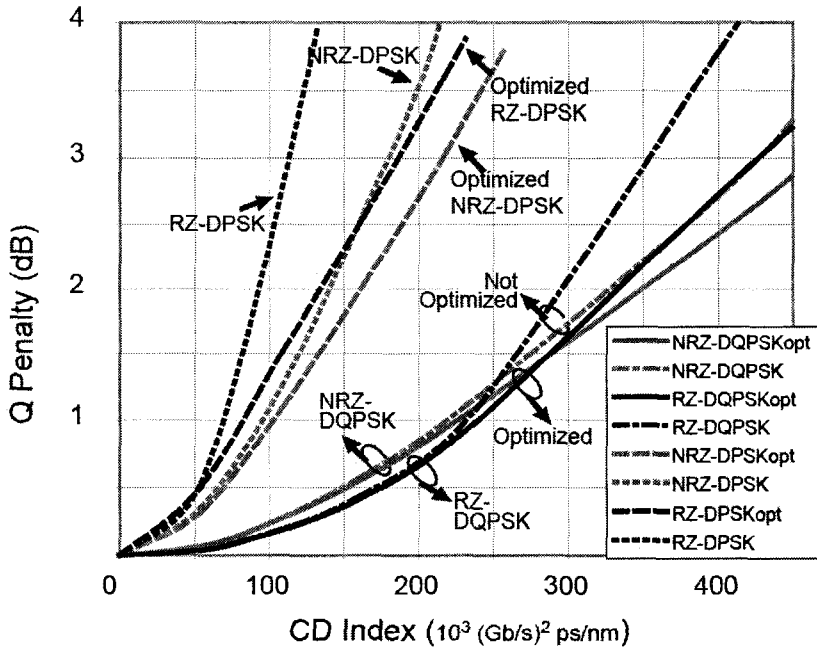


FIGURE 17. CHROMATIC DISPERSION TOLERANCES FOR RZ- AND NRZ-, DPSK AND DQPSK. THE INCREASE IN CHROMATIC DISPERSION WHEN BOTH OPTICAL FILTERING AND FSR ARE OPTIMIZED IS GREATER PERCENTAGE WISE FOR THE DPSK FORMATS BUT ROUGHLY THE SAME IN ABSOLUTE VALUES.

For RZ-DQPSK with optimal OF, the optimal FSR/R value is 1. With tighter filtering, larger FSR yields better performance. With optimal parameters, CD tolerance increases by about 20% at 3 dBQ penalty as illustrated in Figure 17. This contrasts with the dramatic improvement for RZ-DPSK of about 65%. Again, since DQPSK is already more tolerant to CD, the CD tolerance improvement in absolute value is similar for RZ-DQPSK and RZ-DPSK (60 versus 70×10^3 (Gb/s) 2 ps/nm).

The required values of optical filtering (OF) and free spectral range (FSR) normalized over baudrate for RZ- and NRZ- DPSK and DQPSK for optimized Q factor when both OF and FSR are optimized simultaneously are illustrated in Figure 18.

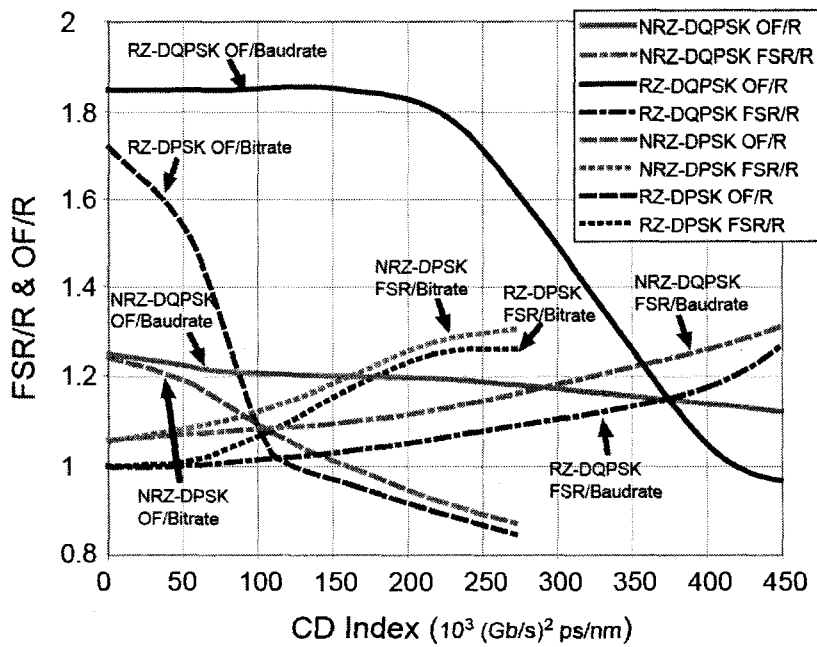


FIGURE 18. REQUIRED VALUES OF OPTICAL FILTERING (OF) AND FREE SPECTRAL RANGE (FSR) NORMALIZED OVER BAUDRATE FOR RZ- AND NRZ- DPSK AND DQPSK FOR OPTIMIZED Q FACTOR (WHEN BOTH OF AND FSR ARE OPTIMIZED SIMULTANEOUSLY).

Conclusion

This thesis has generator some interesting discoveries on the DPSK modulation format. Until recently, optical communication systems strictly employed conventional intensity (IM) modulation signals in either non return-to-zero (NRZ) or return-to-zero (RZ) format. After years in the lab, DPSK is finally a viable format and is being deployed worldwide. The goal of this thesis was to investigate the DPSK modulation format in fibre optic communications systems to further the understanding, improve the performance and enable novel ways to utilize the modulation format.

In the six papers of this thesis we investigated the *generation, transmission and demodulation* of DPSK.

1. We proposed and demonstrated a novel low-cost method to encode optical packets using DPSK.
2. We proposed and demonstrated a transmission effects monitoring using a novel partial-bit delay interferometer-assisted clock tone monitoring method for sensitive optical-signal-to-noise ratio (OSNR), chromatic dispersion (CD) and polarization mode dispersion (PMD) monitoring.
3. We investigated the reduced tolerances and power penalties of DPSK demodulation when more than one bit delay is used in the interferometer and concluded that laser linewidth and frequency offset

tolerance were greatly reduced.

4. We proposed and experimentally demonstrated an optical error correction method combining DPSK optical logic gates with electronic logic gates to improve receiver sensitivity and chromatic dispersion tolerances.
5. We demonstrated the important effect of the optimization of optical filtering and the free-spectral range of the delay-line interferometer to improve chromatic dispersion tolerances.

Finally, we attempted to put our work in the perspective of the next generation of modulation formats such as DQPSK and coherent demodulation and try to understand how the lessons learned in our work on DPSK could be applied and extended.

References

- [1] A. Gnauck, "40-Gb/s RZ-differential phase shift keyed transmission," presented at OFC 2003 - Optical Fiber Communication Conference and Exhibition. Technical Digest, Atlanta, GA, 2003.
- [2] A. H. Gnauck and P. J. Winzer, "Optical phase-shift-keyed transmission," *Journal of Lightwave Technology*, vol. 23, pp. 115-30, 2005.
- [3] P. J. Winzer and R. J. Essiambre, "Advanced modulation formats for high-capacity optical transport networks," *Journal of Lightwave Technology*, vol. 24, pp. 4711-28, 2006.
- [4] R. A. Linke and A. H. Gnauck, "High-capacity coherent lightwave systems," *Journal of Lightwave Technology*, vol. 6, pp. 1750-69, 1988.
- [5] L. Mach, "Uber einer Interferenzrefractor," *Zeitschr. f. Instrkde.*, vol. 12, pp. 89-93, 1892.
- [6] L. Zehnder, "Ein neuer Interferenzrefractor," *Zeitschr. f. Instrkde.*, vol. 11, pp. 275-285, 1891.
- [7] X. Liu, "Nonlinear effects in phase shift keyed transmission," presented at Optical Fiber Communication Conference (OFC), Los Angeles, CA, 2004.
- [8] X. Liu, R. C. Giles, Y. H. Kao, and M. Movassaghi, "High tolerance to coherent crosstalk of differential-phase-shift-keying," presented at Optical Fiber Communication Conference (OFC), Los Angeles, CA, 2004.
- [9] L. Becouarn, T. Boissau, B. Julien, G. Grandpierre, S. Dupont, P. Plantady, and J. F. Marcerou, "Investigation on a stabilised DPSK receiver at 10 Gb/s with a 5111 km-long transmission," presented at 31st European Conference on Optical Communication, Glasgow, UK, 2005.
- [10] L. Becouarn, G. Vareille, S. Dupont, P. Plantady, J. F. Marcerou, A. Klekamp, R. Dischler, W. Idler, and G. Charlet, "42×42.7 Gb/s RZ-DPSK transmission over a 4820 km long NZDSF deployed line using C-band-only EDFA," presented at Optical Fiber Communication Conference (OFC), Los Angeles, CA, 2004.
- [11] J. X. Cai, D. G. Foursa, C. R. Davidson, Y. Cai, G. Domagala, H. Li, L. Liu, W. W. Patterson, A. N. Pilipetskii, M. Nissov, and N. S. Bergano, "A DWDM demonstration of 3.73 Tb/s over 11,000 km using 373 RZ-DPSK channels at 10 Gb/s," presented at OFC 2003 - Optical Fiber Communication Conference

and Exhibition. Postdeadline Papers, Atlanta, GA, 2003.

- [12] J. X. Cai, D. G. Foursa, L. Liu, C. R. Davidson, Y. Cai, W. W. Patterson, A. J. Lucero, B. Bakhshi, G. Mohs, P. C. Corbett, V. Gupta, W. Anderson, M. Vaa, G. Domagala, M. Mazurczyk, H. Li, S. Jiang, M. Nissov, A. N. Pilipetskii, and N. S. Bergano, "RZ-DPSK field trial over 13 100 km of installed non-slope-matched submarine fibers," *Journal of Lightwave Technology*, vol. 23, pp. 95-103, 2005.
- [13] G. Charlet, E. Corbel, J. Lazaro, A. Klekamp, R. Dischler, P. Tran, W. Idler, H. Mardoyan, A. Konczykowska, F. Jorge, and S. Bigo, "WDM transmission at 6-Tbit/s capacity over transatlantic distance, using 42.7-Gb/s differential phase-shift keying without pulse carver," *Journal of Lightwave Technology*, vol. 23, pp. 104-7, 2005.
- [14] G. Charlet, P. Tran, H. Mardoyan, M. Lefrancois, T. Fauconnier, F. Jorge, and S. Bigo, "151 \times 43 Gb/s transmission over 4080 km based on return-to-zero-differential quadrature phase-shift keying," presented at 31st European Conference on Optical Communication, Glasgow, UK, 2005.
- [15] A. H. Gnauck, G. Raybon, S. Chandrasekhar, J. Leuthold, C. Doerr, L. Stulz, A. Agarwal, S. Banerjee, D. Grosz, S. Hunsche, A. Kung, A. Marhelyuk, D. Maywar, M. Movassaghi, X. Liu, C. Xu, X. Wei, and D. M. Gill, "2.5 Tb/s (64 \times 42.7 Gb/s) transmission over 40 \times 100 km NZDSF using RZ-DPSK format and all-Raman-amplified spans," presented at Optical Fiber Communications Conference (OFC), Anaheim, CA, 2002.
- [16] A. H. Gnauck, G. Raybon, S. Chandrasekhar, J. Leuthold, C. Doerr, L. Stulz, and E. Burrows, "25 \times 40-Gb/s copolarized DPSK transmission over 12 \times 100-km NZDF with 50-GHz channel spacing," *IEEE Photonics Technology Letters*, vol. 15, pp. 467-9, 2003.
- [17] C. Rasmussen, T. Fjelde, J. Bennike, L. Fenghai, S. Dey, B. Mikkelsen, P. Mamyshev, P. Serbe, P. van der Wagt, Y. Akasaka, D. Harris, D. Gapontsev, V. Ivshin, and P. Reeves-Hall, "DWDM 40G transmission over trans-pacific distance (10 000 km) using CSRZ-DPSK, enhanced FEC, and all-Raman-amplified 100-km UltraWave fiber spans," *Journal of Lightwave Technology*, vol. 22, pp. 203-7, 2004.
- [18] T. Tsuritani, K. Ishida, A. Agata, K. Shimomura, I. Morita, T. Tokura, H. Taga, T. Mizuochi, N. Edagawa, and S. Akiba, "70-GHz-spaced 40 \times 42.7 Gb/s transpacific transmission over 9400 km using prefiltered CSRZ-DPSK signals, all-Raman repeaters, and symmetrically dispersion-managed fiber spans," *Journal of Lightwave Technology*, vol. 22, pp. 215-24, 2004.
- [19] B. Zhu, L. E. Nelson, S. Stulz, A. H. Gnauck, C. Doerr, J. Leuthold, L. Gruner-Nielsen, M. O. Pedersen, J. Kim, R. Lingle, Jr., Y. Emori, Y. Ohki, N. Tsukiji, A. Oguri, and S. Namiki, "6.4-Tb/s (160 \times 42.7 Gb/s) transmission with 0.8 bit/s/Hz spectral efficiency over 32 \times 100 km of fiber using CSRZ-DPSK

format," presented at OFC 2003 - Optical Fiber Communication Conference and Exhibition. Postdeadline Papers, Atlanta, GA, 2003.

- [20] T. Chikama, T. Naitou, H. Onaka, T. Kiyonaga, S. Watanabe, M. Suyama, M. Seino, and H. Kuwahara, "1.2 Gbit/s, 201 km optical DPSK heterodyne transmission experiment using a compact, stable external fibre cavity DFB laser module," *Electronics Letters*, vol. 24, pp. 636-7, 1988.
- [21] T. Chikama, S. Watanabe, T. Naito, H. Onaka, T. Kiyonaga, Y. Onoda, H. Miyata, M. Suyama, M. Seino, and H. Kuwahara, "Modulation and demodulation techniques in optical heterodyne PSK transmission systems," *Journal of Lightwave Technology*, vol. 8, pp. 309-22, 1990.
- [22] R. A. Linke, B. L. Kasper, N. A. Olsson, R. C. Alferness, L. L. Buhl, and A. R. McCormick, "Coherent lightwave transmission over 150 km fiber lengths at 400 Mb/s and 1 Gb/s data rates using DPSK modulation," presented at IOOC-ECOC '85. 5th International Conference on Integrated Optics and Optical Fibre Communication and 11th European Conference on Optical Communication. Technical Digest, Venice, Italy, 1985.
- [23] J. C. Livas, "High sensitivity optically preamplified 10 Gb/s receivers," presented at OFC '96. Optical Fiber Communication. Vol.2 1996 Technical Digest Series. Postconference Edition, San Jose, CA, 1996.
- [24] S. J. B. Yoo, "Optical packet and burst switching technologies for the future photonic Internet," *Journal of Lightwave Technology*, vol. 24, pp. 4468-92, 2006.
- [25] N. Chi, L. Xu, L. Christiansen, K. Yvind, J. Zhang, P. Holm-Nielsen, C. Peucheret, C. Zhang, and P. Jeppesen, "Optical label swapping and packet transmission based on ASK/DPSK orthogonal modulation format in IP-over-WDM networks," presented at OFC 2003 - Optical Fiber Communication Conference and Exhibition. Technical Digest, Atlanta, GA, 2003.
- [26] N. Chi, L. Xu, J. Zhang, P. V. Holm-Nielsen, C. Peucheret, Y. Geng, and P. Jeppesen, "Transmission and optical label swapping for 4 \times 40 Gb/s WDM signals deploying orthogonal ASK/DPSK labeling," *IEEE Photonics Technology Letters*, vol. 17, pp. 1325-1327, 2005.
- [27] T. Koonen, G. Morthier, J. Jennen, H. de Waardt, and P. Demeester, "Optical packet routing in IP-over-WDM networks deploying two-level optical labeling," presented at Proceedings 27th European Conference on Optical Communication, Amsterdam, Netherlands, 2001.
- [28] T. Koonen, Sulur, I. Tafur Monroy, J. Jennen, and H. de Waardt, "Optical labeling of packets in IP-over-WDM networks," presented at ECOC 2002. 28th European Conference on Optical Communication, Copenhagen, Denmark, 2002.
- [29] M. Hickey and L. Kazovsky, "Combined frequency and amplitude modulation for the STARNET WDM computer communication network," *IEEE Photonics*

Technology Letters, vol. 6, pp. 1473-5, 1994.

- [30] G. K. Chang, J. H. Schaffner, M. Z. Iqbal, G. Ellinas, G. L. Tangonan, J. K. Gamelin, and J. L. Pikulski, "Clear channel transmission of ATM/SONET and subcarrier multiplexed signals in a reconfigurable multiwavelength all-optical network testbed," *IEEE Photonics Technology Letters*, vol. 8, pp. 1394-6, 1996.
- [31] C. W. Chow and H. K. Tsang, "Orthogonal label switching using polarization-shift-keying payload and amplitude-shift-keying label," *IEEE Photonics Technology Letters*, vol. 17, pp. 2475-7, 2005.
- [32] T. Flarup, C. Peucheret, J. J. V. Olmos, Y. Geng, J. Zhang, I. T. Monroy, and P. Jeppesen, "Labeling of 40 Gbit/s DPSK payload using in-band subcarrier multiplexing," presented at 2005 Optical Fiber Communications Conference Technical Digest, Anaheim, CA, 2005.
- [33] J. J. V. Olmas, *Label-Controlled Optical Switching Nodes*. Eindhoven, Netherlands: Technische Universiteit Eindhoven, 2006.
- [34] C. Ting-Kuang, S. K. Agrawal, D. T. Mayweather, D. Sadot, C. F. Barry, M. Hickey, and L. G. Kazovsky, "Implementation of STARNET: a WDM computer communications network," *IEEE Journal on Selected Areas in Communications*, vol. 14, pp. 824-39, 1996.
- [35] N. Chi, C. Mikkelsen, X. Lin, Z. Jianfeng, P. V. Holm-Nielsen, H. Ou, J. Seoane, C. Peucheret, and P. Jeppesen, "Transmission and label encoding/erasure of orthogonally labelled signal using 40 Gbit/s RZ-DPSK payload and 2.5 Gbit/s IM label," *Electronics Letters*, vol. 39, pp. 1335-7, 2003.
- [36] N. Chi, L. Xu, J. Zhang, P. V. Holm-Nielsen, C. Peucheret, C. Mikkelsen, H. Ou, J. Seoane, and P. Jeppesen, "Orthogonal optical labeling based on a 40 Gbit/s DPSK payload and a 2.5 Gbit/s IM label," presented at Optical Fiber Communication Conference (OFC), Los Angeles, CA, 2004.
- [37] X. Liu, X. Wei, Y. Su, J. Leuthold, Y.-H. Kao, I. Kang, and R. C. Giles, "Transmission of an ASK-labeled RZ-DPSK signal and label erasure using a saturated SOA," *IEEE Photonics Technology Letters*, vol. 16, pp. 1594-1596, 2004.
- [38] M.-H. Cheung, L.-K. Chen, and C.-K. Chan, "PMD-insensitive OSNR monitoring based on polarization-nulling with off-center narrowband filtering," *IEEE Photon. Technol. Lett.*, vol. 16, pp. 2562-2564, 2004.
- [39] C. Dorrer and X. Liu, "Noise monitoring of optical signals using RF spectrum analysis and its application to phase-shift-keyed signals," *IEEE Photonics Technology Letters*, vol. 16, pp. 1781-3, 2004.
- [40] X. Liu, Y.-H. Kao, S. Chandrasekhar, I. Kang, S. Cabot, and L. L. Buhl, "OSNR Monitoring Method for OOK and DPSK Based on Optical Delay

Interferometer," *IEEE Photonics Technology Letters*, vol. 19, pp. 1172-1174, 2007.

[41] T. Xiangqing, Y. Su, H. Weisheng, L. Lufeng, H. Peigang, H. Hao, D. Yi, and L. Yi, "Precise in-band OSNR and spectrum monitoring using high-resolution swept coherent detection," *IEEE Photonics Technology Letters*, vol. 18, pp. 145-7, 2006.

[42] J. H. Lee, D. K. Jung, C. H. Kim, and Y. C. Chung, "OSNR monitoring technique using polarization-nulling method," *IEEE Photon. Technol. Lett.*, vol. 13, pp. 88-90, 2001.

[43] M. D. Feuer, "Measurement of OSNR in the presence of partially polarized ASE," *IEEE Photon. Technol. Lett.*, vol. 17, pp. 435-437, 2005.

[44] C. Xie, D. C. Kilper, L. Möller, and R. Ryf, "Orthogonal polarization heterodyne OSNR monitoring technique insensitive to polarization effects," presented at Optical Fiber Communications Conference, Anaheim, CA, 2006.

[45] Y.-C. Ku, C.-K. Chan, and L.-K. Chen, "A novel robust OSNR monitoring technique with 40-dB dynamic range using phase modulator embedded fiber loop mirror," presented at Optical Fiber Communications Conference, Anaheim, CA, 2006.

[46] E. Wong, K. L. Lee, and A. Nirmalathas, "Novel in-band optical signal-to-noise ratio monitor for WDM networks," presented at OECC, Seoul, South Korea, 2005.

[47] C. Dorrer and X. Liu, "Advanced optical performance monitoring of differential phase-shift keyed signal using RF spectrum analysis," presented at Conference on Lasers and Electro-Optics (CLEO), San Francisco, CA, 2004.

[48] K. S. Abedin, "Rapid, cost-effective measurement of chromatic dispersion of optical fibre over 1440-1625 nm using Sagnac interferometer," *Electronics Letters*, vol. 41, pp. 469-71, 2005.

[49] A. L. Campillo, "Chromatic dispersion-monitoring technique based on phase-sensitive detection," *IEEE Photonics Technology Letters*, vol. 17, pp. 1241-3, 2005.

[50] T. Kuen Ting and W. I. Way, "Chromatic-dispersion monitoring using an optical delay-and-add filter," *Journal of Lightwave Technology*, vol. 23, pp. 3737-47, 2005.

[51] A. Liu, G. J. Pendock, and R. S. Tucker, "Chromatic dispersion monitoring for systems using dual-drive Mach-Zehnder modulators," presented at 2005 IEEE LEOS Annual Meeting, Sydney, NSW, Australia, 2005.

[52] S. M. R. M. Nezam, L. Ting, J. E. McGeehan, and A. E. Willner, "Enhancing the monitoring range and sensitivity in CSRZ chromatic dispersion monitors

using a dispersion-biased RF clock tone," *IEEE Photonics Technology Letters*, vol. 16, pp. 1391-3, 2004.

[53] L. Ning, Z. Wen-De, S. Ping, L. Chao, and W. Yixin, "Improved chromatic dispersion monitoring technique," *Optics Communications*, vol. 259, pp. 553-61, 2006.

[54] Z. Pan, Q. Yu, Y. Xie, S. A. Havstad, A. E. Willner, D. S. Starodubov, and J. Feinberg, "Chromatic dispersion monitoring and automated compensation for NRZ and RZ data using clock regeneration and fading without adding signaling," presented at OFC 2001. Optical Fiber Communication Conference and Exhibition. Technical Digest, Anaheim, CA, 2001.

[55] M. N. Petersen, Z. Pan, S. Lee, S. A. Havstad, and A. E. Willner, "Online chromatic dispersion monitoring and compensation using a single inband subcarrier tone," *IEEE Photonics Technology Letters*, vol. 14, pp. 570-2, 2002.

[56] Y. Qian, P. Zhongqi, Y. Lian-Shan, and A. E. Willner, "Chromatic dispersion monitoring technique using sideband optical filtering and clock phase-shift detection," *Journal of Lightwave Technology*, vol. 20, pp. 2267-71, 2002.

[57] I. Shake, H. Takara, K. Uchiyama, and Y. Yamabayashi, "Quality monitoring of optical signals influenced by chromatic dispersion in a transmission fiber using averaged Q-factor evaluation," *IEEE Photonics Technology Letters*, vol. 13, pp. 385-7, 2001.

[58] P. S. Westbrook, B. J. Eggleton, T. Her, G. Raybon, and S. Hunsche, "Application of self-phase modulation and optical filtering to measurement of residual chromatic dispersion," presented at Optical Fiber Communications Conference (OFC), Anaheim, CA, 2002.

[59] P. S. Westbrook, B. J. Eggleton, G. Raybon, S. Hunsche, and H. Tsing Hua, "Measurement of residual chromatic dispersion of a 40-Gb/s RZ signal via spectral broadening," *IEEE Photonics Technology Letters*, vol. 14, pp. 346-8, 2002.

[60] S. Ying, C. Minghua, M. Nan, and X. Shizhong, "Chromatic dispersion monitoring technique employing SOA spectral shift in 40Gbit/s system," *Optics Communications*, vol. 249, pp. 79-84, 2005.

[61] Q. Yu, Z. Pan, L.-S. Yan, and A. E. Willner, "Chromatic dispersion monitoring technique using sideband optical filtering and clock phase-shift detection," *Journal of Lightwave Technology*, vol. 20, pp. 2267-2271, 2002.

[62] K. Yuen-Ching, C. Chun-Kit, and C. Lian-Kuan, "Chromatic dispersion monitoring technique using birefringent fiber loop," presented at OFCNFOEC 2006. 2006 Optical Fiber Communication Conference and National Fiber Optic Engineers Conference, Anaheim, CA, 2006.

- [63] S. M. R. M. Nezam, J. E. McGeehan, and A. E. Willner, "Degree-of-polarization-based PMD monitoring for subcarrier-multiplexed signals via equalized carrier/sideband filtering," *Journal of Lightwave Technology*, vol. 22, pp. 1078-85, 2004.
- [64] S. M. R. M. Nezam, Y. W. Song, S. Z. Pan, and A. E. Willner, "PMD monitoring in WDM systems for NRZ data using a chromatic-dispersion-regenerated clock," presented at Optical Fiber Communications Conference (OFC), Anaheim, CA, 2002.
- [65] S. D. Dods and T. B. Anderson, "Optical performance monitoring technique using delay tap asynchronous waveform sampling," presented at 2006 Optical Fiber Communication Conference, and the 2006 National Fiber Optic Engineers Conference, Anaheim, CA, United States, 2006.
- [66] L. Guo-Wei, C. Man-Hong, C. Lian-Kuan, and C. Chun-Kit, "Simultaneous PMD and OSNR monitoring by enhanced RF spectral dip analysis assisted with a local large-DGD element," *IEEE Photonics Technology Letters*, vol. 17, pp. 2790-2, 2005.
- [67] Y. K. Lize, L. Christen, Y. Jeng-Yuan, P. Saghari, S. Nuccio, A. E. Willner, and R. Kashyap, "Independent and simultaneous monitoring of chromatic and polarization-mode dispersion in OOK and DPSK transmission," *IEEE Photonics Technology Letters*, vol. 19, pp. 3-5, 2007.
- [68] T. T. Ng, J. L. Blows, M. Rochette, J. A. Bolger, I. Littler, and B. J. Eggleton, "In-band OSNR and chromatic dispersion monitoring using a fibre optical parametric amplifier," *Optics Express*, vol. 13, 2005.
- [69] Z. Pan, Y. Wang, Y. Song, R. Motaghian, S. Havstad, and A. Willner, "Monitoring chromatic dispersion and PMD impairments in optical differential phaseshift-keyed (DPSK) systems," presented at OFC 2003 - Optical Fiber Communication Conference and Exhibition, Atlanta, GA, 2003.
- [70] G. Rossi, T. E. Dimmick, and D. J. Blumenthal, "Optical performance monitoring in reconfigurable WDM optical networks using subcarrier multiplexing," *Journal of Lightwave Technology*, vol. 18, pp. 1639-48, 2000.
- [71] Y. K. Lize, J.-Y. Yang, L. Christen, S. Nuccio, A. E. Willner, and R. Kashyap, "Simultaneous and Independent Monitoring of OSNR, Chromatic and Polarization Mode Dispersion for NRZ-OOK, DPSK and Duobinary," presented at Optical Fiber Optic Communication Conference, Anaheim, CA, 2007.
- [72] S. B. Jun, K. Hoon, P. K. J. Park, J. H. Lee, and Y. C. Chung, "Pilot-tone-based WDM monitoring technique for DPSK systems," *IEEE Photonics Technology Letters*, vol. 18, pp. 2171-3, 2006.
- [73] A. B. Sahin, L. S. Yan, Y. Qian, M. Hauer, Z. Pan, and A. E. Willner, "Dynamic

dispersion slope monitoring of many WDM channels using dispersion-induced RF clock regeneration," presented at Proceedings 27th European Conference on Optical Communication, Amsterdam, Netherlands, 2001.

- [74] X. Liu, C. Xu, and X. Wei, "Performance analysis of time-polarization multiplexed 40-Gb/s RZ-DPSK DWDM transmission," *IEEE Photonics Technology Letters*, vol. 16, pp. 302-4, 2004.
- [75] I. Kang, C. Xie, C. Dorrer, and A. Gnauck, "Implementations of alternate-polarisation differential-phase-shift-keying transmission," *Electronics Letters*, vol. 40, pp. 333-5, 2004.
- [76] A. H. Gnauck, G. Raybon, P. G. Bernasconi, J. Leuthold, C. R. Doerr, and L. W. Stulz, "1-Tb/s (6×170.6 Gb/s) transmission over 2000-km NZDF using OTDM and RZ-DPSK format," *IEEE Photonics Technology Letters*, vol. 15, pp. 1618-20, 2003.
- [77] M. Nazarathy and E. Simony, "Multichip differential phase encoded optical transmission," *IEEE Photonics Technology Letters*, vol. 17, pp. 1133-5, 2005.
- [78] Y. Yadin, A. Bilenca, and M. Nazarathy, "Soft detection of multichip DPSK over the nonlinear fiber-optic channel," *IEEE Photonics Technology Letters*, vol. 17, pp. 2001-3, 2005.
- [79] F. Seguin and F. Gonthier, "Tunable All-Fiber delay-line interferometer for DPSK demodulation," in *2005 Optical Fiber Communications Conference Technical Digest*, vol. 6. Anaheim, CA: IEEE, 2005, pp. OFL5.
- [80] Y. K. Lize, L. Christen, M. Nazarathy, S. Nuccio, X. Wu, A. E. Willner, and R. Kashyap, "Combination of Optical and Electronic Logic Gates for Error Correction in Multipath Differential Demodulation," *Optics Express*, vol. 15, pp. 6831-6839 2007.
- [81] M. Nazarathy and Y. Yadin, "Simplified decision-feedback-aided multichip binary DPSK receivers," *IEEE Photonics Technology Letters*, vol. 18, pp. 1771-3, 2006.
- [82] T. Mizuochi, K. Kubo, H. Yoshida, H. Fujita, H. Tagami, M. Akita, and K. Motoshima, "Next generation FEC for optical transmission systems," presented at OFC 2003, Atlanta, GA, 2003.
- [83] D. Lombard and J. C. Imbeaux, "Multidifferential PSK-Demodulation for TDMA transmission satellite links," presented at International Conference on Satellite Communication Systems Technology, London, UK, 1975.
- [84] F. Buchali, G. Thielecke, and H. Bulow, "Viterbi equalizer for mitigation of distortions from chromatic dispersion and PMD at 10 Gb/s," presented at OFC 2004, Anaheim, CA, 2004.
- [85] H. Haunstein, R. Schlenk, K. Stiebt, A. Dittrich, W. Sauer-Greff, and R.

Urbansky, "Optimized filtering for electronic equalizers in the presence of chromatic dispersion and PMD," presented at OFC, Anaheim, CA, 2004.

- [86] R. Urbansky, A. Dittrich, W. Sauer-Greff, and H. Haunstein, "Electrical equalization and error correction coding for optical channels," presented at Holey Fibers and Photonic Crystals/Polarization Mode Dispersion/Photonics Time/Frequency Measurement and Control, Digest of the LEOS Summer Topical Meetings, 2003.
- [87] G. Bosco and P. Poggiolini, "The impact of receiver imperfections on the Performance of optical direct-Detection DPSK," *Journal of Lightwave Technology*, vol. 23, pp. 842-8, 2005.
- [88] H. Kim and P. Winzer, "Frequency offset tolerance between optical source and delay interferometer in DPSK and DQPSK systems," presented at OFC 2003 - Optical Fiber Communication Conference and Exhibition, Atlanta, GA, 2003.
- [89] P. J. Winzer and H. Kim, "Degradations in balanced DPSK receivers," *IEEE Photonics Technology Letters*, vol. 15, pp. 1282-4, 2003.
- [90] E. Iannone, F. S. Locati, F. Matera, M. Romagnoli, and M. Settembre, "High-speed DPSK coherent systems in the presence of chromatic dispersion and Kerr effect," *Journal of Lightwave Technology*, vol. 11, pp. 1478-85, 1993.
- [91] W. Jin and J. M. Kahn, "Impact of chromatic and polarization-mode dispersions on DPSK systems using interferometric demodulation and direct detection," *Journal of Lightwave Technology*, vol. 22, pp. 362-71, 2004.
- [92] J. P. Gordon and L. F. Mollenauer, "Phase noise in photonic communications systems using linear amplifiers," *Optics Letters*, vol. 15, pp. 1351-3, 1990.
- [93] Y. K. Lize, L. Christen, P. Saghari, S. Nuccio, A. E. Willner, R. Kashyap, and L. Paraschis, "Implication of Chromatic Dispersion on Frequency Offset and Bit Delay Mismatch Penalty in DPSK Demodulation," presented at 32th European Conference on Optical Communication. ECOC 2006, Cannes, France, 2006.
- [94] Y. K. Lize, L. Christen, X. Wu, J.-Y. Yang, S. Nuccio, T. Wu, A. E. Willner, and R. Kashyap, "Free spectral range optimization of return-to-zero differential phase shift keyed demodulation in the presence of chromatic dispersion," *Optics Express*, vol. 15, pp. 6817-6822, 2007.
- [95] C. Malouin, J. Bennike, and T. Schmidt, "DPSK Receiver Design - Optical Filtering Considerations," presented at OFCNFOEC 2007. 2007 Optical Fiber Communication Conference and National Fiber Optic Engineers Conference, Anaheim, CA, 2007.
- [96] B. Mikkelsen, C. Rasmussen, P. Mamyshev, and F. Liu, "Partial DPSK with excellent filter tolerance and OSNR sensitivity," *Electronics Letters*, vol. 42, pp. 1363-5, 2006.

- [97] Y. K. Lize, X. Wu, L. Christen, M. Faucher, and A. E. Willner, "Free Spectral Range and Optical Filtering Optimization in NRZ-, RZ- and CSRZ-DPSK Demodulation," presented at IEEE Lasers and Electro-Optics Society (LEOS) Annual Meeting, Orlando, Florida, 2007.
- [98] "Wireless LAN Medium Access Control (MAC) and Physical Layer (PHY) specifications," IEEE Std 802.11b-1999 (R2003), 2003.
- [99] "<http://www.bluetooth.com/Bluetooth/Learn/Technology/Specifications/>."
- [100] Y. K. Lize, X. Liu, and R. Kashyap, "Payload and label encoding with high receiver sensitivity using a single Mach-Zehnder modulator," presented at 31st European Conference on Optical Communication, Glasgow, UK, 2005.
- [101] Y. K. Lize, M. Faucher, É. Jarry, P. Ouellette, É. Villeneuve, A. Wetter, and F. Séguin, "Phase-Tunable Low-Loss, S-, C-, and L-band DPSK and DQPSK Demodulator," *IEEE Photonics Technology Letters*, vol. 19, pp. 1886-1888, 2007.
- [102] S. M. R. M. Nezam, Y.-W. Song, C. Yu, J. E. McGeehan, A. B. Sahin, and A. E. Willner, "First-order PMD monitoring for NRZ data using RF clock regeneration techniques," *Journal of Lightwave Technology*, vol. 22, pp. 1086-1093, 2004.
- [103] K. T. Tsai and W. I. Way, "Chromatic-dispersion monitoring using an optical delay-and-add filter," *Journal of Lightwave Technology*, vol. 23, pp. 3737-47, 2005.
- [104] X. Wei, X. Liu, and C. Xu, "Numerical simulation of the SPM penalty in a 10-Gb/s RZ-DPSK system," *IEEE Photonics Technology Letters*, vol. 15, pp. 1636-8, 2003.
- [105] C. P. Kaiser, P. J. Smith, and M. Shafi, "An improved optical heterodyne DPSK receiver to combat laser phase noise," *Journal of Lightwave Technology*, vol. 13, pp. 525-33, 1995.
- [106] M. Nazarathy and E. Simony, "Generalized Stokes parameters shift keying approach to multichip differential phase encoded optical modulation formats," *Optics Letters*, vol. 31, pp. 435-7, 2006.
- [107] J. Wang and J. M. Kahn, "Impact of chromatic and polarization-mode dispersions on DPSK systems using interferometric demodulation and direct detection," *Journal of Lightwave Technology*, vol. 22, pp. 362-71, 2004.
- [108] L. Christen, Y. K. Lize, S. Nuccio, J. Y. Yang, P. Saghari, A. E. Willner, and L. Paraschis, "Fiber Bragg grating balanced DPSK demodulation," presented at 2006 IEEE LEOS Annual Meeting Conference, Montreal, Que., Canada, 2006.
- [109] Y. K. Lize, L. Christen, M. Nazarathy, Y. Atzmon, S. Nuccio, P. Saghari, R. Gomma, J.-Y. Yang, R. Kashyap, A. E. Willner, and L. Paraschis, "Tolerances and Receiver Sensitivity Penalties of Multi-bit Delay Differential Phase Shift

Keying Demodulation," *IEEE Photonics Technology Letters*, vol. 19, 2007.

- [110] H. Kim and P. J. Winzer, "Robustness to laser frequency offset in direct-detection DPSK and DQPSK systems," *Journal of Lightwave Technology*, vol. 21, pp. 1887-91, 2003.
- [111] X. Zhou, J. Yu, T. Wang, and G. Zhang, "Impact of strong optical filtering on DQPSK modulation formats," presented at European Conference on Optical Communications (ECOC), 2007.
- [112] M. Harris, J. Yu, and G.-K. Chang, "Impact of Free Spectral Range on RZ/NRZ DQPSK modulation format with strong optical filtering for ultra-high data systems," presented at IEEE Lasers and Electro-Optics Society Annual meeting, Orlando, Florida, 2007.
- [113] Y. K. Lize, X. Wu, M. Nazarathy, Y. Atzmon, L. Christen, S. Nuccio, M. Faucher, N. Godbout, and A. E. Willner, "Chromatic dispersion tolerance in optimized NRZ-, RZ- and CSRZ-DPSK demodulation," *Optics Express*, vol. 16, pp. 4228-4236 2008.

Appendices

Appendix I

Single Modulator Payload/Label Encoding and Node Operations for Optical Label Switching

Yannick Keith Lizé, *Student Member, IEEE*, Xiang Liu, *Senior Member, IEEE*, and Raman Kashyap, *Member, IEEE*

Abstract—We present and analyze payload/label encoding based on a single Mach–Zehnder modulator, in which the payload is differential phase-shift keyed and the label is amplitude-shift keyed through modulation of either the modulator bias or the amplifier gain. The encoding is analyzed numerically and experimentally. Simultaneous encoding of a 10-Gb/s payload and a 155-Mb/s label is demonstrated with high receiver sensitivities. Penalty-free transmission over 80 km of standard single-mode fiber is achieved for both the payload (with dispersion compensation) and the label (without dispersion compensation). Furthermore, polarization-independent label processing and payload wavelength conversion at intermediate nodes are proposed for potentially cost-effective node operations.

Index Terms—Differential phase-shift keying (DPSK), Mach–Zehnder modulator (MZM), optical label switching.

I. INTRODUCTION

OPTICAL packet switching (OPS) and optical burst switching (OBS) are regarded as promising next-generation transport technologies [1]. One optically labeled packet transmission scheme is based on an orthogonal intensity modulation/differential phase-shift keying (IM/DPSK) modulation format, in which the payload is amplitude-shift keyed and the label is differential phase-shift keyed [3]. Other schemes with the payload modulation being frequency-shift keying [4], subcarrier modulation [5], or polarization-shift keying [6], have also been demonstrated. It was recently found that using DPSK/IM for payload/label modulation and using a balanced receiver for DPSK detection provide superior receiver sensitivity for both the label and payload [7], [8]. In these optical label encoding schemes, two optical modulators are required, one for the payload encoding and the other for the label encoding. More recently, a single modulator has been used for simultaneous payload and label encoding [9]. In this letter, we present detailed theoretical and experimental analyses of the single modulator-based payload/label encoding scheme. We also propose novel polarization-independent label processing and payload wavelength conversion schemes at intermediate nodes.

Manuscript received January 24, 2006; revised February 12, 2006. The work of Y. K. Lizé and R. Kashyap was supported by the Canadian Institute for Photonic Innovations (CIP) and by the Canadian Research Chairs Program.

Y. K. Lizé and R. Kashyap are with the Advanced Photonics Laboratory, Physics Engineering Department, Ecole Polytechnique de Montréal, Montréal, QC H3C 3A7, Canada (e-mail: yannick.lize@polymtl.ca).

X. Liu is with Bell Laboratories, Lucent Technologies, Holmdel, NJ 07733 USA (e-mail: xliu20@lucent.com).

Digital Object Identifier 10.1109/LPT.2006.873925

II. THEORY

The output optical field of a Mach–Zehnder modulator (MZM) biased at extinction can be expressed as

$$E_{\text{out}}(t) = E_{\text{in}} \cdot \frac{(\mu e^{j\varphi_{\text{upper}}(t)} - e^{-j\varphi_{\text{lower}}(t)})}{2} \quad (1)$$

where E_{in} and E_{out} are the input and output optical fields, respectively, and φ_{upper} and φ_{lower} are induced phase changes in the upper and lower arms of the MZM by applied voltages. With balanced driving, we have $\varphi_{\text{upper}}(t) = -\varphi_{\text{lower}}(t) = \varphi(t)$ and

$$\varphi(t) = \frac{\pi}{V_{\pi}} [V_p D_p(t) + \Delta V_{\text{bias}}] \quad (2)$$

where V_p is the amplitude of the data modulation, $D_p(t) = \pm 0.5$ is the ac-coupled payload data, and ΔV_{bias} is the bias voltage offset from the extinction point. A nonreturn-to-zero signal is generated with $V_p = \Delta V_{\text{bias}} = 0.5V_{\pi}$, and an ideal DPSK signal is generated with $V_p = V_{\pi}$ and $\Delta V_{\text{bias}} = 0$. One advantageous feature of DPSK generation is that even when the MZM is not fully driven or not perfectly biased, exact phase encoding can still be achieved over the center portion of each bit period. This feature is exploited to modulate the amplitude of a high-speed DPSK payload signal for label encoding [9]. In the first single MZM label/payload encoding scheme illustrated in Fig. 1 (top), the RF port of the MZM is used to encode the DPSK payload while the label is encoded by modulating the bias port between the null point and a small fraction of V_{π} . The phase modulation $\varphi(t)$ can be expressed as

$$\varphi(t) = \frac{\pi}{V_{\pi}} [V_p D_p(t) + V_l D_l(t) + \Delta V_{\text{bias}}] \quad (3)$$

where V_l is the amplitude of the label modulation and $D_l(t) = \pm 0.5$ is the label data. In the second scheme illustrated in Fig. 1 (bottom), the drive voltage output of the RF driver is modulated between V_p and $(V_p - V_l)$ by the label data. Preferably, $V_p = V_{\pi}$. The phase modulation $\varphi(t)$ can be expressed as

$$\varphi(t) = \frac{\pi}{V_{\pi}} V_p D_p \cdot \left[1 - \frac{V_l}{V_p} (0.5 - D_l) \right]. \quad (4)$$

III. NUMERICAL AND EXPERIMENTAL RESULTS

The experimental setup is illustrated on Fig. 2. For both schemes, direct detection of the label is achieved with an inexpensive low-speed receiver while the DPSK payload is decoded by using an optical 1-bit delay interferometer before detection by either a single or a balanced detector. A pseudorandom binary sequence pattern of $2^{15} - 1$ is used for the payload

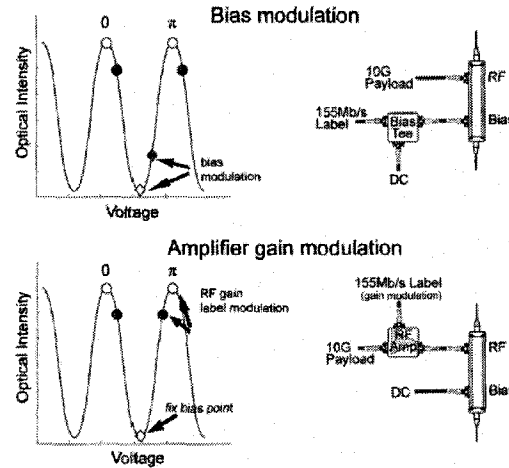


Fig. 1. Transfer functions and implementations of label encoding through bias modulation (top) and drive-voltage modulation (bottom). Empty (filled) circles illustrate payload modulation when label bit is a "1" ("0"). Diamonds mark the bias position.

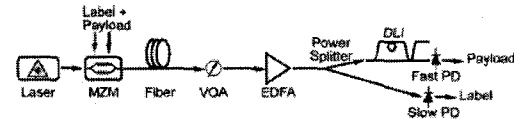


Fig. 2. Experimental setup for testing the two schemes for optical label encoding using a single MZM.

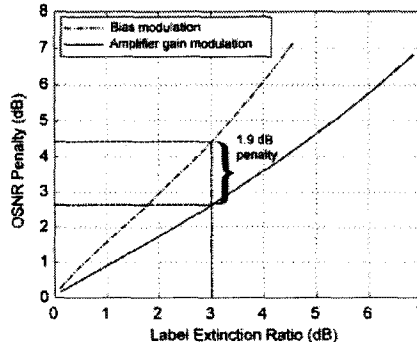


Fig. 3. Simulated payload OSNR penalty as a function of the label ER for the two encoding schemes.

while a $2^7 \sim 1$ for the label, the payload is at 10 Gb/s and the label is 155 Mb/s. The effective bandwidth of the bias port used is ~ 300 MHz, and the gain modulation bandwidth of the RF amplifier is ~ 500 MHz. These bandwidths and, therefore, the label bit rate can be increased through better RF packaging.

Fig. 3 illustrates the payload optical signal-to-noise ratio (OSNR) penalty versus the label extinction ratio (ER) showing better performance for the amplifier gain modulation scheme. Fig. 4 shows the measured BER versus the received power for

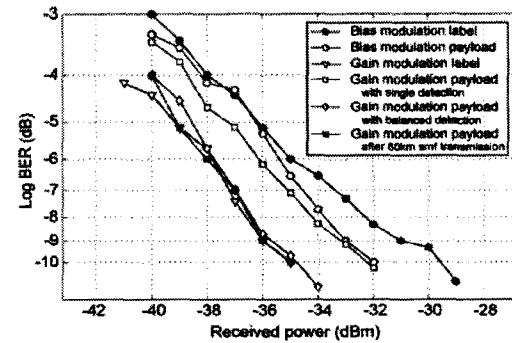


Fig. 4. Measured back-to-back BER versus received optical power. As expected, a 3-dB improvement is observed between single detection and balanced detection. No penalty is observed after 80-km transmission.

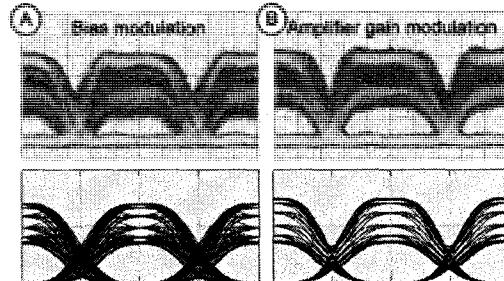


Fig. 5. Eye diagrams of the 10-Gb/s payload with label encoded through (a) the bias modulation and (b) amplifier gain modulation with similar ER for the label in each case.

a 3-dB label ER. In the bias modulation scheme, the measured receiver sensitivities (at $\text{BER} = 10^{-9}$) are -31 dBm for the label and -33 dBm for the payload, respectively. In the amplifier gain modulation scheme, the receiver sensitivities for the label and payload are both -36 dBm. The payload receiver sensitivity becomes -33 dBm when a single detector is used for the DPSK detection. No penalty is observed on both the label and payload after 80-km transmission through a standard single-mode fiber.

Both simulation and experiment show that the amplifier gain label modulation scheme outperforms the bias modulation scheme by about 2 dB for a 3-dB label ER. Fig. 5 shows the experimental and simulated eye diagrams of the payload. Simulation results show that timing jitter [9] and higher frequency components in the bias modulation scheme may explain the difference in performance.

IV. LABEL PROCESSING AND WAVELENGTH CONVERSION

In an optical label switched network, label swapping, including label removal and label reinsertion, must be realizable at intermediate nodes. Different methods to perform these functions inexpensively have been studied and implemented [10]–[15]. Using a polarization-insensitive saturated semiconductor optical amplifier [11], these functions can be achieved in

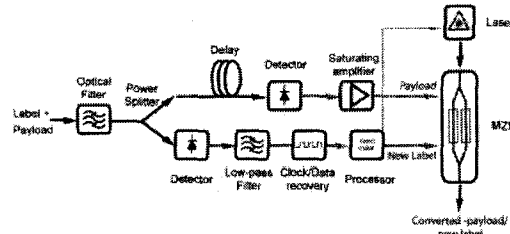


Fig. 6. Label processing and payload wavelength conversion in an intermediate node.

the optical domain for the DPSK/IM encoding scheme where the slow intensity variation can be effectively erased while the payload remains intact. By taking advantage of the single modulator techniques and readily available RF components, label erasure, label reinsertion, and wavelength conversion may be achieved more economically in the RF domain, with no concern for the polarization dependence. For label removal at an intermediate node, a saturating RF amplifier can be used after the payload/label signal is detected, as shown in Fig. 6.

Although wavelength conversions can be performed through nonlinear processes, they are intrinsically polarization dependent, have limited bandwidth, and require sufficiently high optical power (through per-channel-based amplification). With the single MZM scheme, wavelength conversion may be cost-effectively realized by using a wavelength-tunable laser, which operates over a very broad wavelength range. A packet leaving a node may also retain its original wavelength, which is not usually feasible in nonlinear wavelength converters.

V. CONCLUSION

We have presented a detailed study on two single modulator-based payload/label encoding techniques for optical label switching. The amplifier gain modulation scheme outperforms the bias modulation scheme by approximately 2 dB. Polarization-independent label processing and payload wavelength conversion at intermediate nodes based on electrical domain signal processing are proposed. By providing simplicity and potential cost-effectiveness, these payload/label encoding techniques and node operation schemes may be attractive in future OPS and OBS networks.

ACKNOWLEDGMENT

The authors thank C. R. Giles and X. Wei for valuable discussions.

REFERENCES

- [1] S. Yoo, "Optical-packet switching and optical-label switching technologies for the next generation optical internet," in *Proc. Optical Fiber Communications (OFC 2003)*, Atlanta, GA, 2003, Paper FS5.
- [2] D. J. Blumenthal, B. E. Olsson, G. Rossi, T. E. Dimmick, L. Rau, M. Masanovic, O. Lavrova, R. Doshi, O. Jerphagnon, J. E. Bowers, V. Kaman, L. A. Coldren, and J. Barton, "All-optical label swapping networks and technologies," *J. Lightw. Technol.*, vol. 18, no. 12, pp. 2058–2075, Dec. 2000.
- [3] T. Koonen, G. Morthier, J. Jeannen, H. Waardt, and P. Demeester, "Optical packet routing in IP-over-WDM networks deploying two-level optical labeling," in *Proc. Eur. Conf. Optical Communications (ECOC 2001)*, 2001, pp. 14–15.
- [4] M. Hickey and L. Kazovsky, "Combined frequency and amplitude modulation for the STARNET WDM computer communication network," *IEEE Photon. Technol. Lett.*, vol. 6, no. 12, pp. 1473–1475, Dec. 1994.
- [5] G.-K. Chang and J. Yu, "Multirate payload switching using a swappable optical carrier suppressed label in a packet-switched DWDM optical network," *J. Lightw. Technol.*, vol. 23, no. 1, pp. 196–202, Jan. 2005.
- [6] C. W. Chow, C. S. Wong, and H. K. Tsang, "Optical packet labeling based on simultaneous polarization shift keying and amplitude shift keying," *Opt. Lett.*, vol. 29, pp. 1861–1863, Aug. 2004.
- [7] X. Liu, Y. Su, X. Wei, J. Leuthold, and R. C. Giles, "Optical-label switching based on DPSK/ASK modulation format with balanced detection for DPSK payload," in *Proc. Eur. Conf. Optical Communications (ECOC 2003)*, Rimini, Italy, 2003, Paper Tu4.4.3.
- [8] X. Liu, X. Wei, Y. Su, J. Leuthold, Y.-H. Kao, I. Kang, and R. C. Giles, "Transmission of an ASK-labeled RZ-DPSK signal and label erasure using a saturated SOA," *IEEE Photon. Technol. Lett.*, vol. 16, no. 6, pp. 1594–1596, Jun. 2004.
- [9] Y. K. Lize, X. Liu, and R. Kashyap, "Payload and label encoding with high receiver sensitivity using a single Mach-Zehnder modulator," in *Proc. Eur. Conf. Optical Communications (ECOC 2005)*, Glasgow, Scotland, 2005, Paper Mo4.4.3.
- [10] J. Yu, G. K. Chang, and Q. Yang, "Optical label swapping in a packet-switched optical network using optical carrier suppression, separation, and wavelength conversion," *IEEE Photon. Technol. Lett.*, vol. 16, no. 9, pp. 2156–2158, Sep. 2004.
- [11] B. Meagher, G. K. Chang, G. Ellinas, Y. M. Lin, W. Xin, T. F. Chen, X. Yang, A. Chowdhury, J. Young, S. J. Yoo, C. Lee, M. Z. Iqbal, T. Robe, H. Dai, Y. J. Chen, and W. I. Way, "Design and implementation of ultra-low latency optical label switching for packet-switched WDM networks," *J. Lightw. Technol.*, vol. 18, no. 2, pp. 1987–1978, Feb. 2000.
- [12] S. J. B. Yoo, H. J. Lee, Z. Pan, J. Cao, Y. Zhang, K. Okamoto, and S. Karner, "Rapidly switching all-optical packet routing system with optical-label swapping incorporating tunable wavelength conversion and a uniform-loss cyclic frequency AWGR," *IEEE Photon. Technol. Lett.*, vol. 14, no. 5, pp. 1211–1213, May 2002.
- [13] N. Chi, J. Zhang, P. V. Holm-Nielsen, L. Xu, I. T. Monroy, C. Peucheret, K. Yvind, L. J. Christensen, and P. Jeppesen, "Experimental demonstration of cascaded transmission and all-optical label swapping of orthogonal IM/FSK labeled signal," *Electron. Lett.*, vol. 39, no. 8, pp. 676–678, 2003.
- [14] W. Huang, C. Chan, L. Chen, and F. Tong, "A bit-serial optical packet label-swapping scheme using DPSK encoded labels," *IEEE Photon. Technol. Lett.*, vol. 15, no. 11, pp. 1630–1632, Nov. 2003.
- [15] J. Yu and G. K. Chang, "A novel technique for optical label and payload generation and multiplexing using optical carrier suppression and separation," *IEEE Photon. Technol. Lett.*, vol. 16, no. 1, pp. 320–322, Jan. 2004.

Appendix II

Independent and Simultaneous Monitoring of Chromatic and Polarization-Mode Dispersion in OOK and DPSK Transmission

Yannick Keith Lizé, *Student Member, IEEE*, Louis Christen, *Student Member, IEEE*, Jeng-Yuan Yang, Poorya Saghari, *Student Member, IEEE*, Scott Nuccio, *Student Member, IEEE*, Alan E. Willner, *Fellow, IEEE*, and Raman Kashyap, *Member, IEEE*

Abstract—We propose and demonstrate a novel technique for a simultaneous chromatic and first-order polarization-mode-dispersion (PMD) monitoring method using a partial bit delay Mach-Zehnder interferometer (MZI) with radio-frequency (RF) clock tone monitoring. RF clock tones at the output of the two branches of the MZI behave oppositely with increasing chromatic dispersion (CD) which improves the sensitivity of the measurement. The technique increases CD monitoring sensitivity over standard clock tone methods by a factor of two for a nonreturn-to-zero intensity modulation format and a factor of five for a differential-phase-shift-keying modulation format. The accuracy of PMD monitoring is also enhanced. Moreover, the partial bit delay allows the signal to pass through the constructive branch of the MZI with no observable degradation of the signal quality, allowing it to be normally detected by a receiver.

Index Terms—Chromatic dispersion (CD), monitoring, optical fiber communication, polarization-mode dispersion (PMD).

1. INTRODUCTION

SIMULTANEOUS and isolated monitoring of the sources of signal degradations is a laudable goal for stable and robust optical communication systems. Such optical performance monitoring could enable networks to efficiently diagnose and compensate deleterious effects. Key degrading effects that a network operator may want to monitor include chromatic dispersion (CD) and polarization-mode dispersion (PMD). Several approaches have been proposed in the literature to monitor CD and PMD: 1) using sideband optical filtering and clock phase-shift detection to monitor CD [1]; 2) CD monitoring technique based on phase-sensitive detection [2]; 3) using a dispersion-biased radio-frequency (RF) clock tone to monitor CD [3]; 4) using an optical delay-and-add filter to monitor CD [4]; and 5) using

Manuscript received July 13, 2006; revised October 27, 2006. This work was supported by the National Science Foundation (NSF) Contract SA3398-22390PG. The work of Y. K. Lizé and R. Kashyap was supported by the Canadian Institute for Photonic Innovations. The work of R. Kashyap was also supported by the Canadian Natural Sciences and Engineering Research Council.

Y. K. Lizé is with Viterbi School of Engineering, Department of Electrical Engineering, University of Southern California, Los Angeles, CA 90089 USA, the Advanced Photonics Concepts Laboratory, École Polytechnique de Montréal, Montréal H3T 1J4, Canada, and also with ITF Laboratories, 400 Montpellier, Montréal H4N 2G7, Canada (e-mail: yannick.lize@polymtl.ca).

L. Christen, J.-Y. Yang, P. Saghari, S. Nuccio, and A. E. Willner are with the Viterbi School of Engineering, Department of Electrical Engineering, University of Southern California, Los Angeles, CA 90089 USA.

R. Kashyap is with the Advanced Photonics Concepts Laboratory, École Polytechnique de Montréal, Montréal H3T 1J4, Canada.

Digital Object Identifier 10.1109/LPT.2006.888039

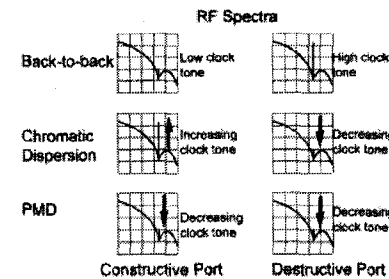


Fig. 1. Conceptual diagram of how the clock tone behaves after the constructive and destructive arm of the partial bit DLI under CD and PMD. The asymmetry in the behaviors allows the isolation of the two effects.

equalized carrier/sideband filtering to monitor degree-of-polarization based PMD [5], CD-regenerated clock tone fading for PMD monitoring [6]. However, all of these techniques either monitor only CD or only PMD, but not both simultaneously. Some reports have presented both CD and PMD monitoring using polarization modulation [7] and asynchronous amplitude histogram evaluation [8], but require more than one monitoring technique.

One simple and cost-effective approach for performance monitoring is to measure the RF power in the clock tone using a narrowband electrical filter and a power meter. This method can be used to track accumulation of either CD or PMD [9]. Unfortunately, it does not allow isolation and simultaneous monitoring given that both effects will have an influence on the clock tone power.

We propose and demonstrate a technique that simultaneously monitors and isolates CD and first-order PMD for nonreturn-to-zero (NRZ) ON-OFF keying (OOK) and differential-phase-shift-keying (DPSK) signals. We monitor the RF clock-tone power at the output ports of an unbalanced Mach-Zehnder delay line interferometer (DLI) with a quarter bit delay in one arm [10]. It is observed that the clock power from the constructive port of the DLI grows with an increase in CD and with a decrease in PMD, whereas the clock power from the destructive port grows with a decrease in both CD and PMD (as in Fig. 1). By appropriately adding and subtracting the constructive and destructive clock powers, we can simultaneously derive the individual contributions of CD and first-order PMD while increasing the sensitivity.

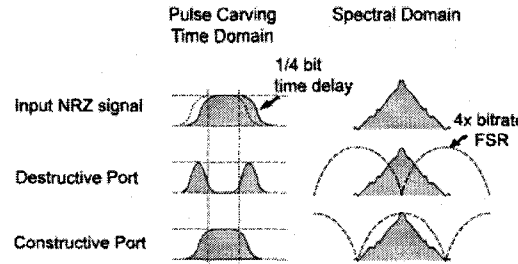


Fig. 2. Partial-bit DLI for NRZ signals. A small fraction of the bit interferes with the following bit for pulse carving in the destructive port, resulting in a strong clock tone. There is little degradation at the constructive port due to the high FSR.

We demonstrate PMD-insensitive CD monitoring over 600 ps/nm at 10 Gb/s while increasing the sensitivity by 220% to 0.055 dB/(ps/nm) for OOK and by 550% to 0.044 dB/(ps/nm) for DPSK over standard clock tone monitoring [3]. We also demonstrate CD-insensitive PMD monitoring over 50 ps with an average sensitivity of 0.25 dB/ps for both OOK and DPSK.

II. BACKGROUND THEORY

We use a DLI similar to that in [7] from ITF Laboratories [11] but with a 1/4-bit-time delay in one arm and without any modifications to the transmitter. The transmission peak of the interferometer is biased at maximum/minimum power in the constructive/deconstructive arm, and both DLI outputs are utilized in the monitoring process. As illustrated in Fig. 2, the response in the constructive port is essentially transparent to the signal due to the high free-spectral range (FSR) ($4 \times$ the data rate). The destructive output of the DLI is a return-to-zero (RZ) signal with a strong RF clock tone present. Inside the DLI, the signal interferes with itself for 3/4 of the bit period and interferes with the phase of the following bit for the other 1/4 of the bit period, resulting in RZ pulses as illustrated in Fig. 2. The 1/4-bit-time value was chosen as a reasonable tradeoff between constructive port penalty for data detection and destructive port pulse-carving for monitoring.

As illustrated in Fig. 1, the 10-G clock tones on the two outputs of the 1/4-bit-delay DLI are dependent on dispersion and PMD. The increase in clock tone power with increasing CD at the constructive port is well known for NRZ [3]. At the destructive port, CD spreads the input pulses in time, thereby lowering the peak power in the output RZ pulses and therefore the clock tone power. The dephasing effect of PMD on the clock tone reduces its intensity [6]. Utilization of this feature allows isolation and simultaneous measurement of CD and PMD. The monitoring can be loosely conceptualized by the two functions

$$f(\text{CD}) \Rightarrow P_{\text{const}}(\uparrow \text{CD}, \downarrow \text{PMD}) - P_{\text{dest}}(\downarrow \text{CD}, \downarrow \text{PMD}) \quad (1)$$

$$f(\text{PMD}) \Rightarrow P_{\text{const}}(\uparrow \text{CD}, \downarrow \text{PMD}) + P_{\text{dest}}(\downarrow \text{CD}, \downarrow \text{PMD}) \quad (2)$$

where P_{const} is the clock tone power at the constructive arm which grows with CD and decreases with PMD. P_{dest} is the

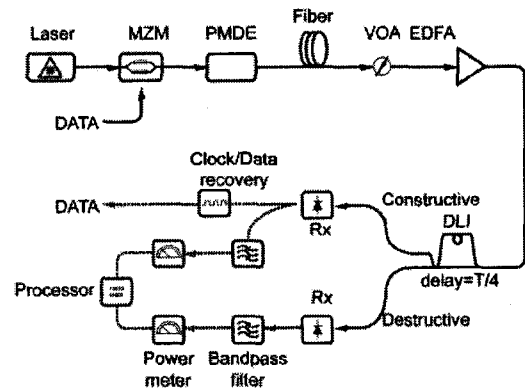


Fig. 3. Experimental setup using fiber for CD and a PMD emulator for DGD. Bandpass filters centered at 10-GHz filter out the clock tone.

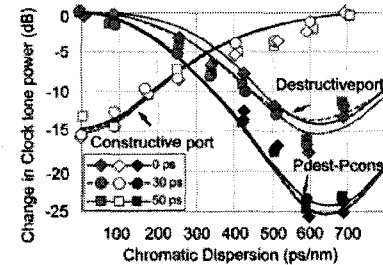


Fig. 4. DPSK clock tone power change versus dispersion for different DGD values. Experiments (dots) and simulation (lines) show that DGD does not affect the change in power versus dispersion. Maximum clock tone power is at 0 ps/nm in the destructive arm and 700 ps/nm for the constructive arm. Subtracting the two curves isolates the effect of CD and increases sensitivity.

clock tone power at the destructive arm which decreases with both CD and PMD. The inverse relationship allows for removal of the PMD in the subtraction and CD in the addition, thereby isolating both effects. This also has the added property of increasing the sensitivity of the CD measurement. Unfortunately this method is not appropriate for RZ-type formats since they already have strong clock tone power and do not benefit from the partial bit delay clock-tone generating DLI.

III. RESULTS

Experimental demonstration was performed using the setup of Fig. 3. Optical fibers were used to vary dispersion and a PMD emulator to vary DGD. The transmission peak of the interferometer was easily adjusted by maximizing power in the constructive arm or minimizing power in the destructive arm.

Figs. 4 and 5 illustrate simulation and experimental results of the change in clock tone power versus dispersion at the constructive and destructive arm of the DLI for different values of DGD. Subtracting the two curves isolates the effect of PMD and increases sensitivity. At a bit-error rate of 10^{-9} , we observed a penalty <0.1 dB in the constructive arm in comparison to direct detection for OOK and DPSK which indicates that the signal

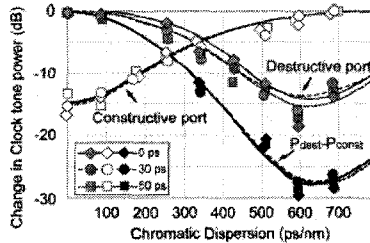


Fig. 5. OOK clock tone power change versus dispersion for different DGD values. Experiments (dots) and simulation (lines) show that DGD does not affect the change in power versus dispersion. Maximum clock tone power is at 0 ps/nm in the destructive arm and 700 ps/nm for the constructive arm. Subtracting the two curves isolates the effect of CD and increases sensitivity.

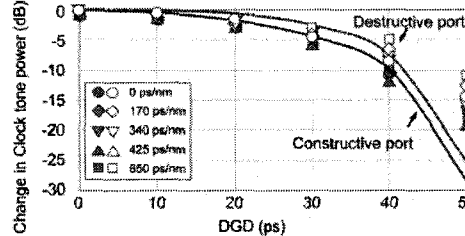


Fig. 6. OOK clock tone power versus PMD values for the constructive and destructive port for different values of CD. Lines are simulation and points are experimental data.

through the constructive port can be used for standard detection.

Although DGD affects the clock tone power [6], it does not affect the change in power versus CD. Experimental results are in agreement with simulations for both PMD and CD measurements.

Using (1) and the results of Figs. 4 and 5, we obtain PMD-insensitive CD measurements to within 0.1 dB. For NRZ-OOK, the monitoring sensitivity is increased by 220% from 0.0245 dB/(ps/nm) for standard clock tone detection to 0.055 dB/(ps/nm) using our method. For DPSK, the sensitivity is increased by 550% from 0.008 dB/(ps/nm) using a single clock tone detection to 0.044 dB/(ps/nm) with our method. Experiments and simulation results show a CD monitoring range from 0–600 ps/nm. We measured up to 50 ps of DGD with an average sensitivity of 0.25 dB/ps for both OOK and DPSK as illustrated in Fig. 6 for OOK and Fig. 7 for DPSK.

IV. CONCLUSION

We have demonstrated a simultaneous CD and first-order PMD monitoring method using a partial bit delay Mach-Zehnder interferometer (MZI)-assisted RF clock tone monitoring which isolates the two effects while improving

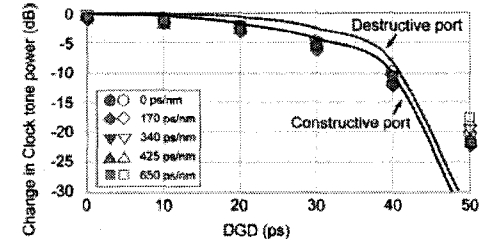


Fig. 7. DPSK clock tone power versus PMD values for the constructive and destructive port for different values of CD. Lines are simulation and points are experimental data.

sensitivity. Monitoring the two branches improves CD monitoring sensitivity over standard clock tone method by a factor of two for NRZ and five for DPSK. In the constructive arm, the MZI acts as an optical bandpass filter reducing the ASE noise without deteriorating the data signal.

REFERENCES

- [1] Q. Yu, Z. Pan, L.-S. Yan, and A. E. Willner, "Chromatic dispersion monitoring technique using sideband optical filtering and clock phase-shift detection," *J. Lightw. Technol.*, vol. 20, no. 12, pp. 2267–2271, Dec. 2002.
- [2] A. L. Campillo, "Chromatic dispersion-monitoring technique based on phase-sensitive detection," *IEEE Photon. Technol. Lett.*, vol. 17, no. 6, pp. 1241–1243, Jun. 2005.
- [3] S. M. R. Motaghian, T. Luo, J. E. McGeehan, and A. E. Willner, "Enhancing the monitoring range and sensitivity in CSRZ chromatic dispersion monitors using a dispersion-biased RF clock tone," *IEEE Photon. Technol. Lett.*, vol. 16, no. 5, pp. 1391–1393, May 2004.
- [4] K. T. Tsai and W. I. Way, "Chromatic-dispersion monitoring using an optical delay-and-add filter," *J. Lightw. Technol.*, vol. 23, no. 11, pp. 3737–3747, Nov. 2005.
- [5] S. M. R. M. Nezam, J. E. McGeehan, and A. E. Willner, "Degree-of-polarization-based PMD monitoring for subcarrier-multiplexed signals via equalized carrier-sideband filtering," *J. Lightw. Technol.*, vol. 22, no. 4, pp. 1078–1085, Apr. 2004.
- [6] S. M. R. M. Nezam, Y.-W. Song, C. Yu, J. E. McGeehan, A. B. Sahin, and A. E. Willner, "First-order PMD monitoring for NRZ data using RF clock regeneration techniques," *J. Lightw. Technol.*, vol. 22, no. 4, pp. 1086–1093, Apr. 2004.
- [7] Y. Shi, M. Chen, and S. Xie, "Simultaneous polarization mode dispersion and chromatic dispersion monitoring method in 40 Gbit/s system by polarization modulation," in *Tech. Dig. OFC 2000*, Baltimore, MD, Paper JTbB39.
- [8] Z. Li and G. Li, "In-service monitoring of chromatic dispersion and polarization mode dispersion for RZ-DPSK signal based on asynchronous amplitude histogram evaluation," in *Tech. Dig. OFC 2006*, Anaheim, CA, Paper OWK3.
- [9] Z. Pan, Q. Yu, Y. Xie, S. A. Havstad, A. E. Willner, D. S. Starodubov, and J. Feinberg, "Chromatic dispersion monitoring and automated compensation for NRZ and RZ data using clock regeneration and fading without adding signaling," in *Tech. Dig. OFC 2001*, Anaheim, CA, Paper WH5-1.
- [10] Y. K. Lize, L. Christen, J.-Y. Yang, P. Saghari, S. Nuccio, A. E. Willner, and R. Kashyap, "Simultaneous monitoring of chromatic dispersion and PMD for OOK and DPSK using partial-bit-delay-assisted clock tone detection," in *Tech. Dig. ECOC 2006*, Cannes, France, Paper Wo4.4.7.
- [11] F. Séguin and F. Gonthier, "Tunable all-fiber delay-line interferometer for DPSK demodulation," in *Tech. Dig. OFC 2005*, Anaheim, CA, Paper OFL5.

Appendix III

Tolerances and Receiver Sensitivity Penalties of Multibit Delay Differential-Phase Shift-Keying Demodulation

Yannick Keith Lizé, *Student Member, IEEE*, Louis Christen, *Student Member, IEEE*,
 Moshe Nazarathy, *Senior Member, IEEE*, Yuval Atzmon, Scott Nuccio, *Student Member, IEEE*,
 Poorya Saghari, *Student Member, IEEE*, Robert Gomma, Jeng-Yuan Yang, Raman Kashyap, *Member, IEEE*,
 Alan E. Willner, *Fellow, IEEE*, and Loukas Paraschis, *Member, IEEE*

Abstract—Multibit delay demodulation of differential-phase shift-keying (DPSK) is finding applications in polarization interleaved modulation, optical time-domain multiplexing (OTDM), and multisymbol DPSK demodulation. Little attention has been paid to the degradation in tolerance and power penalty associated with multibit delay demodulation. We assess experimentally, numerically, and analytically the power penalties and tolerances associated with multibit delay DPSK demodulation. Numerical and analytical results show that the power penalty scales by a small factor of 0.2–0.35 dB per integer bit delay due to laser linewidth (LW) while experimental back-to-back results show a significant 1.2 dB per integer bit delay due to frequency offset penalty of longer bit delays. Frequency offset tolerance scales as 1/bit-delay and the delay-mismatch tolerance decreases by 20% for delays longer than 1 bit. A simple analytic model accounts for the combined effect of LW, frequency offset, and amplified spontaneous emission.

Index Terms—Delay lines, demodulation, differential phase shift keying (DPSK), frequency stability, optical time-domain multiplexing (OTDM), polarization interleaving.

I. INTRODUCTION

DIFFERENTIAL-PHASE shift keying (DPSK) is currently under serious consideration as a deployable data-modulation format for high-capacity optical communication systems due to its high receiver sensitivity and tolerance to certain nonlinear effects. The typical binary DPSK [1] receiver uses a Mach-Zehnder delay-line interferometer (DLI) with balanced detection, and 1-bit delay in one arm, demodulating the differential phase between each data bit and its successor. There has been much recent interest in the concept of modified DLIs with multibit delay in one arm, demodulating the differential phase between successive data bits that are a fixed number

of bit time slots apart. DPSK receivers equipped with such a function are used in the following applications. 1) Demodulating data streams that have been time-multiplexed using polarization interleaving, such that each bit is compared to a previous bit in the same polarization state [2], [3], which can mitigate certain nonlinear effects. 2) Demodulating an optically time-division-multiplexed (OTDM) data stream, such that each data bit is compared to a previous bit from the same transmitter [4]. This is also important in laboratory experiments when using a single transmitter, where the OTDM multiplexer does not provide phase stability. 3) A DPSK receiver using several DLIs of various bit delays, with the DLI outputs all combined using postprocessing, to achieve higher receiver sensitivity [5], [6]. Although DPSK demodulation has been extensively investigated [7]–[10], there has been little discussion on the actual system penalty incurred by multibit delay demodulation [11].

We present experimental results, and numerical and analytic analysis of the penalties associated with multibit DPSK demodulation due to frequency offset (FO) as described in Fig. 1, laser linewidth (LW), and the bit delay offset. Simulation results along with a simple analytic model indicate that the optical signal-to-noise ratio (OSNR) penalty associated with detection through multibit delay scales as 0.2–0.35 dB per integer bit delay at 10 Gb/s with a 10-MHz LW. We also find that the FO tolerance scales as the inverse of the bit delay. Furthermore, the bit delay mismatch penalty increases for 2-bit delay demodulation, but no further degradation occurs for longer delays. These key limitations may reduce the effectiveness of multibit delay methods in some applications.

II. MODEL AND EXPERIMENTAL SETUP

Over a realistic fiber optic link, it has been shown that the total linear and nonlinear phase noise has a nearly Gaussian distribution [12]. Extending the Gaussian approximation to laser-induced phase noise [13], a simple analytic model is derived for M -ary DPSK detection, with Q^2 -factor of the total demodulated Gaussian noisy angle given by

$$Q^2 = (\pi/M - \gamma)^2 / (\sigma_{LN+NL}^2 + \sigma_{LPN}^2) \quad (1)$$

where $\gamma \equiv 2\pi\Delta\nu_c T d$ is the phase offset between the two DLI arms, with $\Delta\nu_c$ the frequency offset away from the optimal optical carrier, σ_{LN+NL}^2 is the variance of the linear and nonlinear phase noise, and the laser phase noise (LPN) variance is given in the first perturbation order by the expression

Manuscript received March 21, 2007; revised August 8, 2007. This work was supported by Cisco Systems and ITL Laboratories.

Y. K. Lizé, L. Christen, S. Nuccio, P. Saghari, J.-Y. Yang, and A. E. Willner are with the Viterbi School of Engineering, University of Southern California, Los Angeles, CA 90089-2565 USA (e-mail: ylize@itl.usc.edu).

M. Nazarathy and Y. Atzmon are with the Electrical Engineering Department, Technion, Israel Institute of Technology, Haifa 32000, Israel.

R. Gomma and R. Kashyap are with the Advanced Photonics Concepts Laboratory, École Polytechnique de Montréal, Montréal, QC H3T 1J4, Canada.

L. Paraschis is with Advanced Technology, Core Routing, Cisco Systems, San Jose, CA 95134 USA.

Color versions of one or more of the figures in this letter are available online at <http://ieeexplore.ieee.org>.

Digital Object Identifier 10.1109/LPT.2007.907577

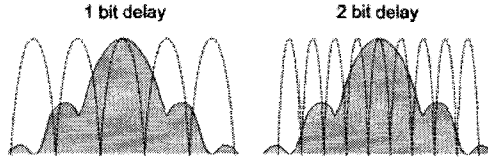


Fig. 1. Spectral response (dash curve) of a 1-bit (left) and 2-bit (right) delay delay-line interferometer overlayed on a DPSK spectrum. The narrower free-spectral range increases the frequency offset sensitivity.

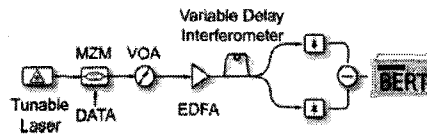


Fig. 2. Experimental setup to obtain receiver sensitivity and OSNR penalty measurements. Different bit delays are obtained through the variable delay interferometer.

$$\sigma_{LPN}^2 = 2\pi\Delta\nu_{LW}T(d - 1/3) \quad (2)$$

with $\Delta\nu_{LW}$ the full-width at half-maximum (FWHM) laser LW, T^{-1} the bit rate, and d the integer number of bit delays. The OSNR penalty in decibel units is readily extracted from (1) and (2) with its functional dependence due to the combined effect of LW, FO, and multibit bit delays

$$-10\log_{10}[1 - 2M\Delta\nu_cTd] + 10\log_{10}\left[1 + \frac{2\pi\Delta\nu_{LW}T(d - \frac{1}{3})}{\sigma_{LN+NL}^2}\right]. \quad (3)$$

The value of σ_{LN+NL}^2 in Figs. 3 and 4 further below was set such that for zero LW and FO penalties the linear phase noise induces a BER of 10^{-9} while the nonlinear phase noise power is zero.

For our experimental results, we constructed a stable delay interferometer with tunable delay providing an FSR ranging from 3.2 to 11 GHz. Two 3-dB fiber couplers were spliced together; one branch wound onto a fixed wheel and the other branch wound on two half wheels with tunable separation, stretching the fiber to provide the variable time delay. The extinction ratio exceeded 15 dB and BER was measured for a 10-Gb/s signal using the setup of Fig. 2.

Simulations were performed for a 10-Gb/s RZ-DPSK signal on a 10-MHz LW laser using 12.5-GHz third-order Gaussian optical filtering and 8-GHz Lorentzian electrical filtering at the receiver. A Karhunen-Loeve expansion for non-Gaussian noise statistics was used with 512 bits simulated at 64 samples per bit. Complete BER versus OSNR curves were simulated and the OSNR penalty at $\text{BER} = 10^{-9}$ was inferred from those curves through a linear fit of the $\log(\text{BER})$ curve.

III. LASER LINewidth PENALTY

With the frequency offset set to zero in (2), the OSNR penalty versus laser LW is illustrated in Fig. 3. At 10-MHz LW and 10 Gb/s, the degradation is ~ 0.35 dB per bit delay. The penalty

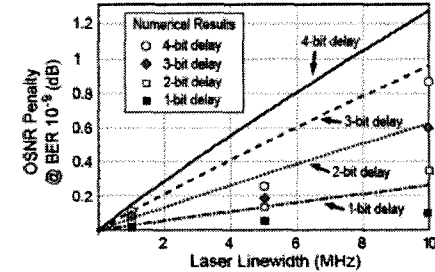


Fig. 3. Analytic (lines) and numerical (dots) results for the OSNR penalty versus laser LW for a 10-Gb/s signal for different bit delay $d = 1, 2, 3, 4$ in the interferometer.

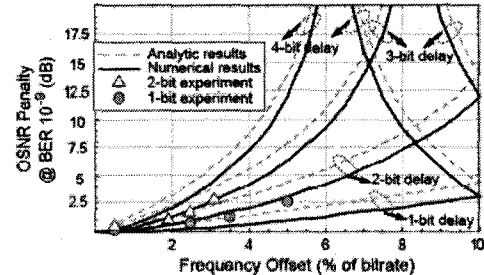


Fig. 4. Analytic, numerical, and experimental results for the OSNR penalty versus frequency offset for different bit delay. The simple analytic model approximates the experimental results while showing similar asymptotic trends of the numerical results.

is associated with the finite coherence time of the laser, or equivalently it is due to the random walk of the phase noise Wiener process, with its variance building up over the multibit delay. For fixed LW and bit delay, increasing the bit rate will decrease the penalty. Simulations show a penalty of 0.2 dB per bit delay at 10 MHz. Since linear phase noise is not exactly Gaussian and our results do not include nonlinear phase noise, there is a small discrepancy between analytic and numerical results.

IV. FREQUENCY OFFSET PENALTY

By setting the laser LW to zero in (2), the analytic penalty due to the frequency offset is as shown in Fig. 4, which also illustrates the simulated frequency offset penalty. The 1-bit delay numerical curve is similar to previously results for 1-bit delay frequency offset [10]. As expected, the frequency offset penalty scales as the inverse of the bit delay such that a 1-dB penalty is obtained for an offset comparable to 4% of the bit rate at 1-bit delay but that the same penalty occurs at 2%, 1.33%, and 1% for 2, 3, and 4 bit delay, as shown in Fig. 4. As expected, the penalty increases with increasing bit delay but decreases with increasing bit rate. Experimental results shown in Fig. 4 exhibit a similar trend as the numerical results, but were found to be more sensitive to frequency offset. Such discrepancy has been observed in other reported experimental results [8]–[10]. There is also a discrepancy between analytic and numerical results which can be explained by the Gaussian phase noise approximation. As

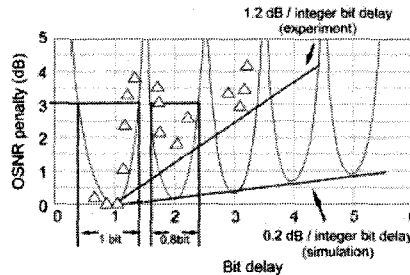


Fig. 5. OSNR penalty versus delay at $\text{BER } 10^{-9}$. Experimental results scale as 1.2 dB per integer bit delay due to frequency offset for longer delays while simulation show a 0.2 dB penalty due to laser LW. The delay mismatch penalty 3 dB range is 1 bit wide around 1-bit delay but only 0.8 bit at greater delays.

expected, both the simple analytic model and simulation results show the same asymptotic behavior versus offset and a decrease in penalty passed 25% of the FSR value. For negligible laser LW, the FO penalty is independent of the linear amplified spontaneous emission (ASE) and nonlinear phase noise (3). This can also be interpreted as independence of the optical filter bandwidth and shape, and was numerically validated.

V. BIT DELAY PENALTY

The OSNR penalty for multibit delay DPSK demodulation in back-to-back transmission is illustrated in Fig. 5. We numerically determined a penalty for multibit delay scaling up with a slope of ~ 0.2 dB per integer bit delay which is in par with analytic and numerical results for laser LW penalty presented in Fig. 4. Experimentally, using a variable delay interferometer, we measured a greater penalty of 1.2 dB per integer bit delay as shown in Fig. 5. We also measured BER versus received power on a different experimental setup using three commercial demodulators with FSRs of 10, 5, and 2.5 GHz. A receiver sensitivity penalty of around ~ 1 dB/integer-bit-delay was again observed.

Our experimental penalty is significantly higher than in the numerical results and also exceeds the previously observed penalty using a 40-Gb/s DPSK signal in a 40-GHz and 10-GHz demodulator [14]. The excess experimental penalty is explained by the use of a tunable FSR demodulator and 5-GHz and 2.5-GHz demodulators that are not phase tunable, causing a frequency offset error due to imperfect alignment of the laser frequency to the transmission peak of the DLLs. Moreover, silica-based interferometers drift with about 1.5 GHz/ $^{\circ}\text{C}$, such that a small temperature change of $\pm 0.1^{\circ}\text{C}$ without active tuning will create a frequency offset of ± 150 MHz. The offset is small for a 40-GHz or 10-GHz demodulator, but will create a significant penalty at 5 or 2.5 GHz.

The bit delay mismatch penalty has been widely investigated [9], [10]. Back-to-back bit delay mismatch penalty can be seen in Fig. 5. The results around 1-bit delay agree with previously reported results. Partial-bit delay mismatch (< 1 bit) incurs a smaller penalty for the same percentage mismatch, since part of the bit interferes with itself, always yielding the same deterministic constructive interference. At multiple bit delays, the time

mismatch translates partial interference with bit n and partial interference with bit $n + 1$ which will yield different interference depending on the phase relationship between n and $n + 1$. The result is that the 3-dB OSNR penalty *bandwidth* on FSR mismatch varies as 1-bit rate for 1-bit delay but tolerance is decreased to 0.8-bit rate for 2-bit delay or more, as illustrated in Fig. 5.

VI. CONCLUSION

The receiver sensitivity penalty associated with multibit delay DPSK demodulation was demonstrated numerically, experimentally, and analytically. The laser LW penalty was shown numerically and analytically to scale as $\sim 0.2\text{--}0.35$ dB per integer bit at 10 Gb/s for a 10-MHz LW. Experimental results show a 1.2-dB penalty per integer bit delay due to reduced frequency offset tolerances which reduce with 1-bit-delay. The delay-mismatch tolerance decreases by 20% for delays longer than one bit. Such limitations may need to be considered for polarization interleaved, OTDM, and multichip DPSK demodulation applications [1].

REFERENCES

- [1] F. Seguin and F. Gonthier, "Tunable all-fiber delay-line interferometer for DPSK demodulation," presented at the 2005 Opt. Fiber Commun. Conf. Tech. Dig., Anaheim, CA, Paper OFL5.
- [2] J. Kang, C. Xie, C. Doerr, and A. Gnauck, "Implementations of alternate-polarisation differential-phase-shift-keying transmission," *Electron. Lett.*, vol. 40, no. 5, pp. 333–335, Mar. 2004.
- [3] X. Liu, C. Xu, and X. Wei, "Performance analysis of time-polarization multiplexed 40-Gb/s RZ-DPSK DWDM transmission," *IEEE Photon. Technol. Lett.*, vol. 16, no. 1, pp. 302–304, Jan. 2004.
- [4] A. H. Gnauck, G. Raybon, P. G. Bernasconi, J. Leuthold, C. R. Doerr, and L. W. Stulz, "1-Tb/s (64 170.6 Gb/s) transmission over 2000-km NZDF using OTDM and RZ-DPSK format," *IEEE Photon. Technol. Lett.*, vol. 15, no. 10, pp. 1618–1620, Nov. 2003.
- [5] M. Nazarathy and Y. Yadin, "Simplified decision-feedback-aided multibit binary DPSK receivers," *IEEE Photon. Technol. Lett.*, vol. 18, no. 16, pp. 1771–1773, Aug. 15, 2006.
- [6] Y. K. Lize, L. Christen, M. Nazarathy, S. Nuccio, X. Wu, A. E. Willner, and R. Kashyap, "Combination of optical and electronic logic gates for error correction in multipath differential demodulation," *Opt. Express*, vol. 15, pp. 6831–6839, 2007.
- [7] G. Bosco and P. Poggiolini, "The impact of receiver imperfections on the performance of optical direct-detection DPSK," *J. Lightw. Technol.*, vol. 23, no. 2, pp. 842–848, Feb. 2005.
- [8] H. Kim and P. J. Winzer, "Robustness to laser frequency offset in direct-detection DPSK and DQPSK systems," *J. Lightw. Technol.*, vol. 21, no. 9, pp. 1887–1891, Sep. 2003.
- [9] Y. K. Lize, L. Christen, X. Wu, J.-Y. Yang, S. Nuccio, T. Wu, A. E. Willner, and R. Kashyap, "Free spectral range optimization of return-to-zero differential phase shift keyed demodulation in the presence of chromatic dispersion," *Opt. Express*, vol. 15, pp. 6817–6822, 2007.
- [10] P. J. Winzer and H. Kim, "Degradations in balanced DPSK receivers," *IEEE Photon. Technol. Lett.*, vol. 15, no. 9, pp. 1282–1284, Sep. 2003.
- [11] Y. K. Lize, L. Christen, S. Nuccio, P. Saghari, R. Gommie, J.-Y. Yang, A. E. Willner, R. Kashyap, and L. Pavesi, "Power penalty in multibit differential phase shift keying demodulation," presented at the 32th Eur. Conf. Opt. Commun., Cannes, France, 2006, Paper Tu3.2.3.
- [12] X. Wei, X. Liu, and C. Xu, "Numerical simulation of the SPM penalty in a 10-Gb/s RZ-DPSK system," *IEEE Photon. Technol. Lett.*, vol. 15, no. 11, pp. 1636–1638, Nov. 2003.
- [13] C. P. Kaiser, P. J. Smith, and M. Shafii, "An improved optical heterodyne DPSK receiver to combat laser phase noise," *J. Lightw. Technol.*, vol. 13, no. 3, pp. 525–533, Mar. 1995.
- [14] C. R. Doerr, M. A. Cappuzzo, E. Y. Chen, A. Wong-Foy, L. T. Gomez, S. S. Patel, S. Chandrasekhar, and A. E. White, "Polarization-insensitive planar lightwave circuit dual-rate Mach-Zehnder delay-interferometer," *IEEE Photon. Technol. Lett.*, vol. 18, no. 16, pp. 1708–1710, Aug. 15, 2006.

Appendix IV

Combination of optical and electronic logic gates for error correction in multipath differential demodulation

Yannick Keith Lize^{1,2,3}, Louis Christen², Moshe Nazarathy⁴, Scott Nuccio⁵, Xiaoxia Wu, Alan E. Willner², Raman Kashyap³

¹Optical ITF Laboratories, 400 Montpellier, Montreal, Québec, H4N 2G7, Canada;

²University of Southern California, Viterbi School of Engineering, Los Angeles, CA, USA;

³École Polytechnique de Montréal, Engineering Physics Department, Montréal, Québec, Canada.,

⁴Techinon, Israel Institute of Technology, EE Department, Haifa, Israel.

yannick.lize@gmail.com

<http://www.itflabs.com>

Abstract: We present an optical multipath error correction technique for differentially encoded modulation formats such as differential-phase-shift-keying (DPSK) and differential polarization shift keying (DPoSK) for fiber-based and free-space communication. This multipath error correction method combines optical and electronic logic gates. The scheme can easily be implemented using commercially available interferometers and high speed logic gates and does not require any data overhead therefore does not affect the effective bandwidth of the transmitted data. It is not merely compatible but also complementary to error correction codes commonly used in optical transmission systems such as forward-error-correction (FEC). The technique consists of separating the demodulation at the receiver in multiple paths. Each path consists of a Mach-Zehnder interferometer with a different integer bit delay used in each path. Some basic logic operations follow and the three paths are compared using a simple majority vote algorithm. Experimental results show that the scheme improves receiver sensitivity by 1.5 dB at BER of 10^{-3} in back-to-back configuration. Numerical results indicate a 1.6 dB improvement in the presence of Chromatic Dispersion for a 25% increase in tolerance for a 3dB penalty from ± 1220 ps/nm to ± 1520 ps/nm. and a 0.35 dB improvement for back-to-back operation.

©2007 Optical Society of America

OCIS codes: (060.2330) Fiber optics communications, (060.5060) Phase modulation, (060.2360) Fiber optics links and subsystems.

References and links

1. A. H. Gnauck and P. J. Winzer, "Optical phase-shift-keyed transmission," *J. Lightwave Technol.* **23**, 115-130. (2005).
2. P. J. Winzer and R. -J. Essiambre, "Advanced modulation formats for high-capacity optical transport networks," *J. Lightwave Technol.* **24**, 4711-4728 (2006).
3. A. H. Gnauck, "40-Gb/s RZ-differential phase shift keyed transmission," in *Proc. OFC2003*, paper ThE1, (2003).
4. X. Liu, "Nonlinear effects in phase shift keyed transmission," in *Proc. OFC2004*, paper ThM4 (2004).
5. X. Liu, Y.-H. Kao, M. Movassaghi, and R. C. Giles, "Tolerance to in-band coherent crosstalk of differential phase-shift-keyed signal with balanced detection and FEC," *IEEE Photon. Technol. Lett.* **16**, 1209-1911 (2004).
6. F. Seguin, and F. Gonthier, "Tunable all-fiber, delay-line interferometer for DPSK demodulation," in *Proc. OFC2005*, paper OFL5, (2005).
7. M. Nazarathy and E. Simony, "Multi-Chip Differential Phase Encoded Optical Transmission," *IEEE Photon. Technol. Lett.* **17**, 1133-1135 (2005).
8. Y. Yadin, A. Bileica, and M. Nazarathy, "Soft detection of multichip DPSK over the nonlinear fiber-optic channel," *IEEE Photon. Technol. Lett.* **17**, 2001-2003 (2005).

9. X. Liu, "Digital implementation of soft detection for 3-chip-DBPSK with improved receiver sensitivity and dispersion tolerance," in Proc. OFC2006, paper OTu12, (2006).
10. M. Nazarathy, X. Liu, Y. Yadin, and M. Orenstein, "Multi-chip detection of optical differential phase-shift keying and complexity reduction by interferometric decision feedback," in Proc. ECOC2006, We3.P.79, (2006).
11. M. Nazarathy and Y. Yadin, "Simplified decision feedback-aided multi-chip binary DPSK receivers," IEEE Photon. Technol. Lett. **18**, 1771 - 1773 (2006).
12. X. Liu, "Receiver sensitivity improvement in optical DQPSK and DQPSK/ASK through data-aided multi-symbol phase estimation," in Proc. ECOC2006, We2.5.6 (2006).
13. X. Liu, X. Liu, S. Chandrasekhar, A. H. Gnauck, C. R. Doerr, I. Kang, D. Kilper, L. L. Buhl, and J. Centanni, "DSP-enabled compensation of demodulator phase error and sensitivity improvement in direct-detection 40-Gb/s DQPSK, postdeadline paper Tb4.4.5 in ECOC'06 Cannes, France, 2006.
14. M. Nazarathy, Y. Yadin, M. Orenstein, Y. K. Lize, L. Christen, and Alan Willner, "Enhanced self-coherent optical decision-feedback-aided detection of multi-symbol M-DPSK/PolSK in particular 8-DPSK/BPolSK at 40 Gbps," Optical Fiber Conference, paper JWA43, Anaheim, CA (2007).
15. L. Christen, Y. K. Lize, S. R. Nuccio, X. Liu, M. Nazarathy, and A. E. Willner, "DPSK error correction using multi-bit detection for enhanced sensitivity and compensation of impairments," in Proc. OFC2007, paper JThA50, Anaheim, CA (2007).
16. T. Mizuochi, K. Kubo, H. Yoshida, H. Fujita, H. Tagami, M. Akita, and K. Motoshima, "Next generation FEC for optical transmission systems," in Proc. OFC 2003, paper ThN1, Atlanta, GA, (2003).
17. D. Lombard and J. C. Imbeaux, "Multidifferential PSK-demodulation for TDMA transmission," in Proc. International Conference on Satellite Communication Systems Technology, (1975), pp. 207-213.
18. F. Buchali, G. Thielecke, and H. Bulow, "Viterbi equalizer for mitigation of distortions from chromatic dispersion and PMD at 10 Gb/s," in Proc. OFC2004, paper MF85, (2004).
19. H. Haunstein, R. Schlenk, K. Stiebt, A. Dittrich, W. Sauer-Greff, and R. Urbansky, "Optimized filtering for electronic equalizers in the presence of chromatic dispersion and PMD," in Proc. OFC2004, paper MF6, (2004).
20. H. Haunstein, R. Schlenk, K. Stiebt, A. Dittrich, W. Sauer-Greff, and R. Urbansky, "Control of combined electrical feed-forward and decision feedback equalization by conditional error counts from FEC in the presence of PMD," in Proc. OFC2003, 2, pp. 474-476.
21. R. Urbansky, A. Dittrich, W. Sauer-Greff, and H. Haunstein, "Electrical equalization and error correction coding for optical channels," Holey Fibers and Photonic Crystals/Polarization Mode Dispersion/Photonics Time/Frequency Measurement and Control, 2003 Digest of the LEOS Summer Topical Meetings, (2003), pp. WB1.1/59-WB1.1/60.
22. Y. K. Lize, L. Christen, S. Nuccio, P. Saghari, R. Gomma, J.-Y. Yang, A. E. Willner, and R. Kashyap, "Power penalty in multibit differential phase shift keying demodulation," in Proc. ECOC2006, paper Tu3.2.3, Cannes, France (2006).

1. Introduction

Differentially encoded optical modulation formats such as differential phase shift keying (DPSK), Quadrature DPSK (DQPSK) and differential polarization shift keying (DPolSK) generated considerable attention in the past 5 years. DPSK is currently under serious consideration as a deployable data-modulation format for high-capacity optical communication systems due to its 3 dB OSNR advantage over intensity modulation and its non-linear tolerance [1-6]. However DPSK OSNR requirements are still 1.2 dB higher than for its coherent counterpart, PSK for a BER of 10^{-3} . Multi-symbol processing strategies have been proposed to reduce this penalty through soft detection, including decision feedback based techniques [7-15], providing \sim 1-3 dB sensitivity improvements for DPSK optical transmission, however the analog or high-speed digital soft detection feedback electronics remain challenging to implement. It would be advantageous to attain comparable processing gains over multiple demodulation paths with hard detection rather than soft detection, i.e. by applying digital logic processing on the balanced outputs of multiple Mach-Zehnder Delay Interferometers (DLI). Forward error correction (FEC) is now commonly used in most types of long-haul transmission systems. With only a 7% overhead, enhanced FEC (eFEC) can convert a 2×10^{-3} error to 1×10^{-15} while Super FEC with a 25% overhead, can correct errors from as low as 6×10^{-3} [16]. When error rates exceed those values, FEC becomes somewhat inefficient. It would be useful to have an error correction algorithm that could take a poor error rate and bring it to a FEC-capable error rate without affecting the effective bandwidth of the transmission.

In this paper we propose and experimentally demonstrate an optical multi-path error correction technique for differentially encoded modulation formats. The scheme can be readily implemented using commercially available DLIs [6] and high-speed logic gates. After optical demodulation and hard detection, basic logic operations are applied on each path to recover the data signal. The partially correlated errors induced by ASE noise are then corrected using a simple majority-vote algorithm [17]. We find through numerical simulations that back-to-back DPSK receiver sensitivity is improved by 0.35 dB at BER of 10^{-3} with optimal filtering and 0.45dB in a 25GHz channel. In chromatic dispersion (CD) -limited channels such as in fiber optic transmission, we numerically obtain a 1.6 dB improvement and the tolerance to CD is increased by 25% from ± 1220 ps/nm to ± 1520 ps/nm. Experimentally we measured a 1.5 dB sensitivity improvement. The main advantage of the proposed method is that it does not require any data overhead and hence its performance improvement is attained without affecting the effective bandwidth of the transmitted data. This diversity demodulation scheme is compatible with and complementary to error correction techniques commonly used in optical transmission systems such as forward-error-correction (FEC). Since the error correction is obtained through hard detection, it is also compatible with soft electronic distortion compensation schemes such as feed forward equalization (FFE), decision feedback equalization (DFE), and maximum likelihood sequence estimation (MLSE) [18-21]. The scheme is differentiated from [7-14] in that it is a hard detection scheme and could therefore be combined with the other soft detection multipath-methods. Furthermore, we present here an experimental and numerical demonstration at 10 Gbps whereas [7-11, 14] were numerical demonstrations.

2. Theory

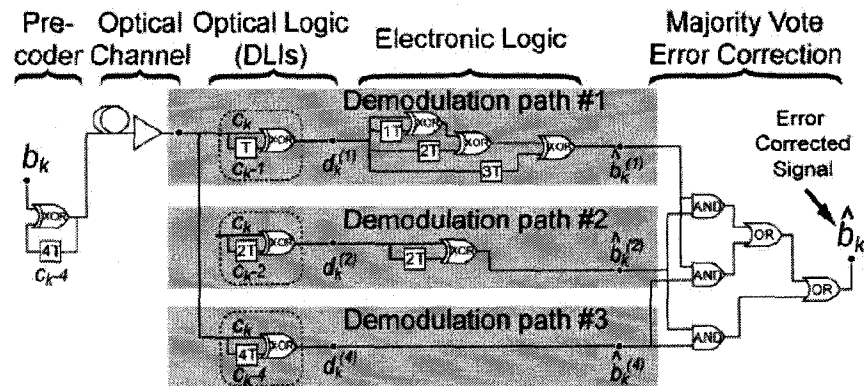


Fig. 1. Conceptual diagram of multipath demodulation with majority vote error correction. The DPSK precoder uses a 4-bit delay. The optical logic is performed by the passive DLI DPSK demodulator. The electronic logic recovers the original signal before majority vote is applied.

The scheme takes advantage of the combination of the optical logical XOR function of the DLI and electronic binary logic gates. A simple logic representation of the system is illustrated in Fig. 1. A modified 4-bit form of Differential Precoding (DP) is performed at the transmitter prior to optical modulation. The received signal is corrupted by amplified spontaneous emission (ASE) noise accumulated along the transmission fiber from amplifiers. Optical demodulation is performed using multiple demodulation paths each consisting of a DLI with a different integer bit-delay. The bits are then detected. The output of the 4-bit delay DLI recovers the proper transmitted bits, since a 4-bit differential precoder is used at the transmitter. Electronic logic blocks consisting of XOR gates and delays follow the outputs of

the 2-bit and 1-bit delay DLIs, re-aligning the three paths together. Finally error-correction is performed through a simple majority vote algorithm. The digital processing can be described by Eqs. (1)-(4), where \oplus , $\&$, $|$ respectively denote the XOR (addition-modulo-2), AND, OR logic functions:

$$c_k = b_k \oplus c_{k-4} \quad (1)$$

represents the differential encoder using a 4 bit delay where b_k is the information message bit in time bin k , and c_k is the differentially encoded message transmitted in the channel, as shown in Fig. 1. Next,

$$\begin{aligned} d_k^{(1)} &= c_k \oplus c_{k-1} \oplus \varepsilon_k^{(1)} \\ d_k^{(2)} &= c_k \oplus c_{k-2} \oplus \varepsilon_k^{(2)} \\ d_k^{(4)} &= c_k \oplus c_{k-4} \oplus \varepsilon_k^{(4)} \end{aligned} \quad (2)$$

represent the optical differential demodulations for the 1-bit, 2-bit and 4-bit delay DLIs, where d is the data after optical demodulation of c , and ε is the noise in the transmitted time bins. Then

$$\begin{aligned} \hat{b}_k^{(1)} &= d_k^{(1)} \oplus d_{k-1}^{(1)} \oplus d_{k-2}^{(1)} \oplus d_{k-3}^{(1)} \\ \hat{b}_k^{(2)} &= d_k^{(2)} \oplus d_{k-2}^{(2)} \\ \hat{b}_k^{(4)} &= d_k^{(4)} \end{aligned} \quad (3)$$

represent the electronic XOR gates necessary to realign all 4 paths to the initial signal where

$$\hat{b}_k = \hat{b}_k^{(1)} \& \hat{b}_k^{(2)} | \hat{b}_k^{(1)} \& \hat{b}_k^{(3)} | \hat{b}_k^{(2)} \& \hat{b}_k^{(3)} \quad (4)$$

represents the majority vote error correction algorithm using the bit stream from all three DLIs.

Referring to the bit intervals $T=1/R$ (with R the bitrate) the DP performs a modulo-2 addition of the current transmitter output bit with the input data bit $4T$ seconds earlier, i.e. it implements an accumulator with 4-bit delay, whereas conventional DPSK uses a DP with 1-bit delay.

First, assume that there are no errors, i.e. $\varepsilon_k^{(1)} = \varepsilon_k^{(2)} = \varepsilon_k^{(4)} = 0$. Applying the identity $a \oplus a = 0$, it follows from (1)-(4) that the output of the 4-bit delay DLI (yielding the estimate $\hat{b}_k^{(4)}$) correctly recovers the transmitted stream, and so do $\hat{b}_k^{(2)}$ and $\hat{b}_k^{(1)}$:

$$\begin{aligned}
\hat{b}_k^{(4)} &= d_k^{(4)} = c_k \oplus c_{k-4} = b_k \oplus c_{k-4} \oplus c_{k-4} = b_k \\
\hat{b}_k^{(2)} &= d_k^{(2)} \oplus d_{k-2}^{(2)} = (c_k \oplus c_{k-2}) \oplus (c_{k-2} \oplus c_{k-4}) \\
&= c_k \oplus c_{k-2} \oplus c_{k-2} \oplus c_{k-4} = c_k \oplus c_{k-4} = d_k^{(4)} = b_k \\
\hat{b}_k^{(1)} &= d_k^{(1)} \oplus d_{k-1}^{(1)} \oplus d_{k-2}^{(1)} \oplus d_{k-3}^{(1)} \\
&= c_k \oplus c_{k-1} \oplus c_{k-1} \oplus c_{k-2} \oplus c_{k-2} \oplus c_{k-3} \oplus c_{k-3} \oplus c_{k-4} = c_k \oplus c_{k-4} = b_k
\end{aligned} \tag{5}$$

Extending the model to include the additively injected error indicators $\varepsilon_k^{(i)}, i = 1, 2, 4$ at the DLI outputs yields after some manipulation

$$\hat{b}_k^{(\Delta)} = b_k \oplus \eta_k^{(i)}, \quad i \in \{1, 2, 4\} \tag{6}$$

where $\eta_k^{(i)}$ are effective binary noise streams at the majority-vote input, given by

$$\eta_k^{(1)} \equiv \varepsilon_k^{(1)} \oplus \varepsilon_{k-1}^{(1)} \oplus \varepsilon_{k-2}^{(1)} \oplus \varepsilon_{k-3}^{(1)}, \quad \eta_k^{(2)} \equiv \varepsilon_k^{(2)} \oplus \varepsilon_{k-2}^{(2)}, \quad \eta_k^{(4)} \equiv \varepsilon_k^{(4)} \tag{7}$$

Notice that the underlying noise bits of the form $\varepsilon_k^{(i)}$ are not statistically independent, hence nor are the effective noise bits $\{\eta_k^{(1)}, \eta_k^{(2)}, \eta_k^{(4)}\}$ independent.

It is apparent that (6) defines an effective binary channel wherein b_k repetition-coded with 3-fold diversity, i.e. the same bit is transmitted over three scalar binary channels corrupted by the partially correlated effective noises. The proposed decoding scheme applies a simple majority-vote strategy reducing the probability of errors, relative to a single use of either one of the three paths, and also provides improvement relative to conventional DPSK. When errors are uncorrelated in each demodulation path, the correction rate of majority vote is determined by the individual Error Rates (ER):

$$[ER^{(1)} \cdot ER^{(2)} \cdot (1 - ER^{(4)})] + [ER^{(1)} \cdot (1 - ER^{(2)}) \cdot ER^{(4)}] + [(1 - ER^{(1)}) \cdot ER^{(2)} \cdot ER^{(4)}]$$

This is the upper limit of majority vote error detection. Since there is only partial correlation between the effective noise bits, there is a low probability that two or three of the paths assume the same value simultaneously. The majority vote correction method is analogous to what has been proposed in the RF domain at MHz speed [17]. Combining soft FEC or soft detection techniques with this method could be done immediately after the interferometers in Fig. 1 before a hard decision is made to obtain $d_k^{(1)}, d_k^{(2)}, d_k^{(4)}$.

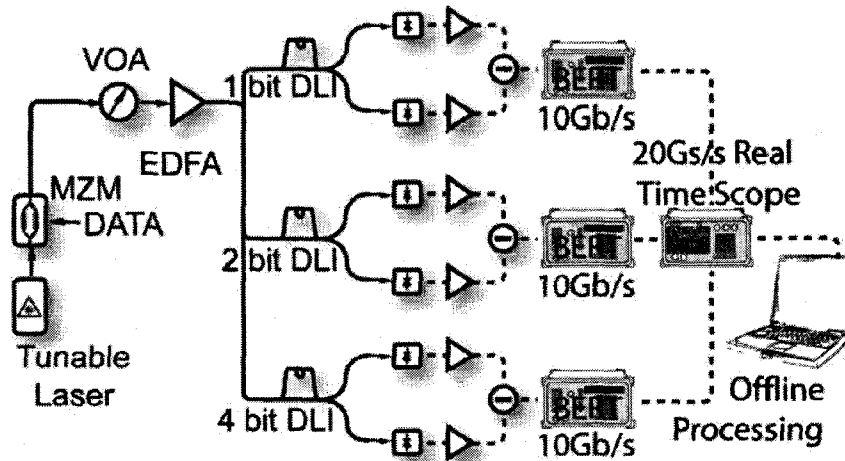


Fig. 2. Experimental setup for the demonstration of multipath DPSK demodulation majority vote error correction. Using 3 commercial DLIs, three 10Gbps bit error rate tester and a 20Gs/s real time scope. Logic operations were processed offline.

3. Results

Monte Carlo simulations were performed using a $2^{15}-1$ pseudo random bit sequence (PRBS) at 10Gbps with 12.5 GHz optical filter and 8 GHz electrical filtering at the receiver. Using these parameters we find an improvement in receiver sensitivity of 0.35dB at BER of 10^{-3} as illustrated in Fig. 3. Our simulation of BER versus OSNR curve for standard back-to-back DPSK, which would overlap with the 4 bit delay demodulation in Fig. 3, agrees with previously published results [9] yielding confidence in our numerical results. Figure 3 also provides the theoretical limit of majority vote error correction (ideal majority vote) assuming the errors were completely uncorrelated, confirming that in multi-path demodulation, errors are partially correlated. The theoretical limit when the demodulation paths are completely independent allows a 1.2×10^{-2} error rate to become 2×10^{-3} suitable for eFEC or it allows a 2.1×10^{-2} error rate to reach 6×10^{-3} suitable for Super FEC. In a back-to-back transmission, errors are somewhat correlated in each demodulation path such that the coding reduces, correcting a 2.6×10^{-3} BER to a 2×10^{-3} BER and 6.92×10^{-3} BER to a 6×10^{-3} BER. Transmission impairments (i.e. chromatic dispersion (CD), polarization mode dispersion (PMD), non-linear phase noise, cross-phase-modulation), and receiver degradations (i.e. non-ideal filtering, DLI's frequency offset) result in decorrelated errors between demodulation paths. Figure 3, also illustrates that error propagation due to the 4-bit precoding doubles the errors of the 2-bit delay demodulation and quadruples the errors in the 1-bit delay. Nonlinear phase is an important degradation in DPSK transmission systems. The other multipath schemes [7-14] also exhibited increased performance in the presence of nonlinear degradations, which can explain the decorrelation of errors between the paths. We would expect majority vote error correction to perform closer to its theoretical limit in the presence of non-linear phase.

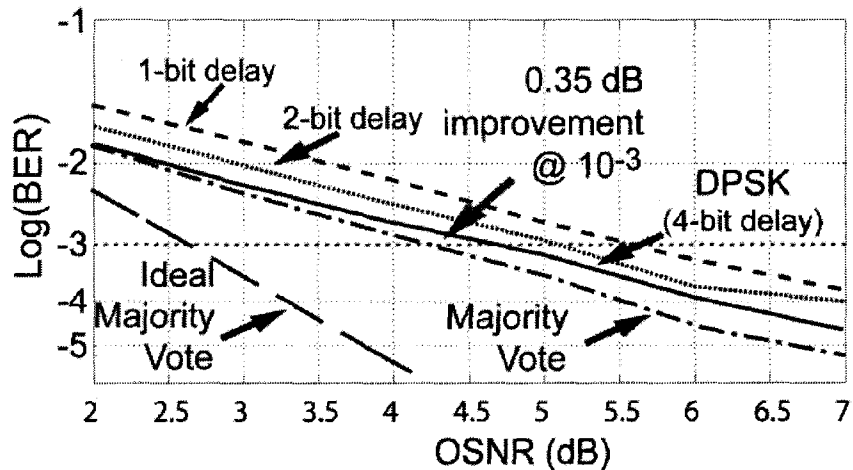
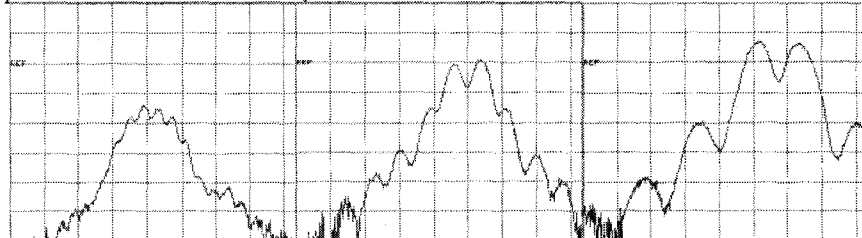


Fig. 3. Numerical results for the 1 bit-delay, the 2 bit delay and 4-bit delay paths and majority vote. Ideal majority vote performance if errors were uncorrelated is shown.

We performed experimental verification using the setup illustrated in Fig. 2. A $2^{15}-1$ PRBS pattern was phased modulated at 10Gbps and then sent through a variable attenuator and erbium amplifier. The DPSK demodulators from ITF Laboratories had FSR's of 10GHz, 5GHz and 2.5GHz providing 1, 2 and 4 bit delay. A 70 Ghz optical filter was used and the 3 photodiodes had bandwidths of approximately 8GHz. The three paths were detected simultaneously using three receivers and three bit-error-rate testers. Only the destructive arm of the DLI was detected since we lacked access to three balanced receivers. The detected bits were then fed into a 20Gsample/s real time oscilloscope with sufficient memory for offline-process of 500 000 bits for each path.



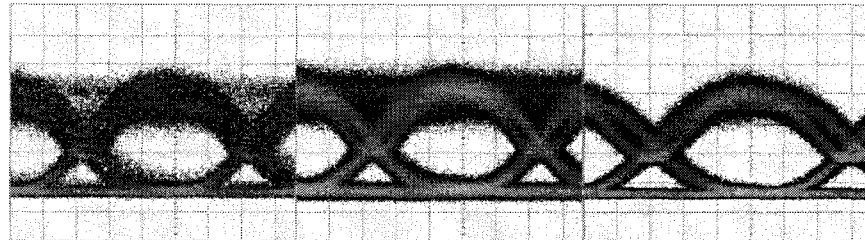


Fig. 5. Eye diagrams of the destructive port for 4 bit delay, 2bit delay and 1 bit delay demodulator. The longer delays demodulator were passive devices in our experiment making them more difficult to align the frequency of the laser to the transmission frequency of the DLI which resulted in a penalty.

The experimental BER improvement is illustrated on Fig. 6. At a BER of 10^{-3} , the back-to-back improvement is 1.5dB and the method was demonstrated capable of correcting a 5×10^{-2} to 2×10^{-3} for eFEC and of 1×10^{-2} to 6×10^{-3} for SuperFEC.

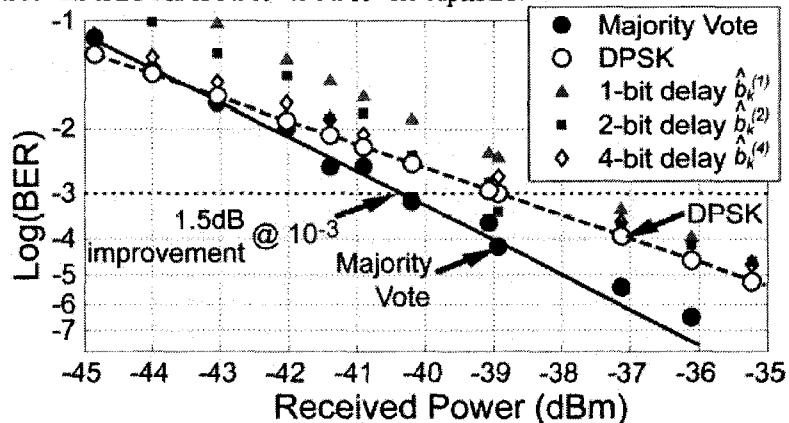


Fig. 6. Experimental results for the 3 paths and the majority vote combined output. A 1.5dB is observed at BER 10^{-3} in back-to-back configuration. The better experimental results are a result of errors being decorrelated between path due to non-optimal optical and electrical filtering and modulator driving voltage slightly less than $2V\pi$.

To explain the superior experimental performance we simulated the required OSNR for a BER of 10^{-3} at 10Gbps for different combinations of optical and electrical filtering bandwidth. Figures 7 & 8 illustrate the simulated contour plots. With majority vote error correction, the effect of optimizing the optical filtering is less significant which can be quite advantageous in multi-wavelength system where filtering is limited to the wavelength demultiplexer. The discrepancy can then be partly explained as due to non-ideal optical and electrical filtering in our experiment. The experimental discrepancy is further explained by frequency offsets on the longer delay DLIs which creates uncorrelated errors [22] in the three paths, thus bringing the performance of majority vote error correction closer to the ideal majority vote theoretical error correction limit illustrated in Fig. 3.

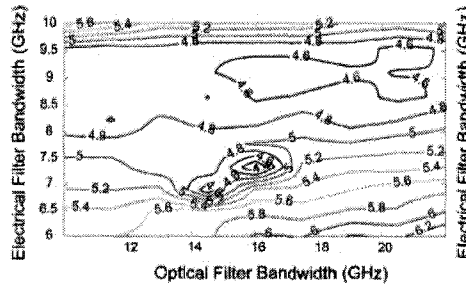


Fig. 7. DPSK contour plot of required OSNR at BER 10^{-3} for electrical and optical filter bandwidth combination.

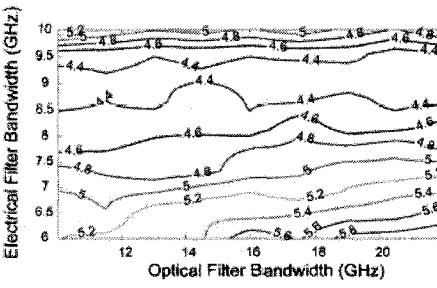


Fig. 8. Majority vote multipath demodulation contour plot showing very good tolerance to optical filtering.

4. Chromatic dispersion sensitivity

Chromatic dispersion in the demodulated signal may lead to beneficial decorrelation of the errors in each path. Such uncorrelated errors improve the performance of the method by bringing the correction efficiency closer to the theoretical limit illustrated in Fig. 3. Figure 5 illustrates numerical results for CD sensitivity. The baseline curve matches previously reported results for CD tolerance for NRZ-DPSK and as expected, majority vote provides a 1.6 dB improvement at a BER of 10^{-3} . Chromatic dispersion tolerance for a 3dB penalty is increased by 25% from ± 1220 ps/nm to ± 1520 ps/nm.

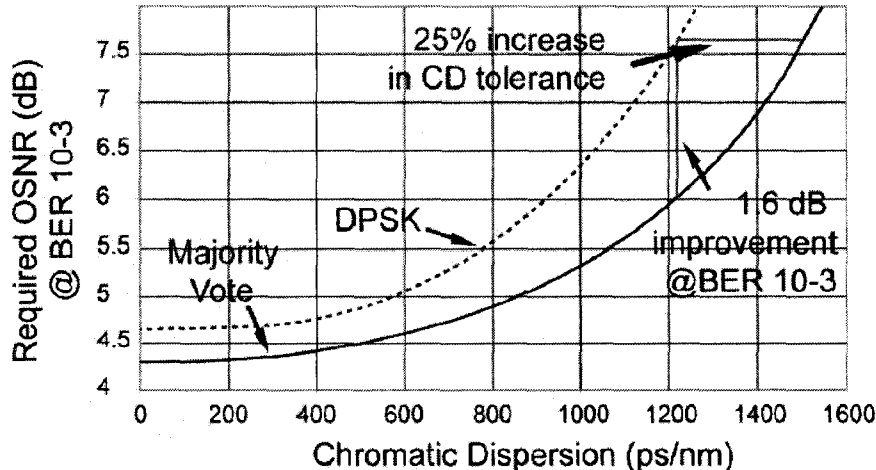


Fig. 9. OSNR penalty versus CD for DPSK and majority vote demodulation. A 25% increase in CD tolerance is found for a 1.6dB improvement at BER= 10^{-3} .

5. Conclusion

We proposed and demonstrated experimentally and numerically an optical multi-path demodulation error correction technique for differentially encoded modulation formats. By combining optical and electronic logic gates we find that DPSK receiver sensitivity is improved by 0.35 dB numerically and 1.5 dB experimentally at BER 10^{-3} . The method increases chromatic dispersion tolerance by 25% while increasing optical and electrical filtering tolerances. The method does not require any error correction overhead and is complementary to other electronic distortion compensation schemes such as MLSE and DFE, and error correction algorithms such as forward-error-correction (FEC).

Appendix V

Free spectral range optimization of return-to-zero differential phase shift keyed demodulation in the presence of chromatic dispersion

Yannick Keith Lize^{1,2,3}, Louis Christen², Xiaoxia Wu², Jeng-Yuan Yang², Scott Nuccio²,
Teng Wu², Alan E. Willner², Raman Kashyap³

¹ITF Laboratories, Montreal, Canada

²Viterbi School of Engineering, University of Southern California, Los Angeles, California, 90089, USA

³Advanced Photonic Concepts Laboratory, École Polytechnique de Montréal, Montreal, Canada

yannick.lize@gmail.com

Abstract: Optical differential phase shift keying is normally demodulated in a delay-line interferometer with a 1-bit delay such that the free-spectral-range of the demodulator is equal to the transmitted bitrate. We show using Karkunen-Loeve expansion simulation that free-spectral-range optimization leads to increased chromatic dispersion tolerances. The optimized delay inversely scales with the amount of chromatic dispersion such that a delay slightly shorter than the bit period increases tolerances with no adverse effect on the polarization-mode-dispersion tolerance or frequency offset penalty at the receiver.

©2007 Optical Society of America

OCIS codes: (060.5060) Phase modulation.

References and links

1. A. H. Gnauck and P. J. Winzer, "Optical phase-shift-keyed transmission," *J. Lightwave Technol.* **23**, 115-130 (2005).
2. P. J. Winzer, and R.-J. Essiambre, "Advanced modulation formats for high-capacity optical transport networks," *J. Lightwave Technol.* **24**, 4711-4728 (2006).
3. K. P. Ho, *Phase Modulated Optical Communication Systems* (Springer, 2005).
4. X. Liu, "Nonlinear effects in phase shift keyed transmission," in *Proc. of C2004*, paper ThM4, Los Angeles, CA (2004).
5. X. Liu, Y.-H. Kao, M. Movassaghi, and R. C. Giles, "Tolerance to in-band coherent crosstalk of differential phase-shift-keyed signal with balanced detection and FEC," *IEEE Photon. Technol. Lett.* **16**, 1209-1911 (2004).
6. F. Seguin and F. Gonthier, "Tunable all-fiber, delay-line interferometer for DPSK demodulation," in *Proc. OFC 2005*, paper OFL5, Anaheim, CA (2005).
7. J. X. Cai, D. G. Foursa, L. Liu, C. R. Davidson, Y. Cai, W. W. Patterson, A. J. Lucero, B. Bakhshi, G. Mohs, P. C. Corben, V. Gupta, W. Anderson, M. Vaa, G. Domagala, M. Mazurczyk, H. Li, S. Jiang, M. Nissov, A. N. Pilipetskii, and N. S. Bergano, "RZ-DPSK field trial over 13 100km of installed non-slope matched submarine fibers," *J. Lightwave Technol.* **23**, 95 (2005).
8. T. Mizuochi, K. Ishida, T. Kobayashi, J. Abe, K. Kimjo, K. Motoshima, K. Kasahara, "A comparative study of DPSK and OOK WDM transmission over transoceanic distances and their performance degradations due to nonlinear phase noise," *J. Lightwave Technol.* **21**, 1933-1943 (2003).
9. G. Charlet, E. Corbel, J. Lazaro, A. Klekamp, R. Dischner, P. Tran, W. Idler, H. Mardoyan, A. Konczykowska, F. Jorge, S. Bigo, "WDM transmission at 6-Tbit/s capacity over transatlantic distance, using 42.7-Gb/s differential phase-shift keying without pulse carver," *J. Lightwave Technol.* **23**, 104-107 (2005).
10. H. Kim and P. Winzer, "Robustness to laser frequency offset in direct-detection DPSK and DQPSK Systems," *J. Lightwave Technol.* **21**, 1887-1891 (2003).
11. P. Winzer and H. Kim, "Degradations in balanced DPSK receivers," *IEEE Photon. Technol. Lett.* **15**, 1282-1284 (2003).
12. K. P. Ho, "The effect of interferometer phase error on direct-detection DPSK and DQPSK signals," *IEEE Photon. Technol. Lett.* **16**, 308-310 (2004).
13. G. Bosco and P. Poggolini, "The impact of receiver imperfections on the performance of Optical Direct-Detection DPSK," *J. Lightwave Technol.* **23**, 842-848 (2005).

14. J. P. Gordon and L. F. Mollenauer, "Phase noise in photonic communications systems using linear amplifiers," *Opt. Lett.* **15**, 1351-1353 (1990).
15. E. Iannone, F. S. Locati, F. Matera, M. Romagnoli, and M. Settembre, "High-speed DPSK coherent systems in the presence of chromatic dispersion and Kerr Effect," *J. Lightwave Technol.* **23**, 842-848 (2005).
16. J. Wang and J. M. Kahn, "Impact of chromatic and polarization-mode dispersions on DPSK systems using interferometric demodulation and direct detection," *J. Lightwave Technol.* **22**, 362-371 (2004).
17. Y. K. Lize, L. Christen, P. Saghari, S. Naccic, A.E. Willner, R. Kashyap, and Paraschis, "Implication of Chromatic dispersion on frequency offset and Bit delay mismatch penalty in DPSK demodulation," in *Proc. ECOC 2006*, paper Mo3.2.5, Cannes, France (2006).
18. B. Mikkelsen, C. Rasmussen, P. Mamyshev, and F. Liu, "Partial DPSK with excellent filter tolerance and OSNR sensitivity," *Electron. Lett.* **42**, 1363-1364 (2006).

1. Introduction

Due to its increased receiver sensitivity and increased tolerance to various fiber-based impairments, differential-phase-shift-keying (DPSK) has been pursued aggressively as an alternative to on-off keying (OOK) [1-6]. After several years of laboratory experiments and field demonstrations [7-9], Return-to-zero (RZ-) DPSK is currently being deployed for next generation high capacity optical networks. In DPSK the information is encoded on the difference of phase between consecutive bit period rather than the absolute phase of the signal, a delay-line Mach-Zehnder interferometer (DLI) [6] is commonly used to convert phase difference into intensity modulation which can be detected by standard photo-diodes. The two arms of the DLI are delayed relative to each other by a single bit time such that the free spectral range (FSR) of the interferometer is equal to the transmitted bitrate. The phase of one bit in the data stream is then compared to the phase of the subsequent bit. The two output ports of the DLI, representing the constructive and destructive interference between the phases of adjacent bits, are connected to balanced receivers where it is the balanced detection that is responsible for most of the advantage of DPSK over OOK.

In back-to-back configuration, the most efficient DLI has a complete one-bit delay such that the phases of two adjacent bits are compared during the entire bit time for maximum eye opening. It has been shown that DLI degradations such as bit delay mismatch and frequency offset [10-13], transmission impairments such as chromatic dispersion (CD), polarization-mode-dispersion (PMD), and nonlinearities [14,16] or the combination of DLI degradations and transmission impairments [17] can distort the phase of the DPSK signal and reduce receiver sensitivity. It might be advantageous to optimize the FSR of the DLI to actually counteract the phase degradation of the transmission impairments in order to enhance the DPSK receiver sensitivity. It was recently demonstrated that FSR optimization can increase optical filtering and CD tolerances for NRZ-DPSK [18].

In this paper we demonstrate that in the presence of CD, offsetting the FSR of the DLI to obtain partial bit delay in the demodulation of a RZ-DPSK signal increases CD tolerance with no adverse effect on the PMD tolerance or frequency offset penalty. We find up to 1dB increase in receiver sensitivity at BER 10^{-3} or a 12.5% increase in CD tolerance. We show a 0.25 dB increase in receiver sensitivity for PMD impairment which although approaching the resolution of the simulation, at the very least indicates that the FSR optimization does not impact PMD tolerance. The optimal FSR scales with CD and PMD. Furthermore, we show that some of the increased degradation stemming from the combination of transmission impairments and frequency offset [17] is actually mitigated by using partial bit delay demodulation.

2. Concept and Theory

Normally in DPSK demodulation, an exact 1 bit delay is used to demodulate the signal. The effect of bit delay mismatch at the interferometer has been extensively studied [11, 13, 17]. As seen in Fig. 1, when less than 1-bit delay is used, part of the bit interferes onto itself which provides deterministic constructive interference for every bit time. This normally creates eye closure in back-to-back OSNR sensitivity measurement but the deterministic interference is

not affected by transmission effects and provides a buffer between bits after demodulation which minimizes inter-symbol interference (ISI). CD and PMD are a main cause of ISI in fiber optic transmission. The ISI tolerance that is provided by the constant interference of partial bit delay demodulation is not as efficient in the presence of PMD since the deterministic interference will occur independently in the two orthogonal polarization states. PMD will cause a time delay between the two polarizations such that the time location of the deterministic interference will drift and ISI will still occur. This also explains why NRZ-DPSK provides a greater improvement than RZ-DPSK for FSR optimization [18] since the RZ formats provides an ISI resistant "buffer" that FSR optimization provides.

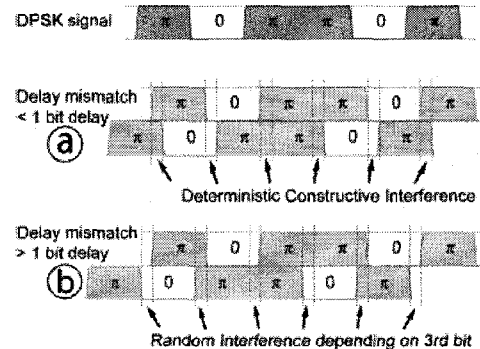


Fig. 1. Concept of bit delay mismatch. For mismatch smaller than one bit period a constant deterministic interference occurs for each bit period leading to greater tolerance to ISI.

It has been shown [11,13,17] that in back-to-back transmission, a DLI with a mismatch greater than 1-bit delay such that the FSR is smaller than the bit rate has larger negative impact than a mismatch of less than 1-bit delay.

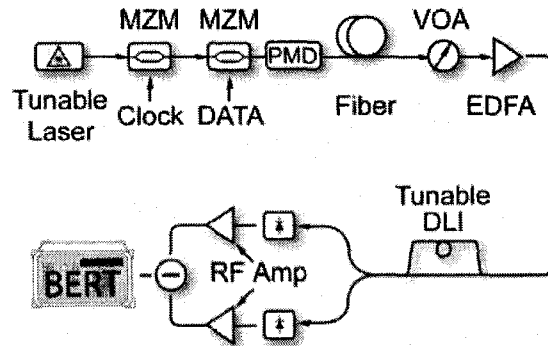


Fig. 2. Diagram of the setup for simulations using a 40Gbps RZ-DPSK signal with 50GHz 3rd order Gaussian optical filter and 32GHz Lorentzian electrical filter. Karkunen-Loeve expansion for non-Gaussian noise statistics was used with 512 bits simulated at 60 samples per bit in a simulation bandwidth of 0.48 THz.

3. Results

Simulations were performed for a 40Gbps RZ-DPSK signal with 50GHz 3rd order Gaussian optical filtering and 32GHz Lorentzian electrical filtering. Karkunen-Loeve expansion for non-Gaussian noise statistics was used with 512 bits simulated at 60 samples per bit in a simulation bandwidth of 0.48 THz. The setup for the simulations is illustrated in Fig. 2.

Results show that the optimal bit delay in the presence of residual CD or PMD is no longer a 1 bit delay. Complete BER curves were simulated for each combination of parameters and OSNR penalty at $BER=10^{-3}$ were inferred from a linear fit of the $\text{Log}(\text{Log}(\text{BER}))$ versus OSNR in dB.

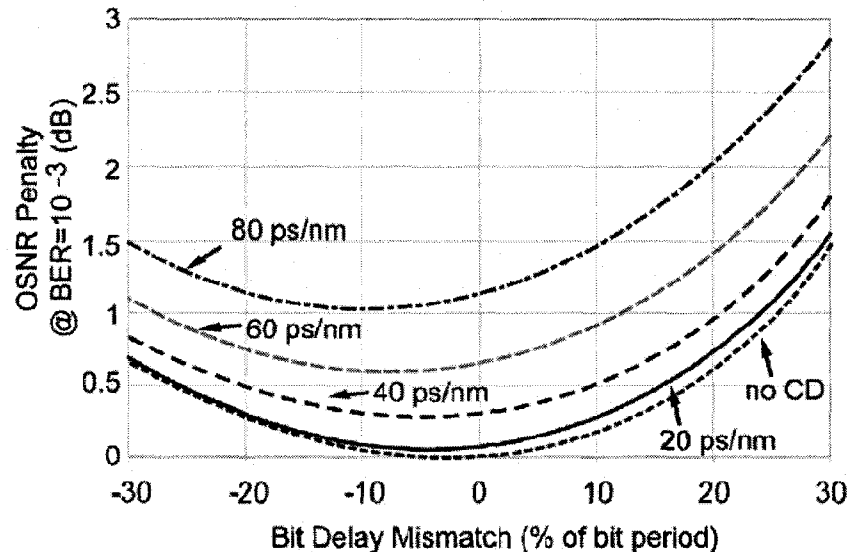


Fig. 3. Bit delay mismatch penalty for different values of chromatic dispersion. The optimal bit delay is no longer 1bit in the presence of CD.

3.1 Chromatic dispersion and bit delay mismatch

The OSNR penalty at $BER=10^{-3}$ versus bit delay mismatch in percentage of the bit period at 40Gbps for an RZ-DPSK signal is illustrated in Fig.3 for different values of CD. The results shown in Fig.3 for no CD are similar but not exactly the same as previously reported results for bit delay mismatch penalty [11-13]. This is explained by the fact our results are for RZ-DPSK and we calculate the OSNR penalties at BER of 10^{-3} . Interestingly with increasing CD, the penalty curve shifts to the left of the zero-delay-mismatch point such that the optimal delay is no longer equal to the bit period. Again, a mismatch larger than the bit period causes a greater penalty than a mismatch smaller than the bit period.

Figure 4 illustrates the OSNR penalty versus CD for a perfect 1-bit delay and with the optimized delay mismatch. Results for 1-bit delay are in agreement with previously reported results for CD tolerance of RZ-DPSK [16]. For optimal bit delay mismatch, full BER versus OSNR curves were simulated for all the combinations CD and delay mismatch to find the optimal point.

We find that RZ-DPSK becomes 12.5% more tolerant to CD at 3dB penalty than standard 1-bit delay demodulation. The Fig. also shows that the optimal mismatch values increase with increasing CD and that the bit delay is about $\frac{1}{4}$ of the bit period at 3dB. The Fig. indicates indicate that at no CD, the optimal point is not zero mismatch but the difference in OSNR penalty at that point is less than 0.01dB which is much lower than the simulation accuracy.

Figure 5 illustrates the OSNR penalty versus PMD for a perfect 1-bit delay and with optimized delay mismatch. As expected the improvement is not as significant as for CD. The PMD tolerance is increased by 2% for a 3dB OSNR penalty which is on the order of the

simulation accuracy. More importantly, it indicates that optimizing the DLI to increase tolerance to CD does not degrade the tolerance to PMD in the RZ-DPSK demodulation.

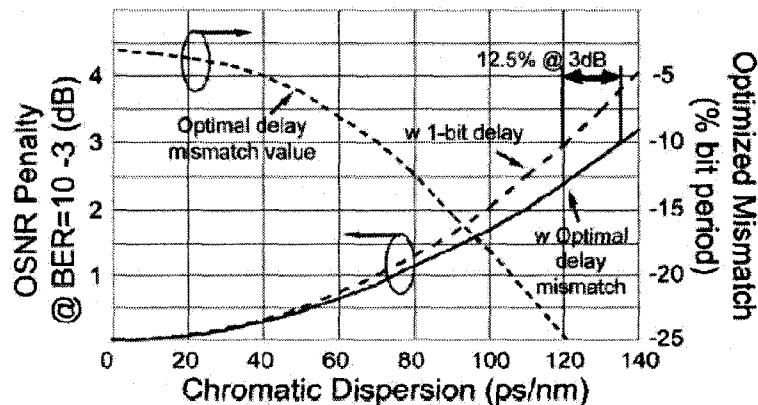


Fig. 4. Numerical results of optimal mismatch as percentage of bit period for CD. Difference in OSNR penalty for exact 1-bit and with optimal bit delay mismatch. An improvement of 12.5% of CD tolerance is observed at 3dB OSNR penalty.

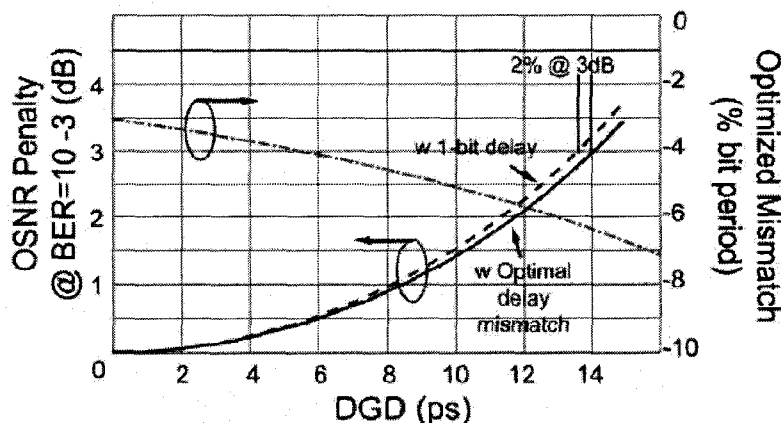


Fig. 5. Numerical results of optimal mismatch as percentage of bit period and OSNR penalty for PMD. The improvement of 2% in PMD tolerance is not significant and within the accuracy of the numerical simulation but it nevertheless indicates that optimized FSR for CD will not be degraded by PMD.

3.2 Frequency Offset, chromatic dispersion and bit delay mismatch

Frequency offset penalty in DPSK demodulation occurs when the transmission peak of the DLI is not aligned to the frequency of the transmitting laser. This is caused by the improper phase tuning of the demodulator [11-14]. It was recently reported that the combination of frequency offset to residual CD at the receiver incurs a greater penalty than the sum of the two degradations [17] because of the combination of phase degradations. Figure 6 illustrates the frequency offset penalty with 140ps/nm of CD for different values of bit-delay mismatch. The baseline curve with no CD is similar to previously reported results [11-14] but we used RZ-DPSK and calculated the OSNR penalty at BER 10^{-3} . A 0.5dB penalty is incurred when the frequency of the signal is offset from the transmission peak of the DLI by about 4% of the bitrate in back-to-back demodulation. The OSNR penalty coming from CD [16] has been

subtracted from Fig. 6 such that only the frequency offset penalty is shown so as to more clearly visualize the OSNR penalty stemming from the *combination* of CD and frequency offset. With 140ps/nm of CD, the frequency offset penalty alone doubles. Again the total OSNR penalty would also incorporate the CD penalty.

If the bit delay mismatch is greater than 1-bit delay, Fig. 6 illustrates that the penalty of combining CD and frequency offset is further increased. For a mismatch of +10% the frequency offset penalty climbs from 0.5dB at 4% offset to a very significant 2dB penalty. The penalty for a 4% offset, is 1.5dB for a perfect one bit delay but reduced to about 1 dB for a -15% mismatch.

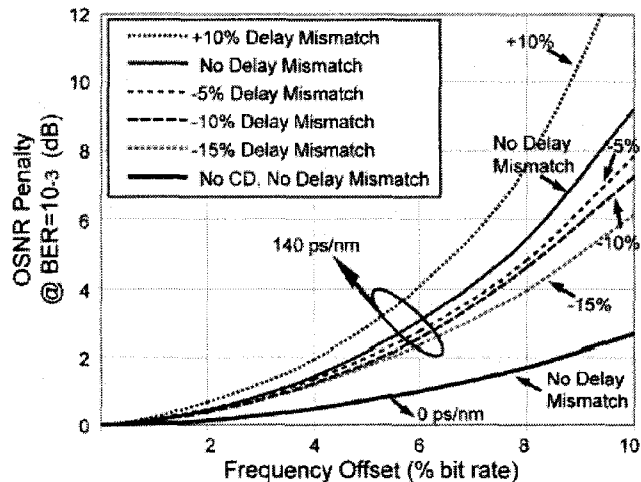


Fig. 6. Combination of frequency offset and CD with the CD penalty subtracted out. Optimized bit-delay mismatch compensates for some of the increased penalty incurred by the combination without reaching the no-CD level.

Unlike in the CD case, the combination of PMD with frequency offset does not yield an increased penalty when the signal is not centered on the transmission frequency of the DLI. Since partial bit delay demodulation has little effect on PMD tolerance, its effect on the combination of frequency offset and PMD also has little effect.

4. Conclusion

We presented the optimization of the bit delay mismatch in RZ-DPSK demodulation in the presence of chromatic dispersion. We showed that by offsetting the FSR of the DLI to obtain partial bit delay in the demodulator, CD tolerance is increased with no adverse effect on the PMD tolerance or frequency offset penalty. We find that up to 1dB increase in receiver sensitivity with a 12.5 % increase in CD tolerance is possible. We show a 0.25 dB increase in receiver sensitivity for PMD impairment demonstrating that the mismatch is not negatively affected by PMD. The optimal delay mismatch scales with CD and PMD.

Appendix VI

Chromatic dispersion tolerance in optimized NRZ-, RZ- and CSRZ-DPSK demodulation

Yannick Keith Lize^{1,2,3}, Xiaoxia Wu², Moshe Nazarathy⁴, Yuval Atzmon⁴, Louis Christen², Scott Nuccio², Mathieu Faucher¹, Nicolas Godbout³, Alan E. Willner²

¹ITF Laboratories, Montreal, Canada

²Viterbi School of Engineering, University of Southern California, Los Angeles, California, 90089, USA

³Engineering Physics Department, Ecole Polytechnique de Montréal, Montréal, Canada

⁴EE Department, Technion Institute of Technology, Haifa, Israel

yannick.lize@gmail.com

Abstract: We present the results of a comprehensive analysis optimizing the performance of DPSK systems with increased FSR and narrow optical filtering, establishing improved chromatic dispersion tolerance of NRZ-DPSK by 20%, RZ-DPSK by 71% and CSRZ-DPSK by 74% approximately. Transmitting a 40Gb/s signals on a spectrally efficient 50GHz DWDM grid still exhibit improvements of 7% for NRZ-DPSK, 37% for RZ-DPSK and 22% for CSRZ-DPSK, relative to a typical DPSK receiver. The optimized delay and optical filtering scale with the amount of chromatic dispersion. We also demonstrate the impact of limited transmitter bandwidth on optimal optical filtering and bit delay parameters.

©2008 Optical Society of America

OCIS codes: (060.5060) Phase modulation.

References and links

1. A. H. Gnauck and P. J. Winzer, "Optical phase-shift-keyed transmission," *J. Lightwave Technol.* **23**, 115-130 (2005).
2. E. Golovchenko, L. Rahman, B. Bakhshi, D. Kovsh, F. Idrovo, and S. Abbott, "Field Deployment of WDM 10 Gb/s Capacity over 10.737 km of Reconfigured Portion of SAM-1 Cable System," in Optical Fiber Conference (OFC 2007)(Anaheim, CA, 2007), p. PDP27.
3. G. Bosco and P. Poggolini, "The impact of receiver imperfections on the Performance of optical direct-Detection DPSK," *J. Lightwave Technol.* **23**, 842-848 (2005).
4. P. J. Winzer and H. Kim, "Degradations in balanced DPSK receivers," *IEEE Photon. Technol. Lett.* **15**, 1282-1284 (2003).
5. Y. K. Lize, M. Faucher, É. Jarry, P. Ouellette, É. Villeneuve, A. Weiter, and F. Séguin, "Phase-Tunable Low-Loss, S-, C-, and L-band DPSK and DQPSK Demodulator," *IEEE Photon. Technol. Lett.* **19** (2007).
6. Y. K. Lize, L. Christen, X. Wu, J.-Y. Yang, S. Nuccio, T. Wu, A. E. Willner, and R. Kashyap, "Free spectral range optimization of return-to-zero differential phase shift keyed demodulation in the presence of chromatic dispersion," *Opt. Express* **15**, 6817-6822 (2007).
7. C. Malouin, J. Bennike, and T. Schmidt, "DPSK Receiver Design - Optical Filtering Considerations," in OFC/NFOEC 2007. 2007 Optical Fiber Communication Conference and National Fiber Optic Engineers Conference(Optical Society of America, Anaheim, CA, 2007), p. 3.
8. B. Mikkelsen, C. Rasmussen, P. Mamyshev, and F. Liu, "Partial DPSK with excellent filter tolerance and OSNR sensitivity," *Electron. Lett.* **42**, 1363-1365 (2006).
9. Y. K. Lize, X. Wu, L. Christen, M. Faucher, and A. E. Willner, "Free Spectral Range and Optical Filtering Optimization in NRZ-, RZ- and CSRZ-DPSK Demodulation," in IEEE Lasers and Electro-Optics Society (LEOS) Annual Meeting(Orlando, Florida, 2007).
10. J. Wang and J. M. Kahn, "Impact of chromatic and polarization-mode dispersions on DPSK systems using interferometric demodulation and direct detection," *J. Lightwave Technol.* **22**, 362-371 (2004).
11. A. Agarwal, S. Chandrasekhar, and P. J. Winzer, "Experimental study of photocurrent imbalance in a 42.7-Gb/s DPSK receiver under strong optical filtering," in 2005 Optical Fiber Communications Conference Technical Digest(IEEE, Anaheim, CA, 2005), p. 3 Vol. 6.
12. P. J. Winzer and R. J. Essiambre, "Advanced modulation formats for high-capacity optical transport networks," *J. Lightwave Technol.* **24**, 4711-4728 (2006).

13. B. Slater, S. Boscolo, T. Broderick, S. K. Turitsyn, R. Freund, L. Molle, C. Caspar, J. Schwartz, and S. Barnes, "Performance analysis of 20Gb/s RZ-DPSK non-slope matched transoceanic submarine links," *Opt. Express* **15**, 10999-11007 (2007).

1. Introduction

Differential phase shift keying (DPSK) in its variants, such as non-return-to-zero (NRZ-), return-to-zero (RZ-) and carrier-suppressed- return-to-zero (CSRZ-) DPSK, is becoming one of the formats of choice in next generation optical communication systems [1, 2]. DPSK is usually demodulated in a delay-line interferometer with a one-bit delay such that the phases of two adjacent bits are compared during the entire bit time [3-5]. It was recently shown that free-spectral-range (FSR) optimization can increase optical filtering (OF) or CD tolerance for RZ-and NRZ-DPSK [6-9]. Although quite convincing, those results fail to identify the optimal value of FSR value versus CD. It was also mentioned in [6-8] that transmitter bandwidth has an impact of optimal FSR parameter but only for NRZ-DPSK and the specific impact and requirements are yet to be fully explored. Most importantly there has been little discussion on the combined effect of FSR optimization and tight OF on the increase of CD tolerances.

In this paper we report a comprehensive analysis of the parameter space of OF bandwidth and FSR for the NRZ-, RZ- and CSRZ-DPSK formats, establishing that *simultaneous* FSR and OF optimization significantly improves CD tolerances. The results can be used as guidelines in designing DPSK receivers according to the maximum amount of chromatic dispersion allowed in the system. The specific impact of transmitter bandwidth on the optimized FSR and OF parameters is also presented. Finally, we show the impact OF and FSR optimization on DWDM DPSK systems with high channel density.

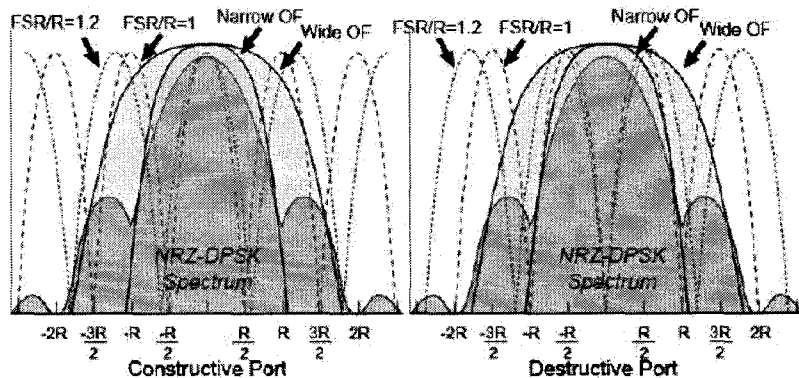


Fig. 1. DPSK spectrum with overlayed transfer functions for optical filtering and delay-line interferometer. Free-spectral-range larger than the bitrate and tighter optical filtering puts a greater emphasis on the optical duobinary (ODB) port (constructive) rather than the alternate-mark-inversion port (destructive).

2. Principle of operation

The optimisation obtained through increasing the FSR of the Delay Interferometer (DI) can be explained using the equivalent baseband model detailed in [10], representing the DPSK link as two parallel paths with Transfer Functions (TF) given in our modified notation by the product $H_L(f) \equiv H_T(f)H_F(f)H_o(f)H_{\pm}(f)$ of the TF $H_T(f)$ of the Transmitter (TX)

pulse-carver, the fiber dispersion $H_F(f)$, the OF $H_0(f)$ and the TFs describing the DI propagation to the constructive (ODB) / destructive (AMI) DI ports:

$$H_{\pm}(f) = [\exp(-j2\pi f/FSR) \pm 1]/2 \quad (1)$$

$$|H_+(f)|^2 = \cos^2(\pi f/FSR)/4 \quad (2)$$

$$|H_-(f)|^2 = \sin^2(\pi f/FSR)/4 \quad (3)$$

The benefit of taking $FSR > R$, (with $R = T_b^{-1}$ the bitrate) is then interpreted as an equalization measure; by reducing the OF bandwidth (BW) we improve the CD tolerance and reduce ASE noise, however this in itself would introduce ISI, which is subsequently equalized by increasing the FSR of the filters in (1) as shown in Fig. 1. The enhanced BW filters (1) then act as equalizers for the other TFs in the chain $H_L(f)$. While the ASE noise reduction due to tighter optical filtering is undone to some extent by the noise enhancement through the enhanced BW equalizers (1), an improvement in CD tolerance is achieved: Up to $f = \pm FSR/2$ the ODB port TF (2) is low-pass, while the AMI port TF (3) is high-pass, accentuating the frequencies farther away from the optical carrier, resulting in emphasis of CD. Increasing the FSR, both TFs are horizontally stretched, on one hand reducing the rolloff of (2) which becomes less of a low-pass, making up for (partially equalizing) the increased rolloff of the tight OF, hence mitigating the ISI induced by the tight OF. On the other hand, stretching the high-pass TF (3) reduces its "rollup" making it less of a highpass, hence diminishing the emphasis of CD at the AMI port. This has similarities with biasing the photocurrent imbalance to favor the ODB port, as was demonstrated in [7].

3. Numerical model

Simulations were performed for a C-band Pseudo random binary signal (PRBS) DPSK signals at bitrate R , modulated with a Mach-Zehnder modulator (MZM) with 20dB of extinction ratio. The RZ- and CSRZ-DPSK signals were generated using a second MZM driven by a $R/2$ clock with a V_{π} drive voltage for CSRZ-DPSK and R clock with V_{π} drive voltage for RZ-DPSK. At the receiver, the signal was filtered through a 2nd order Gaussian OF and demodulated in an MZ delayline interferometer (DLI). Balanced detection was followed by \sqrt{R} 4th-order Bessel electrical filter. The bit error rate (BER) was estimated by means of a Karhunen-Loeve expansion for non-Gaussian noise statistics, with 1024 simulated bits at 64 samples per bit in a simulation BW of $25R$. The OSNR in 0.1 nm was set using $OSNR = 10\log(R)$ dB corresponding to 10, 16 and 20 dB of OSNR at 10, 40 and 100 Gb/s respectively. The CD was varied from 0 to 272 in normalized units of 10^3 (Gb/s)² ps/nm using $CD_{\text{index}} = R^2 LD$ [10] where L is the fiber length and D the CD in ps/nm/km. The Q parameter was calculated from the BER value as in [3, 7] using $Q = 20\log\sqrt{2}\text{erfc}^{-1}(2BER)$, with erfc^{-1} the inverse complementary error function.

4. Results

Similarly to what has been reported elsewhere, we find that the optimal OF for NRZ-, RZ- and CSRZ-DPSK for a one-bit back-to-back demodulation to be around $1.25R$ for NRZ-, $1.75R$ for RZ- and $1.8R$ for CSRZ-DPSK. The optimal FSR varies over the OF BWs but is also very dependent on CD. The results indicate that either tighter optical filtering or larger FSR tends to increase CD tolerance but their *combination* leads to optimal CD performance.

For RZ-DPSK with optimal OF, the optimal FSR/R value is 1 as was noted in [4]. With tighter filtering, larger FSR yields better performance. Figure 2 illustrates the dramatic impact of optimizing the FSR and OF in the presence of CD. For 0 CD, by drawing a line on the contour plot at OF 1.75R, 0.88R and 0.75R, we obtain results similar to [7]. On the 0 CD plot, the orientation of the contour line for tight optical filtering clearly demonstrate the effect of increasing the FSR. The advantage of having complete results shown as contour plot is that it provides the penalty curve for a wide range of OF bandwidth which is practical if optimal OF bandwidth is not possible.

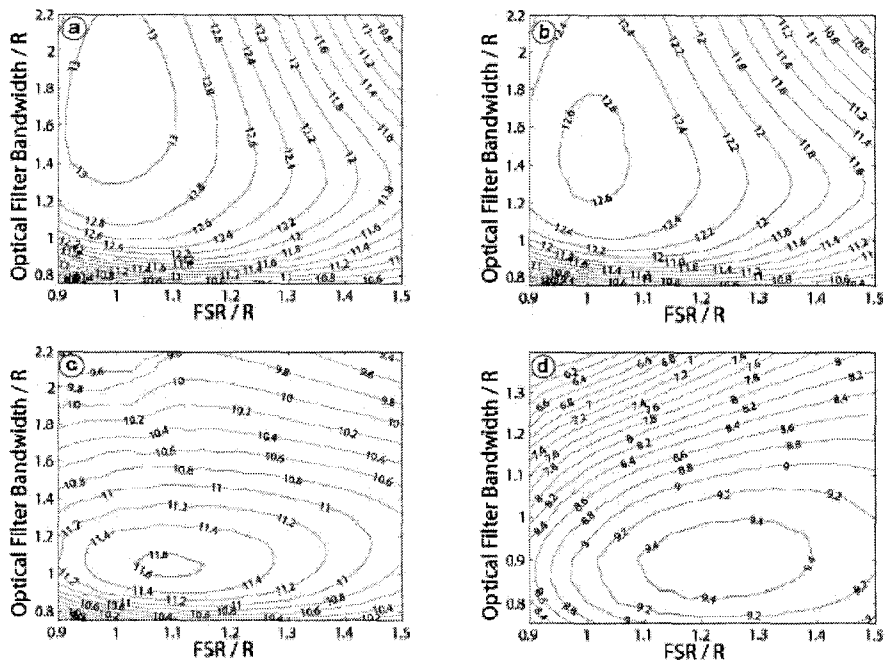


Fig. 2. RZ-DPSK Q-factor versus free spectral range and optical filtering bandwidth for CD index of a) 0, b) 24, c) 110 and d) 218×10^3 (Gb/s)² ps/nm

As CD is increased to 54, 110 and 218×10^3 (Gb/s)² ps/nm, the optimal OF bandwidth drops dramatically while the optimal FSR value increases almost linearly. With optimal parameters, CD tolerance increases by 71% at 9.8 dBQ as shown in Fig. 3. Using the normalized values for a 40Gb/s RZ-DPSK signal, the results translate into an OSNR of 16dB and residual CD tolerance increase from 74 ps/nm to 127.5 ps/nm.

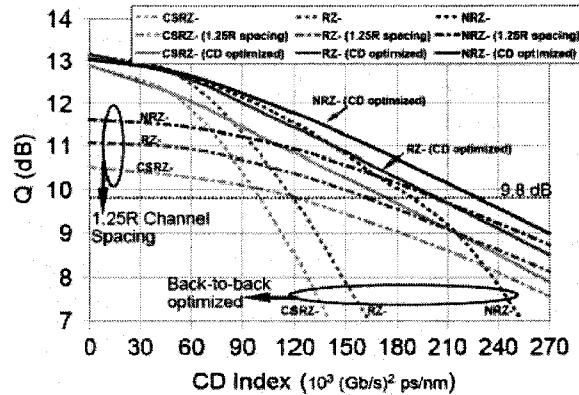


Fig. 3. Chromatic dispersion tolerance improvement using FSR and optical filtering optimized for best back-to-back performance versus using optimized parameters. Using channel spacing of 1.25R (50Ghz for 40G signal) with optimized parameters yields better results than a single non-optimized channel.

Although the improvement may be considered small on an absolute scale, it may be of great importance for short distance office to office 40 Gb/s systems which cannot afford chromatic dispersion compensation.

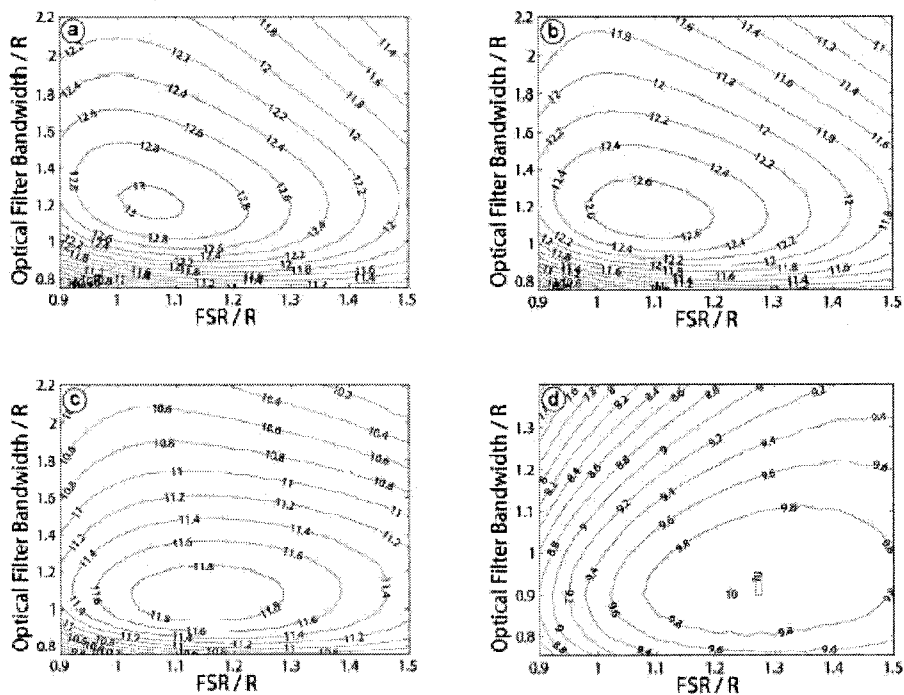


Fig. 4. NRZ-DPSK Q-factor versus free spectral range and optical filtering bandwidth for CD index of a) 0, b) 54, c) 110 and d) $218 \times 10^3 (\text{Gb/s})^2 \text{ ps/nm}$.

Such systems are currently being deployed using the ODB modulation format because of its high chromatic dispersion tolerances [12]. For dispersion compensated systems, the method provides an increase in tolerances to varying residual CD or improper dispersion slope compensation. Another interesting observation from the contour plot is that at 110×10^3 (Gb/s)² ps/nm, if the OF is not reduced, increasing the FSR does not improve CD tolerances.

The impact of optimising the FSR and OF in the presence of CD is also apparent for NRZ-DPSK as shown in Fig. 4. With optimal parameters, CD tolerance increases by 20% as illustrated in Fig. 3. For a 40Gb/s signal it translates into residual CD tolerance increase from 118 ps/nm to 142 ps/nm. For CSRZ-DPSK, the same phenomenon is observed as illustrated in Fig. 5. With optimal parameters, CD tolerance increases by 74% as illustrated in Fig. 3. Similarly to RZ-, the contour plots for NRZ- and CSRZ- at 110×10^3 (Gb/s)² ps/nm show that if OF bandwidth is not reduced, CD tolerances and not improved significantly by increasing the FSR.

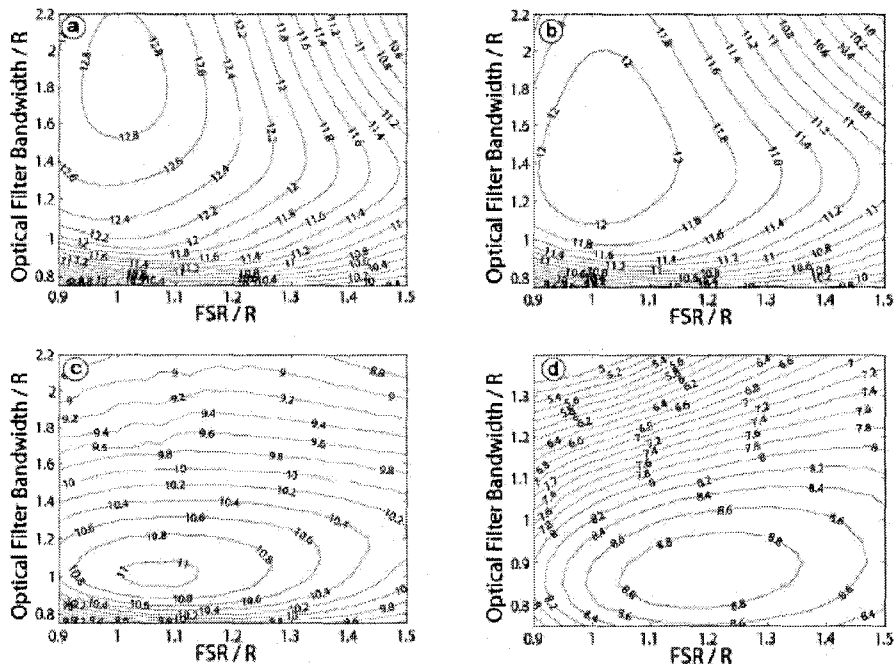


Fig. 5. CSRZ-DPSK Q-factor versus free spectral range and optical filtering bandwidth for CD index of a) 0, b) 54, c) 110 and d) 218×10^3 (Gb/s)² ps/nm.

The optimal values of FSR and OF can be selected depending on the amount of CD in the system. As shown in Fig. 6, OF BW values for RZ- and CSRZ- drop drastically for 0 to 100 $\times 10^3$ (Gb/s)² ps/nm CD index. For the three formats, the OF BW then decreases linearly with CD index. The optimal FSR increases with CD as shown in Fig. 6. Interestingly, the optimal

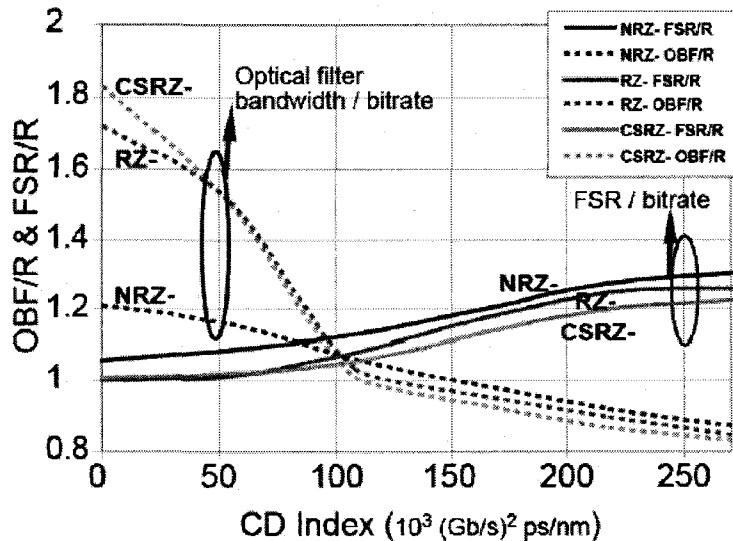


Fig. 6. Optimized values of optical filtering (OF) and free spectral range (FSR) normalized over bitrate for RZ-, NRZ- and CSRZ- DPSK optimized Q factor (with both OF and FSR are optimized simultaneously). But choosing OF and FSR parameters optimized for a specific amount of CD yields only a small penalty which effectively flattens the curve of penalty versus CD which can be very beneficial in a DPSK system.

FSR/R value for NRZ-DPSK is not unity even in the absence of CD as was also shown in [8].

Tunable bandwidth optical filter and tunable FSR interferometer are not readily available or easily integrated in a DPSK receiver. Fortunately the results of Figs. 2-6 do not indicate that a tunable solution is required to properly demodulate a DPSK signal. By choosing the FSR and OF parameters for a specific amount of CD, the penalty without CD is not significant. For example in Fig. 2 for RZ-DPSK at 218×10^3 (Gb/s)² ps/nm of CD, the optimal parameters are OF/R=0.9 and FSR/R=1.25 as shown in Fig. 5. Using those values for zero CD gives a Q of 11.8dB for an insignificant penalty 1.2dBQ. Alternatively, using a standard 1.75 OF/R and 1 FSR/R which would be optimized for back-to-back demodulation, would incur a penalty greater than 5dBQ and a Q smaller than 5dBQ for 218×10^3 (Gb/s)² ps/nm of CD. Choosing OF bandwidth and FSR optimized for the maximum CD tolerances, effectively flattens the penalty curve versus CD which can be very beneficial in a system. The conclusion is not however that CD compensation will no longer be required in all types of DPSK networks. The increased CD tolerances could reduce the requirements on accuracy, end of life requirements or group delay ripple for fixed or tunable CD compensators in networks with large amount of CD or with significant time-varying CD.

5. Channel spacing and transmitter bandwidth

It was remarked in [8] that FSR optimization enables minimizing channel spacing in DWDM systems. To quantify this benefit, we ran simulations observing the center channel in five independent DWDM channels separated in frequency by 1.25R and pre-filtered before multiplexing with FSR and OF values re-optimized to maximize the Q-factor at the receiver.

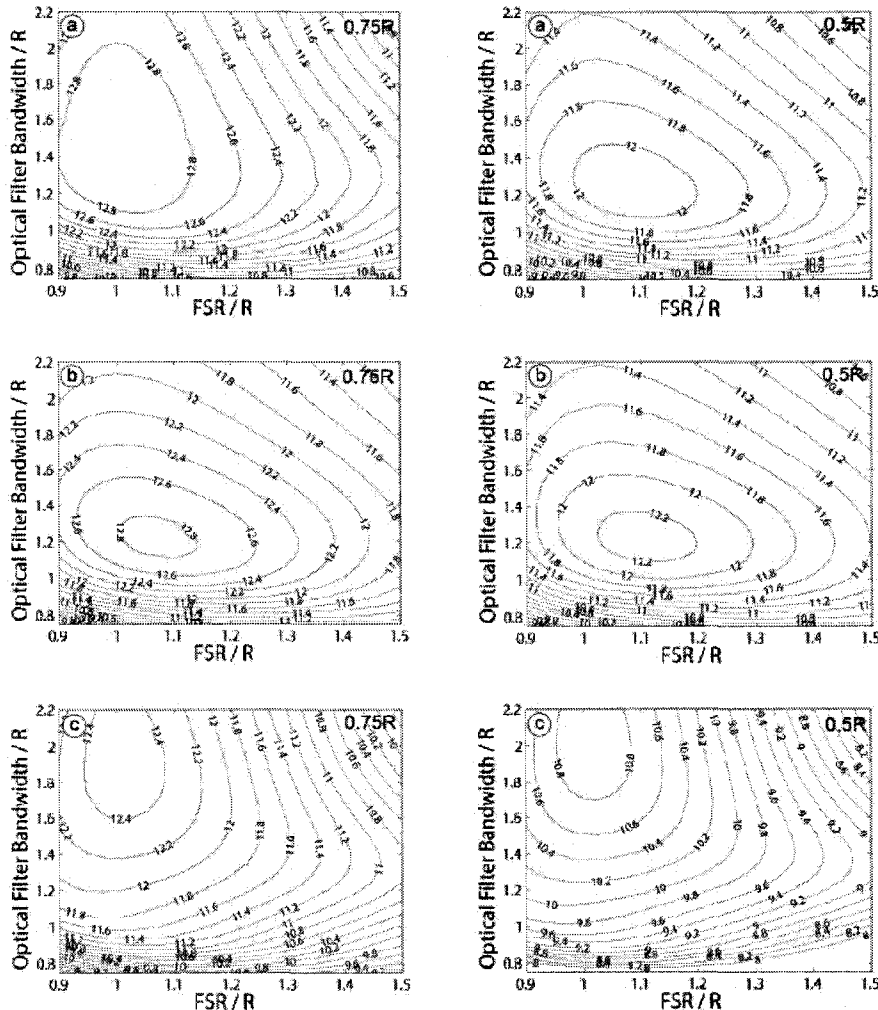


Fig. 7. Effect of modulator bandwidth on FSR and OF optimization in back to back detection for a) RZ- b) NRZ, and c) CSRZ- for 0.75R (left) and 0.5R(right) modulator bandwidth.

The results shown in Fig. 3 indicate that all three DPSK formats with optimized FSR and OF using 1.25R channel spacing, outperform a single non-optimized channel. The CD tolerance using a 40Gb/s DWDM system with 50GHz channel spacing with 16dB of OSNR is increased by 37% for RZ-DPSK, 7% for NRZ-DPSK and 22% for CSRZ-DPSK, relative to a single channel with non-optimized demodulation.

Finally, as was noted by [7, 8], transmitter bandwidth impacts the optimal FSR for NRZ-DPSK. We thoroughly studied this effect for three DPSK formats with 0.75R and 0.5R modulator and modulator driver BW and found that this effect is also true for RZ-DPSK. The results presented in Fig. 7 indicate that when comparing with the 0-CD contour plots of Fig. 2, 4 and 5, reducing the optical filtering and increasing the FSR improves performance of a lower BW transmitter. The results open the potential of using lower bandwidth electronic components, for example using 10Gb/s modulators and drivers, for 20Gb/s DPSK

transmission [13]. The smaller transmitter bandwidth provides a narrower spectrum and the penalty is somewhat compensated by using an optimized FSR and OF bandwidth. The penalty is only 1dBQ for RZ-DPSK and 0.8 dBQ for NRZ-DPSK. Interestingly, CSRZ-DPSK is not improved when using a larger FSR or narrower OF filtering bandwidth. Nevertheless, the method could enable lower-cost transponders with substantial improvements in CD tolerance by combining larger FSR, narrow optical filter and smaller transmitter bandwidths.

5. Conclusion

We reported a comprehensive analysis of the parameter space of OF bandwidth and FSR for the NRZ-, RZ- and CSRZ-DPSK formats, establishing that *simultaneous* FSR and OF optimization significantly improves CD tolerances. The results can be used as guidelines in designing DPSK receivers according to the maximum amount of chromatic dispersion allowed in the system. The specific impact of transmitter bandwidth on the optimized FSR and OF parameters is also presented. Finally, we show the impact OF and FSR optimization on DWDM DPSK systems with high channel density.